

The Peregrine

Virginia
Tech

VIRGINIA POLYTECHNIC INSTITUTE
AND STATE UNIVERSITY
AEROSPACE ENGINEERING

2003/2004 AIAA Undergraduate Team Aircraft Design Competition



-an E/STOL, Airport Adaptive Regional Jet-

Designed by Team ASCENT



The Peregrine

-an E/STOL, Airport Adaptive Regional Jet-

Designed by Team ASCENT



2003/2004 AIAA Undergraduate Team Aircraft Design Competition

Virginia Polytechnic Institute & State University

June 4, 2004

Name	Signature	Focus	AIAA #
Joe Adelman, Team Leader	_____	Weight, CG, Powered Lift	235569
Chris Bang	_____	Mission, Cost	238079
Matt Eluk	_____	Stability and Control	238089
Adam Entsminger	_____	Configuration, CAD	239781
Jessica Hill	_____	Aerodynamics	237236
Jason Mostaccio	_____	Propulsion, Powered Lift	235572
Derek Reimer	_____	Structures, Systems	235414

Faculty Advisors

W.H. Mason _____

M.A. Cavanaugh _____



Executive Summary

The Peregrine provides an innovative solution to the growing problem of airport congestion as well as serving the nation through homeland security and military support. By incorporating a hybrid, powered lift, double-slotted flap system into a 49-passenger regional jet it was possible to satisfy the 2003/2004 AIAA undergraduate RFP. Team Ascent has incorporated these advanced technologies into a unique design to be a flexible, efficient and cost effective regional jet that will revolutionize air transportation and improve national security.

Multiple Missions

The cost of the aircraft is split between the baseline cost of the regional jet and the additional, government-subsidized cost of converting the Peregrine to its secondary mission configuration. The Peregrine is capable of many missions including: wildfire support, air ambulance to urban and rural areas, air transport to and from combat areas and emergency evacuation. The main cabin is outfitted with quick-release seats that are easily removable to accommodate firemen, military response teams and medical personnel. To further assist with the additional missions, the auxiliary engines can be used as power sources for medical equipment and other necessary devices. The baggage area under the cabin is used to store mission support equipment such as fire suppressant canisters and an extra cargo door is installed to accommodate loading and unloading in adverse conditions.

The Peregrine is designed to land on unprepared runways using landing gear with a low turnover angle and four wheels per bogey for improved weight distribution. The landing gear features long stroke shock struts and a Central Tire Inflation System for efficient use on various runways. The Peregrine is outfitted with features to address survivability in dangerous missions such as, 4 mm aluminum plating under the cockpit, self-sealing fuel tanks, fire extinguishers within the engine nacelles and separated redundant flight controls. Countermeasures are available in the form of chaff and flares.

Powered Lift

The Peregrine's hybrid, powered lift system integrates two main thrusting engines, and two auxiliary, turboprop engines. The main engines produce lift through an externally blown flap arrangement. The lift generated from external blowing is dependent on exhaust plume diameter, vertical flap spacing and effective flap length. Accounting for the lift produced by the externally blown flaps and the wing, the maximum C_L achieved is 3.48. This



lift coefficient is insufficient to meet the STOL requirements of the RFP, therefore, an additional lifting source is required.

Two auxiliary engines are mounted next to the fuselage, under the wing root near the primary source of application, the inboard trailing edge flaps. Each engine is connected to a high efficiency fan, which directs air through a duct that curves up into the bottom of the airfoil and fans out towards thirteen cutouts within the aft wing spar. The air then flows over the trailing edge flaps to produce the necessary lift through internal blowing.

The combination of these unique lifting systems allows the aircraft to achieve a BFL of 1,016 ft. during primary mission operations and a BFL of 1,244 ft. during secondary mission operations. These remarkable performance characteristics enable the Peregrine to effectively complete multiple missions with a minimal cost increase.

Landing Conditions

To address the SNI approach and automated spiral descent there are several technologies integrated into the Peregrine. The Rockwell Collins FCS-4000 automatic flight control system stabilizes the spiral descent, as well as aiding the pilot with pedal-force for the rudder deflections, stabilizer deflections and bank control. During engine out conditions, the high lift system allows the Peregrine to stably continue the SNI approach and achieve a stall speed as low as 65 knots with a descent rate of 12 fps.

The Peregrine



Specs	
TOGW (lbs)	55,000
Capacity	49 pax+ 3 crew
T/W	0.335
Main Engines	2 x GE CF34-3 turbofan (9,220 lb.)
Main Engine High Lift System	External Blowing Double Slotted Flaps
Auxiliary Engines	2 x Rolls Royce Model 250-C40B Turboprop (715 hp)
Auxiliary Engine High Lift System	Internal Blowing Double Slotted Flaps
Wind Area (sq. ft.)	1080
Aspect Ratio	10.11
Span (ft.)	103.7
Length (ft.)	87.2
Primary Mission BFL (ft.)	1016
Primary Mission Takeoff Distance (ft.)	846
Primary Mission Landing Distance (ft.)	852
Secondary Mission Additional Missions	Wildfire Support Air Ambulance Combat Air Transport Emergency Evacuation
Secondary/Additional Mission BFL (ft.)	1244
Secondary/Additional Mission Takeoff Distance (ft.)	1018
Secondary/Additional Mission Landing Distance (ft.)	1145
Structural Makeup	80% Composite, Primarily CFRP and GLARE 20% Aluminum and Titanium
Airfoil	Supercritical (max t/c=.14)
CL-MAX	8.75
Stall Speed (kts.)	52
Engine Out Stall Speed (kts.)	65
Static Stability (%)	9 - 14 in normal operations



RFP Data Requirements	Report Location
1. Justify the final design and describe in detail the technologies and technical approach used to meet the mission requirements.	Throughout report
2. Provide carpet plots used to optimize the final selected design.	Figure 3.2 , pg 9
3. Include a dimensioned 3-view general arrangement drawing.	Foldout 3 , pg 15
4. Include an inboard profile showing the general internal arrangement.	Foldout 2 , pg 14
5. Include an illustrated description of the primary load bearing airframe structure and state rationale for material selection.	Foldouts 4 & 5 , pgs 30 & 40
6. Include a V-n diagram.	Figure 6.1 , pg 33
7. Show an estimated drag build up and drag polar for the cruise configuration, the takeoff configuration and the landing configuration.	Figures 4.8-4.10 , pgs 22-23
8. Show a weight breakdown of major components and systems, and center of gravity travel.	Table 3.1 , pg 10, Figure 3.3 , pg 11
9. Provide performance estimates and demonstrate aircraft stability for all flight and loading conditions.	Chapter 8 , pgs 59-66 Chapter 9 , pgs 67-72
10. Describe any advanced technologies and their relative benefits as used to obtain performance improvements.	Sections 5.3-5.5 , pgs 26-29
11. Provide flyaway cost and direct operating cost plus interest (DOC+I) estimates for a production runs of 150, 500, and 1500 aircraft. Increments to flyaway and direct operating costs plus interest incurred for including Homeland Security mission capability will need to be identified.	Section 10.4 , pg 76 Section 11.4 , pg 80 Section 11.7 , pg 82



Table of Contents

Executive Summary	iii
Multiple Missions.....	iii
Powered Lift.....	iii
Landing Conditions.....	iv
RFP Data Requirements	vi
List of Foldouts	ix
List of Figures	ix
List of Tables	x
List of Symbols	xi
Chapter 1: Introduction, Problem Statement and RFP Analysis	1
1.1 Introduction.....	1
1.2 Opportunity Statement.....	1
1.3 RFP Analysis.....	1
Chapter 2: Introduction of Concepts	3
2.1 Peregrine.....	3
2.2 X-03.....	5
2.3 Decision.....	6
Chapter 3: Peregrine Configuration Design Description	8
3.1 Constraint Diagrams and Sizing.....	8
3.2 Weights.....	10
3.3 Internal Arrangement.....	11
Chapter 4: Aerodynamics	17
4.1 High-Lift Technologies.....	17
4.2 Airfoil Selection.....	18
4.3 Lifting Capabilities.....	20
4.4 Drag Analysis.....	21
Chapter 5: Propulsion and Powered Lift	24
5.1 Introduction.....	24
5.2 Main Engine Selection.....	25
5.3 Powered Lift: External Blowing-Main Engines.....	26
5.4 Powered Lift: Internal Blowing-Auxiliary Engines.....	27
5.5 Benefits of the Auxiliary Fans.....	29
5.6 Take-off Analysis.....	30
5.7 Landing Analysis.....	31
5.8 Engine Out Landing.....	31
Chapter 6: Structures	32
6.1 Loads.....	32
6.2 Material Selection.....	34
6.3 Structural Concept.....	38
Chapter 7: Systems	43
7.1 Electrical System.....	43
7.2 Auxiliary/Emergency Power.....	44
7.3 Air Management System.....	45
7.4 Hydraulics.....	45
7.5 Avionics.....	47
7.6 Automatic Flight Control System.....	48
7.7 Fuel System.....	48
7.8 Emergency Exits and Escapes.....	50
7.9 Water and Waste System.....	51
7.10 Noise Reduction.....	51
7.11 Landing Gear.....	54



Chapter 8: Stability and Control	59
8.1 Analysis Method.....	59
8.2 Trim.....	61
8.3 Crosswind/Tailwind	62
8.4 Engine Out	63
8.5 SNI Landing.....	63
8.6 Dynamic Response	65
Chapter 9: Mission Performance	67
9.1 Primary Mission	67
9.1.1 Take-Off Analysis	67
9.1.2 Landing Analysis.....	68
9.2 Secondary Mission	70
9.2.1 Landing Analysis.....	71
Chapter 10: Conversion Configuration	73
10.1 Baseline.....	73
10.2 Additional Components.....	73
10.3 Multiple Mission Configuration	75
10.4 Cost Difference.....	76
Chapter 11: Cost	77
11.1 Research, Development, Test & Evaluation.....	77
11.2 Manufacturing	79
11.3 Acquisition.....	80
11.4 Direct Operating Cost.....	80
11.5 Disposal	81
11.6 Life Cycle Cost.....	81
11.7 Flyaway Cost.....	82
Chapter 12: Conclusion	84
Appendix A: CF34 Engine Decks	85
References	86



List of Foldouts

Foldout 1: The Peregrine with key specifications and features listed	v
Foldout 2: Inboard Profile	14
Foldout 3: 3-view General Arrangement	15
Foldout 4: 3-view Structural Layout	39
Foldout 5: Peregrine 3-D Structural Layout	40

List of Figures

Figure 1.1 Primary Mission Profile	2
Figure 1.2 Secondary Mission Profile	2
Figure 2.1 Peregrine Concept	4
Figure 2.2 X-03 Concept	6
Figure 3.1 Constraint Diagram	8
Figure 3.2 Peregrine Weight Carpet Plot	9
Figure 3.3 Weight-CG Excursion Diagram	11
Figure 3.4 Peregrine General Cross Section	12
Figure 3.5 Future Growth	16
Figure 4.1 Planform Diagram of Wing	17
Figure 4.2 Externally Blown Double-Slotted Flap Arrangement	18
Figure 4.3 Internally Blown Double-Slotted Flap Arrangement	18
Figure 4.4 NACA 23012 at Cruise C_L	19
Figure 4.5 Supercritical at Cruise C_L	19
Figure 4.6 2-D Lift Coefficient	20
Figure 4.7 3-D Lift Coefficient	21
Figure 4.8 Peregrine Drag Polar for Take-Off	22
Figure 4.9 Peregrine Drag Polar for Cruise	23
Figure 4.10 Peregrine Drag Polar for Landing	23
Figure 5.1 Propulsion and Hybrid Powered Lift Configuration	24
Figure 5.2 Engine Nacelle for the CF34-3 Turbofan Engine	25
Figure 5.3 Installation of Active Core Exhaust (Ref. 11)	26
Figure 5.4 Externally Blown Flap Configuration with the CF34-3 Turbofan Engine	26
Figure 5.5 Rolls Royce Model 250-C40B Turboprop Engine (Ref. 13)	27
Figure 5.6: Installation of Auxiliary Fan Assembly with the Wing and Inboard Trailing Edge Flaps	28
Figure 5.7 Model 250 Turboprop Shafted to the High Efficiency Fan, with Extended Compressor Inlet Duct and Exhaust Duct	29
Figure 5.8 Installation of Auxiliary Fan with Ducting Highlighted	29
Figure 6.1 The Maneuver and Gust V-n Diagram for the Peregrine at TOGW at Sea Level	33
Figure 6.2 Comparison of Fatigue Resistance and Mechanical Strength of CFRP with Other Structural Composites and Metals	36
Figure 6.3 ACE Implementation Reduces Thermal Loading on Flaps	37
Figure 6.4 Comparison of Thermal Characteristics of CFRP and Other Materials	38
Figure 6.5 Bulkhead-Wing Box Integration	41
Figure 6.6 Location of Peregrine’s Main Landing Gear Mounts	42
Figure 7.1 Peregrine’s Integrated Electrical System	43
Figure 7.2 Electro-Hydrostatic Actuator (EHA) Operating Diagram	46
Figure 7.3 Messier-Bugatti Pump for Flight Control EHA	47
Figure 7.4 Fuel System Layout and Survivability Features	50
Figure 7.5 Emergency Exit Provisions for the Peregrine	51
Figure 7.6 FAR §36 Noise Requirements Applicable to Peregrine	52
Figure 7.7 Active Tuned Vibration Attenuator (ATVN), Decreases Airframe Vibration and Cabin Noise	53
Figure 7.8 GE CF34 Experiences 2.5 EPNdB Noise Reduction Using “Chevron” Nozzle	54
Figure 7.9 Peregrine Landing Gear Geometry	55



Figure 7.10 Peregrine Landing Gear Kinematics	57
Figure 7.11 Peregrine's Landing Gear Blister	57
Figure 8.1 Horizontal Tail Constraint Diagram (X-plot)	60
Figure 8.2 Pitching Moments for Various Flight Conditions	62
Figure 8.3 SNI Landing Conditions	64
Figure 8.4 SNI Landing & Engine Out Conditions	64
Figure 8.5 Time History of Aircraft	65
Figure 9. 1 Primary Mission	69
Figure 9.2 Secondary Mission	72
Figure 10.1 Secondary Mission Configuration	75
Figure 11.1 RDT&E Cost Breakdown	78
Figure 11.2 Flight Test of Aircraft Breakdown	79
Figure 11.3 Direct Operating Cost	81
Figure 11.4 Estimated Unit Price per Plane	82
Figure A.1: CF34 Turbofan Engine Performance Charts for Maximum Thrust Setting	85
Figure A.2: CF34 Turbofan Engine Performance Charts for Minimum Thrust Setting	85

List of Tables

Table 2.1 Comparator Aircraft	3
Table 2.2 2-D Lift Coefficients for Various High Lift Systems	3
Table 2.3 Peregrine PRO/CON Chart	4
Table 2.4 X-03 PRO/CON Chart	5
Table 2.5 Decision Matrix	7
Table 3.1 Weights and Centers of Gravity	10
Table 4.1 Component Contribution to C_{D0}	22
Table 5.1 Benefits of the Hybrid Lift System: Auxiliary Fan Concept vs. Two Engine Configuration	30
Table 5.2 Engine Out Landing Analysis at 5,000 ft. Altitude	31
Table 6.1 Conventional vs. Composite Aileron on L-1011	34
Table 6.2 Composites Used in Commercial Aircraft	35
Table 6.3 Peregrine Material Locations	36
Table 7.1 Aircraft Sub-Systems Requiring Electrical Support	44
Table 7.2 Electro-Hydrostatic Actuation Applications	45
Table 7.3 Allowable Tire Pressures for Various Surfaces	56
Table 7.4 Peregrine Tire Specifications	56
Table 8.1 J-Kay VLM Program Results	61
Table 8.2 Stability Parameters	65
Table 8.3 Time to Bank	66
Table 9.1 Normal Take-Off	68
Table 9.2 One Engine Inoperable	68
Table 9.3 Landing Analysis	68
Table 9.4 Secondary Normal Take-Off	70
Table 9.5 Secondary One Engine Inoperable	71
Table 9.6 Secondary Landing	71
Table 10.1 Subsidized Flyaway Cost	76
Table 10.2 Subsidized Direct Operating Cost plus Interest	76
Table 11.1 RDT&E Cost Breakdown	77
Table 11.2 Flight Test Cost (RDT&E)	78
Table 11.3 Manufacturing Cost Breakdown	80
Table 11.4 Total Price	82
Table 11.5 Price Comparison	83



List of Symbols

α = angle of attack
 A_b = ratio of primary jet area to nozzle area
AR = aspect ratio
 A_{db} = ratio of diffuser exit area to nozzle area
 β = sideslip angle
 C_D = drag coefficient
 C_{D0} = zero lift drag coefficient
 C_L = 3-D lift coefficient
 $C_{L\alpha}$ = lift curve slope
 C_{Lmax} = maximum lift coefficient
 C_{l_a} = roll moment due to aileron deflection derivative
 $C_{l\beta}$ = roll moment due to sideslip derivative
 C_{m_e} = pitch moment due to elevator deflection derivative
 C_{n_a} = yaw moment due to aileron deflection derivative
 $C_{n\beta}$ = yaw moment due to sideslip derivative
 C_{n_r} = yaw moment due to rudder deflection derivative
 C_{n_T} = yaw moment due to engine out derivative
 C_μ = momentum coefficient
 C_w = weight coefficient
 $C_{Y\beta}$ = side force due to sideslip derivative
 C_{Y_r} = side force due to rudder deflection derivative
 δ = deflection
 δ_a = aileron deflection angle
 δ_{flap} = flap deflection angle
 δ_r = rudder deflection angle
 e = wing efficiency
FAR = Federal Aviation Regulation
 L/D = lift to drag ratio
 T/W = thrust to weight ratio
 γ_{climb} = climb angle = $\sin^{-1}[T/W - 1/(L/D)]$
 γ_{min} = min. climb angle = 0.030 for a 4 engine configuration
 $G = \gamma_{climb} - \gamma_{min}$
 $h_{obstacle}$ = height of obstacle = 35 ft. for civilian aircraft
 Λ = wing sweep
 \dot{m}_{jet} = mass flow rate of jet exhaust
MAC = mean aerodynamic chord
OEI = One Engine Out
 $\sigma_{blowing}$ = blowing augmentation ratio
 ϕ = bank angle
 ρ = density
 ρ_{SL} = density at sea level
 q = dynamic pressure = $\frac{1}{2} \rho V_e^2$
 S = wing area
 S_{blown} = blown wing area
 S_{ref} = reference wing area
 σ = control effectiveness ratio
 $U = 0.01C_{Lmax} + 0.02$ for flaps in takeoff position
 V_e = free-stream velocity
 V_{jet} = jet exhaust velocity
 W/S = wing loading
 x_{cg} = location of center of gravity

Chapter 1: Introduction, Problem Statement and RFP Analysis

1.1 Introduction

This proposal presents a design that meets the requirements of the 2003/2004 AIAA Undergraduate Aircraft Design Competition RFP with an aircraft that is superior in both performance and cost. The Peregrine concept meets or exceeds all of the RFP requirements by providing an efficient multi-mission regional jet with ESTOL with capabilities.

1.2 Opportunity Statement

Many airports have excessive wait time for available runways resulting from the inability to handle arriving and departing aircraft capacity demands, leading to increased airport operating costs. This also decreases the number of daily flights and potential profits. Additionally, many runways go unused because they are not long enough to support current regional jet operations. To utilize these runways there exists a need for a regional jet that can take off and land in shorter distances. Finally, current regional jets are inflexible and lack multiple mission capabilities. In order to support the United States during times of national crisis, the government requires a fleet of regional jets capable of commercial operations as well as Homeland Disaster Response, Military Support and National Defense. The government will subsidize the additional cost required to develop an aircraft capable of performing these secondary missions.

The Peregrine meets the requirements of the RFP, allowing for the opportunity to increase the number of daily flights to current airports, to allow access to smaller airports that have been unable to support regional jet operations, and to provide an aircraft capable of supporting government funded relief missions.

1.3 RFP Analysis

During primary mission operation the aircraft must accommodate 49 passengers, 3 crewmembers and their baggage. The RFP requires a balanced field length of 2500 ft. on a hot day (95 °F) at sea level. Short takeoff and landing capabilities will be necessary to comply with this requirement dictating the use of high-lift systems. The aircraft must be capable of a maximum cruise speed of at least 400 knots with a block range of 1500 nmi. and FAR 121 reserves. The regional jet must be able to complete a spiral descending approach in IMC (Cat 3C) conditions and land at 65 kts with one engine out. These conditions further support the need for STOL capabilities, increased



control surface sizing for stability and the need for a heads-up display to aid in the inclement weather landing requirement.

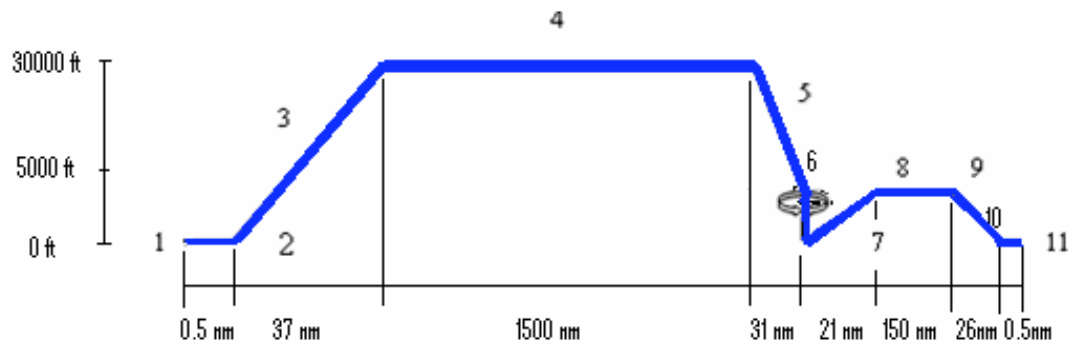


Figure 1.1 Primary Mission Profile

During secondary mission operation the aircraft must convert from its primary mission configuration to allow for 20 fire fighters, their equipment and 2000 lb. of fire suppressant. The RFP requires the aircraft to operate out of a balanced field length of 2000 ft. with 50 ft. obstacles, 250 ft. from either end of the runway at 5000 ft. MSL. The aircraft must be capable of a maximum cruise speed of at least 400 kts. with a range of 750 nmi. and is required to return to the start point minus the payload without refueling. It must land in a 25 kt. crosswind with a 5 kt. component tailwind. The government will subsidize the cost difference to convert the aircraft from its primary mission configuration to its secondary mission configuration.

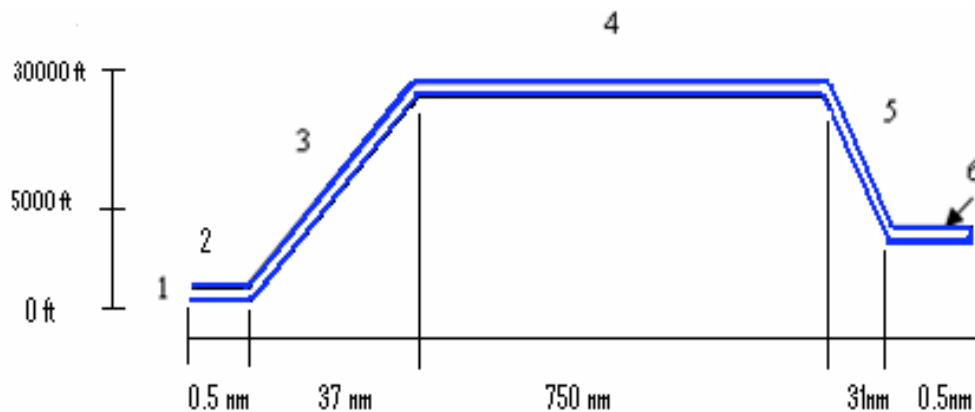


Figure 1.2 Secondary Mission Profile



Chapter 2: Introduction of Concepts

After analyzing the RFP it was necessary to research the capabilities of current regional jets in today's market. The ERJ-145 and the ATR-72 exhibit the basic characteristics of passenger capacity and takeoff gross weight required in the RFP. This provided an initial sizing estimate for developing concept aircraft. It is apparent from Table 2.1 that neither of these aircraft exhibit the required STOL capabilities. Therefore, it was decided to integrate powered lift into the concept aircraft. Although the ATR-72 can operate from unprepared runways, neither comparator aircraft can perform the required secondary mission. This led to the development of two, initial concepts, the Peregrine and the X-03.

Table 2.1 Comparator Aircraft

	ERJ-145	ATR-72
PAX	50	66
TOGW (lbs)	48,500	49,000
T/W	0.290	0.368
BFL (ft)	7,448	4,019

2.1 Peregrine

The Peregrine utilizes a hybrid, powered lift system integrating two main thrusting engines and two auxiliary turboprop engines. The main engines produce lift through an externally blown flap arrangement. The auxiliary engines are mounted next to the fuselage, under the wing root and produce additional lift through internal blowing. The Peregrine's auxiliary engines were an attractive feature based on historical data indicating that the highest lift coefficients were obtained from internally blown flap systems. Table 2.2 compares a variety of high lift systems.

Table 2.2 2-D Lift Coefficients for Various High Lift Systems
(Adapted from Advanced Topics in Aerodynamics, Ref. 1)

System	CL	Cl_{max}
Internally Blown Flap	4 ÷ 9	9
Upper Surface Blowing	4 ÷ 8	8
Externally Blown Flap	5 ÷ 7	7
Augmentor Flap	4 ÷ 7	7



To ensure efficient mission conversion the main cabin is outfitted with quick-release seats that are easily removable to accommodate firemen, military response teams and medical personnel. To further assist with the additional missions, the auxiliary engines can be used as power sources for medical equipment and other necessary devices. The PRO/CON chart in Table 2.2 provides an efficient means of determining the advantages and disadvantages of the Peregrine concept. A 3-View schematic is shown in Figure 2.1.

Table 2.3 Peregrine PRO/CON Chart

PRO	CON
<ul style="list-style-type: none"> • Short BFL and Takeoff/Landing Distance • Fuel Efficient • Cost Efficient • Multiple Mission Capability • Rapid Additional Mission Conversion • Safe Operation with Engine Out • Relatively Light Weight 	<ul style="list-style-type: none"> • High Drag • Complex Lifting System • Fire Suppressant Loading System

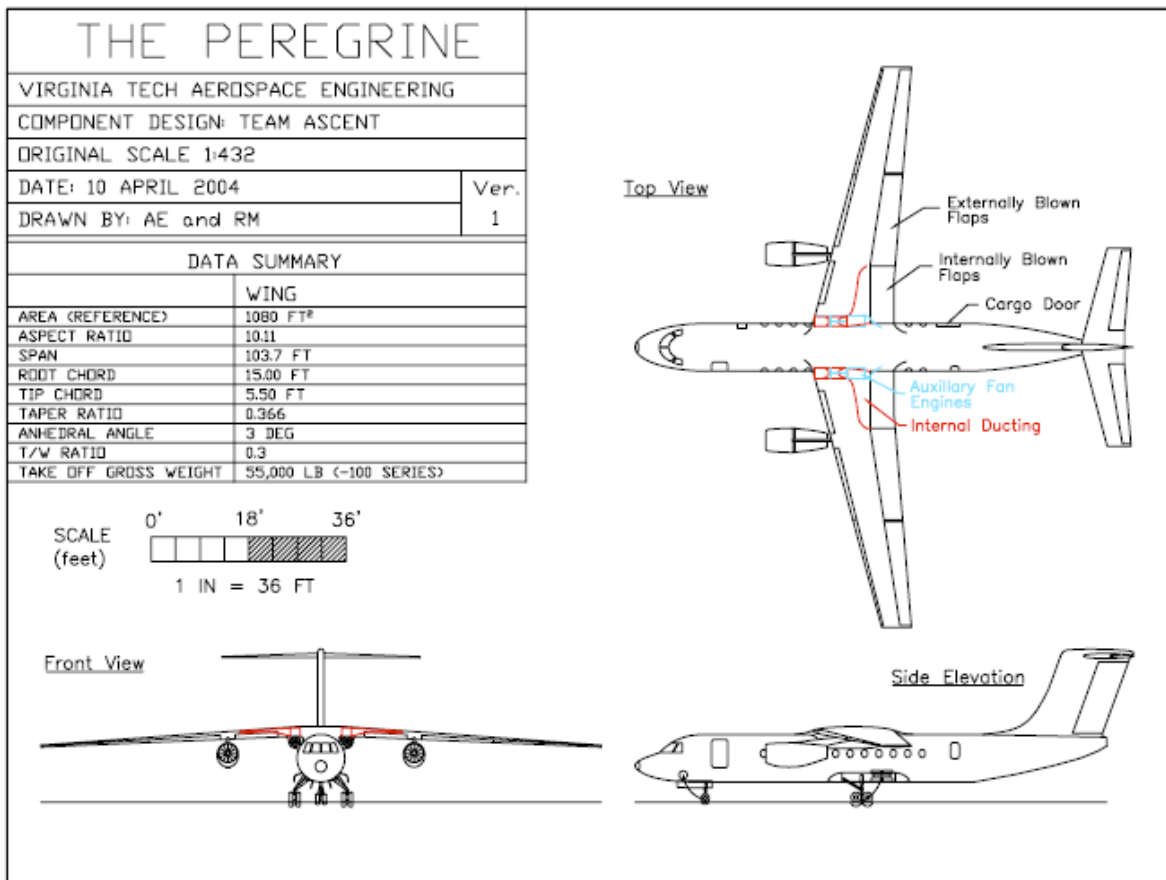


Figure 2.1 Peregrine Concept



2.2 X-03

To meet the necessary STOL requirements the X-03 incorporates two advanced technologies in a four engine configuration. The outboard engines are integrated into an externally blown flap arrangement and the inboard engines will use vectored thrust for take off and landing enabling STOL capabilities. To further enhance the aircraft's performance, winglets were added to effectively increase the wingspan. To ensure efficient additional mission conversion, the main cabin is outfitted with quick-release seats that are easily removable to accommodate firemen, military response teams and medical personnel. The PRO/CON chart in Table 2.3 provides an efficient means of determining the advantages and disadvantages of the X-03 concept. A 3-View schematic is shown in Figure 2.2.

Table 2.4 X-03 PRO/CON Chart

PRO	CON
<ul style="list-style-type: none">• Short BFL and Takeoff/Landing Distance• Multiple Mission Capability• Rapid Additional Mission Conversion• Excess Reserve Thrust	<ul style="list-style-type: none">• Complex Lifting System• Hot Gas Ingestion• Additional Pilot Training• Engine Out Stability• Cost• Weight• Fire Suppressant Loading System

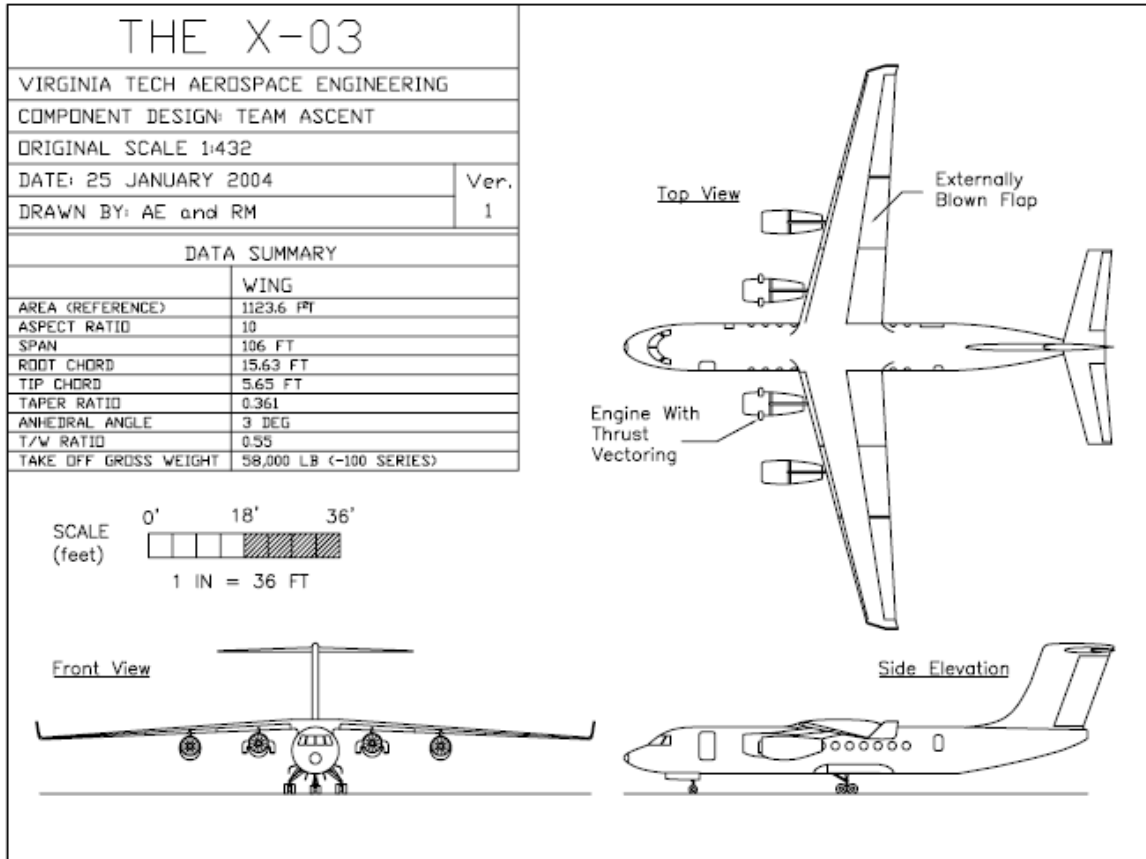


Figure 2.2 X-03 Concept

2.3 Decision

The Peregrine produces the greatest lift through a light-weight, low cost, fuel efficient design. The addition of an internally blown flap lifting system enables the Peregrine to perform ESTOL operations and maintain engine out stability. The X-03 is more prone to engine failure and instability during engine out situations. During STOL operations, the induced ground vortices cause recirculation of the exhaust leading to less thrust and ultimately, compressor stall. The four-engine configuration is heavier, more expensive and less fuel efficient.

These issues combined with the concerns addressed in the PRO/CON charts have been compiled in a decision matrix in Table 2.1. This matrix provides a weighted system comparing key aircraft parameters that fulfill the RFP. Each aircraft parameter was graded on a scale of 1-10 and multiplied by a scaling factor from 1-3.



Table 2.5 Decision Matrix

	Scaling Factor	Peregrine	X-03	ERJ-145	ATR-72
TOGW	1	8	7	10	9
Cost	2	8	6	9	10
Safety	3	9	6	9	8
BFL	2	10	8	0	0
Cruise Speed	1	7	8	8	6
Range	1	8	8	8	8
Secondary Mission	2	9	9	0	5
Conversion	1	9	9	0	10
Total		113	96	71	87

The result of the decision matrix determined the optimal candidate to be developed in the preliminary design phase.

The Peregrine is clearly the best option to fulfill an airport adaptive regional transport role while augmenting homeland security.



Chapter 3: Peregrine Configuration Design Description

3.1 Constraint Diagrams and Sizing

To provide an initial sizing with a range of required capabilities, a feasible design space needs to be determined with respect to T/W and W/S . The constraints that define this space are dictated by the RFP and FAR Parts 25 and 36. This design considers the constraints: a take-off balance field length of 2,500 feet at an altitude of 5,000 feet on a hot day, an initial climb segment over a 50 foot obstacle at a climb gradient of 3.7 percent, a second segment climb gradient of 2.4 percent with OEI, a minimum max cruise speed of 400 knots (with T/W scaled from cruise altitude of 30,000 feet to sea level), and a stall speed of 52 knots. Equations adapted from Roskam (Ref. 2) take into account some approximate values, such as an AR of 10, a Mach of 0.7, a C_{D0} of 0.025, and a C_{Lmax} of 8.7, and an L/D max of 16. The results are plotted on a graph of T/W and W/S in Figure 3.1.

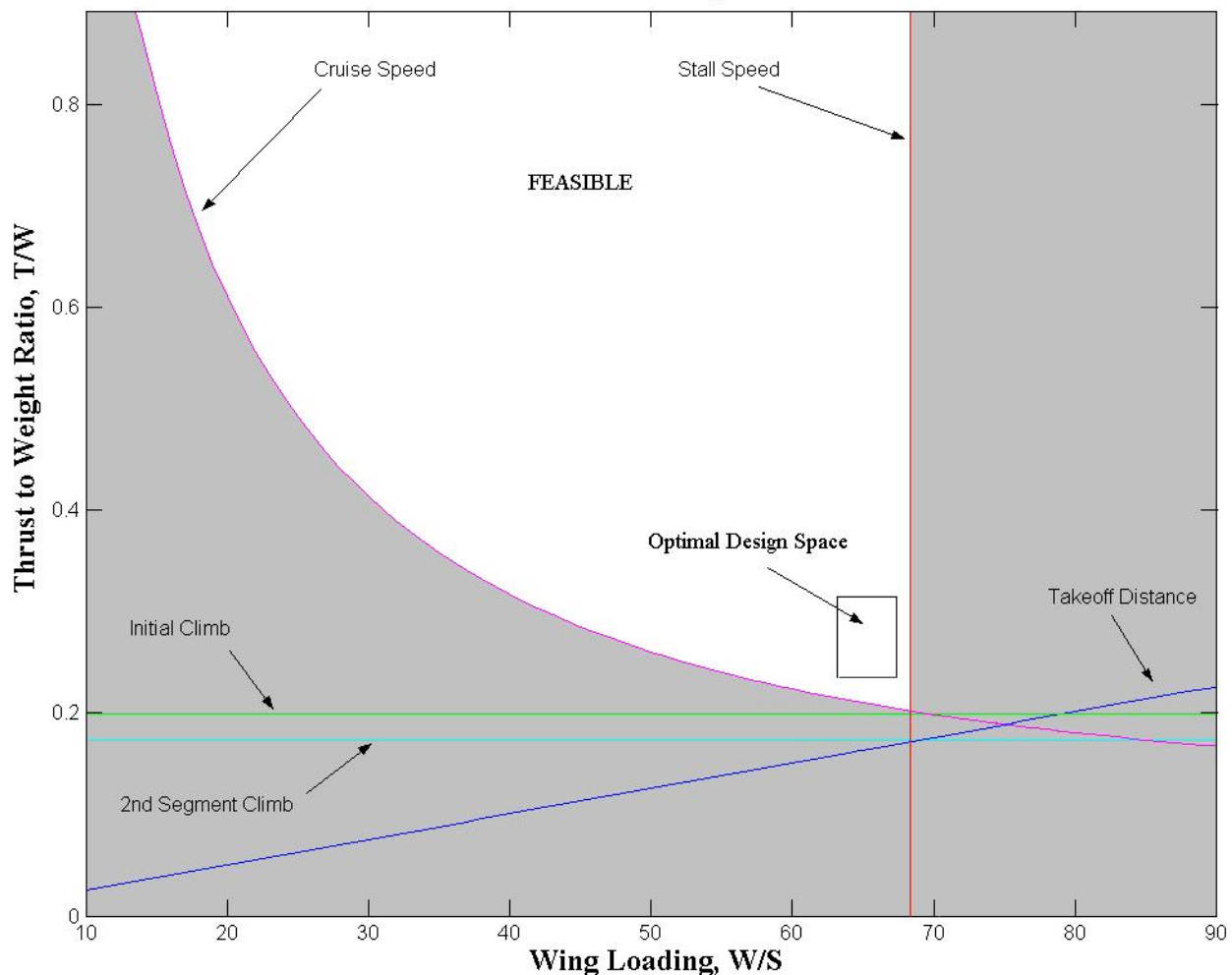


Figure 3.1 Constraint Diagram



The infeasible side of each constraint is shown by the grey area. The optimal region is defined here from comparator aircraft values. For this mission a T/W of between 0.3 to 0.4 should be sufficient and the W/S is then considered. A high W/S is required for a cruise efficient aircraft, while a low W/S is required for a low stall speed. To make a wise decision in designing a cost efficient and well performing aircraft, $TOGW$ needs to be considered as it varies with the constraints, T/W , and W/S . Using Raymer's method (Ref. 9), an iterative program was created in Matlab to show these variations. The output can be seen in Figure 3.2.

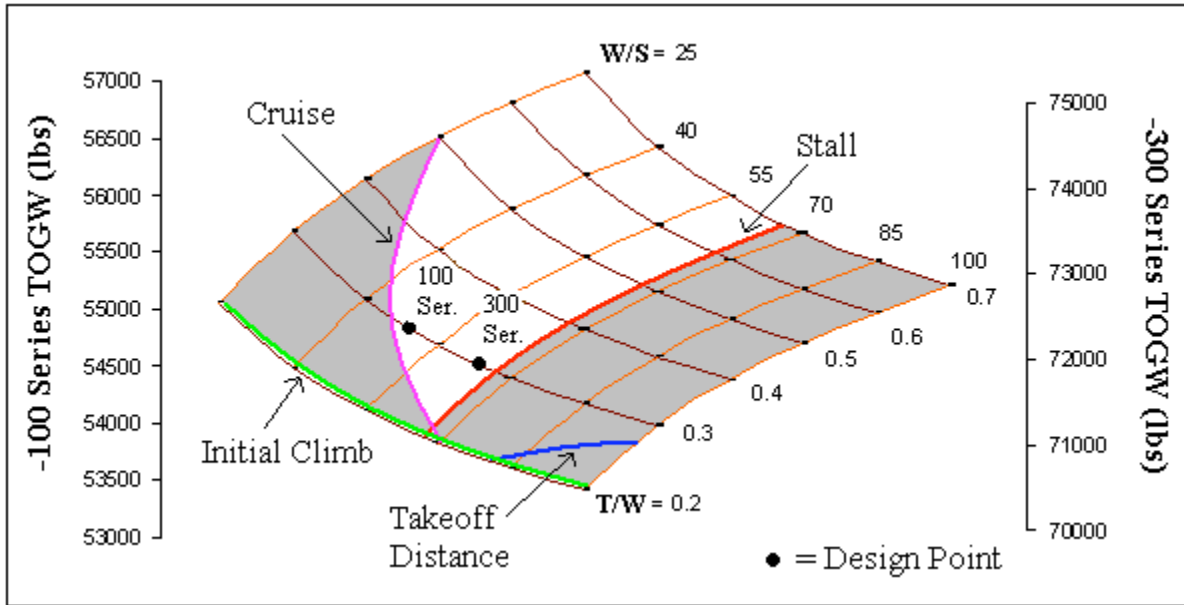


Figure 3.2 Peregrine Weight Carpet Plot

This figure shows that a higher wing loading will reduce the $TOGW$, which in turn will affect the cost. Another consideration in this design is to oversize the wing, which will reduce the manufacturing cost when future -200 and -300 family models are produced. Minimizing the $TOGW$, allowing for an oversized wing, and allowing a small factor of safety to ensure no constraints are violated due to future design changes, the T/W of 0.3 is supported. The W/S is found to be 66.6 for the approximately 72,000 pound -300 model while the W/S is now 50 for the 55,000 pound -100 model. This sizing gives an uncompromised -300 series and an effectively lower W/S for the -100 series, which will lower its cruise efficiency. However, the lower W/S will decrease future manufacturing costs and help to provide enhanced performance for take-off and landing, which are certainly drivers in the RFP. From the estimated weight, W/S , and chosen AR of 10, a common wing size is found. The wing area is 1080 ft.² with a span of 103 ft. 8in. and an average chord of 10 ft. 3in.



3.2 Weights

After determining an initial size for the aircraft concepts based on current regional jets and the RFP requirement to allow for 49 passengers plus 3 crewmembers and baggage, a refined take off gross weight was determined using the method in Roskam (Ref. 2). A MatLab computer code was written and, after employing an iterative process, an improved estimate of TOGW was determined to be 65,900 pounds. Although this sizing method was more accurate than the initial sizing, it required additional refinement.

After many design modifications a final TOGW was found using the method in Roskam (Ref. 3). After determining these weights, the center of gravity of each item was found using the method in Roskam (Ref. 4). This allowed for the calculation of the center of gravity travel of the Peregrine. Table 3.1 shows the aircraft's weight breakdown and the center of gravity of each item.

Table 3.1 Weights and Centers of Gravity

Component	Weight (lbs)	X-CG (in)	Y-CG (in)
Wing	6985	514.57	137.7875
Empennage	1430		
h.t.	723.6	1034.8	333.4
v.t.	382.4	821	234.8617
Fuselage	6490	510.2	88.56
Nacelles	1017.5	362.3	91.1409
Landing Gear	3850	507	26.725
Powerplant and inst.	5225	375	91.1409
Fixed Equipment	6820	531.5	81.36
Empty Weight, WE	31817.5		
Trapped Fuel and Oil (TFO)	275	531.5	134.7875
Fuel	11000	514.57	137.7875
Crew	600	96	81.36
Pax	9065	481.4	81.36
Baggage	2205	525.4	51.46
TOGW	54962.5		

*Note: All X-distances are measured from the tip of the fuselage
All Y-distances are measured from the ground

During regular aircraft operation $X\text{-CG}_{\text{MIN}} = 489.4$ in. (27.0% MAC). This center of gravity accounts for the aircraft operating weight empty and the weight of the crew. During regular aircraft operation $X\text{-CG}_{\text{MAX}} = 495.7$ in. (32.0% MAC). This center of gravity accounts for the aircraft operating weight empty, the weight of the crew and the fuel weight. Figure 3.3 is a weight-cg excursion diagram. The blue lines represent the center of gravity travel during normal aircraft operation. The red lines represent the center of gravity travel during extreme loading cases. The extreme $X\text{-CG}_{\text{MIN}}$ (17.2% MAC) occurs with the three crewmembers in the cockpit, the first three rows filled



with passengers with their baggage beneath them and the aircraft at operating weight empty. The extreme X-CG_{MAX} (41.2% MAC) occurs with two crewmembers in the cockpit, one crewmember in the tail cone, no passengers on board and the maximum allowable passenger baggage stored in the tail cone.

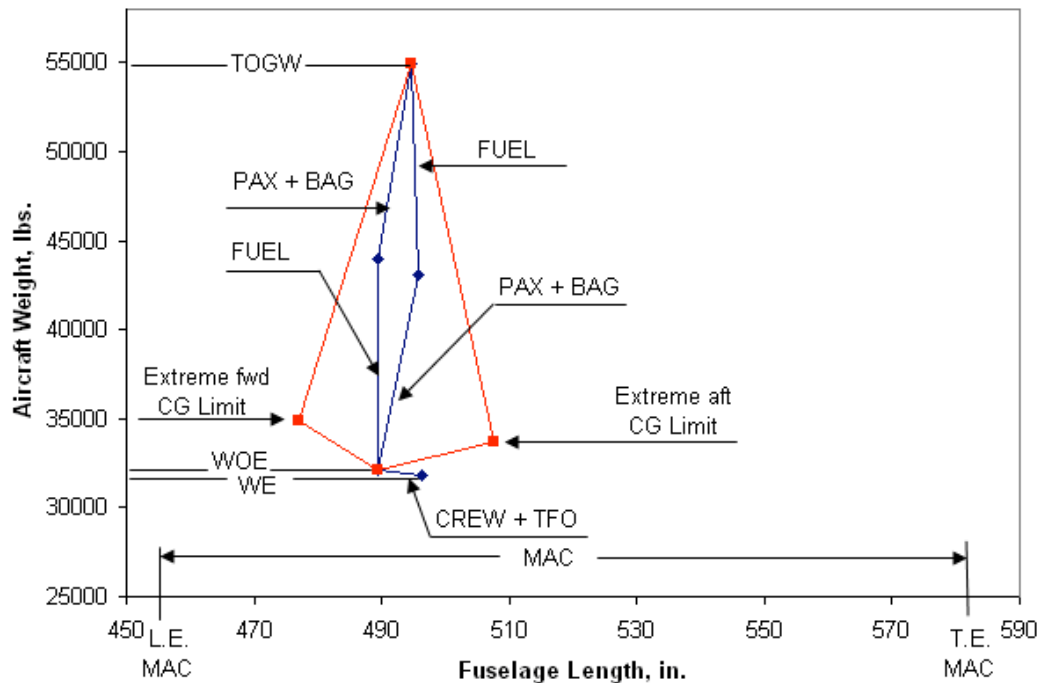


Figure 3.3 Weight-CG Excursion Diagram

3.3 Internal Arrangement

The internal arrangement was mostly dictated by the RFP, calling for a single class seating arrangement of 49 passengers at 230 lbs. each (including luggage) with 2 pilots and 1 flight attendant. The suggested seat pitch was 32 in., which seemed reasonable for passenger comfort. Before the fuselage could be laid out, the cross section had to be defined so that the length of the cabin could be determined. The shape of the fuselage cross section was chosen to be circular because of its strength, simplicity, and easy pressurization. To shorten the fuselage length, allow for more comfort in this and future models, and allowing more baggage area per unit length, a 4 abreast seating arrangement was chosen over a 3 abreast. Using the Bombardier CRJ-200 as a comparator aircraft due to its similarity in cross section geometry, the diameter was set at 8 ft. 10in. with a 4.21 in. wall thickness. The floor was shifted down from the center by 20 percent of the fuselage diameter to allow for an aisle height of approximately 6 ft., centered in the cross section. This height is reasonable when looking at comparator aircraft and larger passengers



should not experience much discomfort since the majority of every flight will be spent in the slightly wider than average regional jet seat width (by about 0.7 in.). FAR 25.815 states that for aircraft with 20+ passengers, the aisle must be at least 20 in. wide at a height 25 in. above the floor.

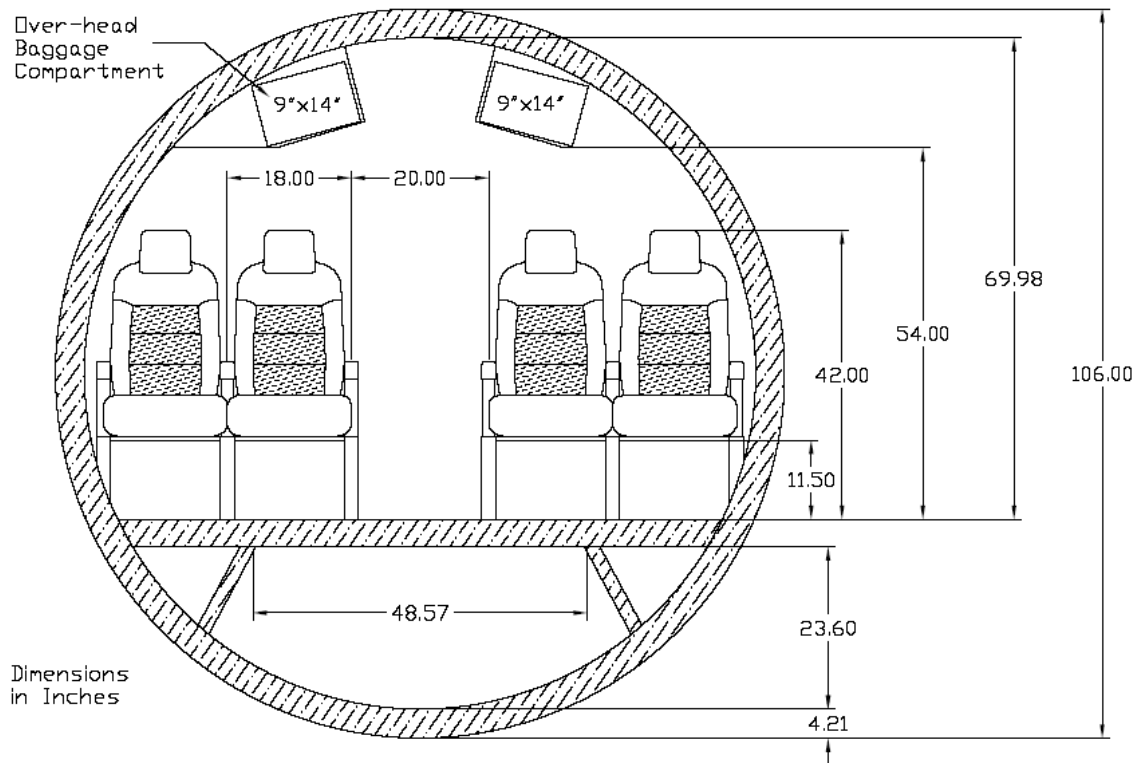


Figure 3.4 Peregrine General Cross Section

To accommodate 49 passengers using the 4 abreast configuration, 13 rows are used with 7 rows on the left and six on the right. There is a closet for passenger's coats and other belongings located across from the main aircraft entrance. The galley is 43 in. wide and located on the starboard side at the front of the aircraft next to service door. Across from the galley is the 38.8 in. by 45 in. lavatory. The single class seating is just aft of the galley and lavatory, giving a cabin length of 48 ft. A 52 in. x 52 in. cargo door is located on the right at the very rear of the cabin. This can be fully opened with top hinged gas springs allowing for an unimpeded path for loading equipment for the secondary mission (which will be discussed more in Chapter 10), or even a stretcher in the case the aircraft is being used as an air-ambulance (tertiary mission). The cargo door also has an option to fold the left half of the door down using bottom hinged gas springs to create an exit with its own stairway. A service door is located in the rear of the cabin, which allows authorized personnel to access the rear baggage compartment for increased aircraft



flexibility. FAR §25.807 requires 1 Type I and 1 Type III emergency exits on each side of the fuselage, which are sized to be at least 24 in. x 48 in. and 20 in. x 36 in. respectively. The main entrance was sized to be 36 in. x 72 in. After setting the cabin length, the rest of the fuselage needed to be established. A nose cone fineness of 1.5 and tail cone fineness of 2.8 allowed adequate room for the cockpit and rear baggage area while maintaining good aerodynamic qualities, such as helping to eliminate separation. The primary mission fuselage layout can be seen in the following inboard profile and is followed by the general arrangement three view drawing.

INBOARD PROFILE

VIRGINIA TECH AEROSPACE ENGINEERING

COMPONENT DESIGN: TEAM ASCENT

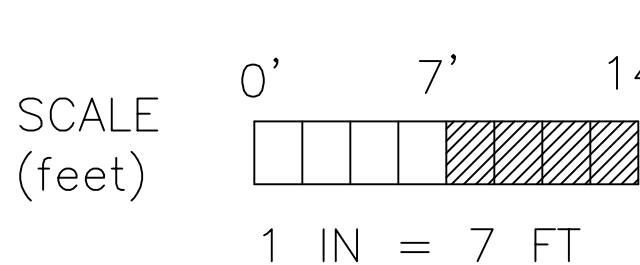
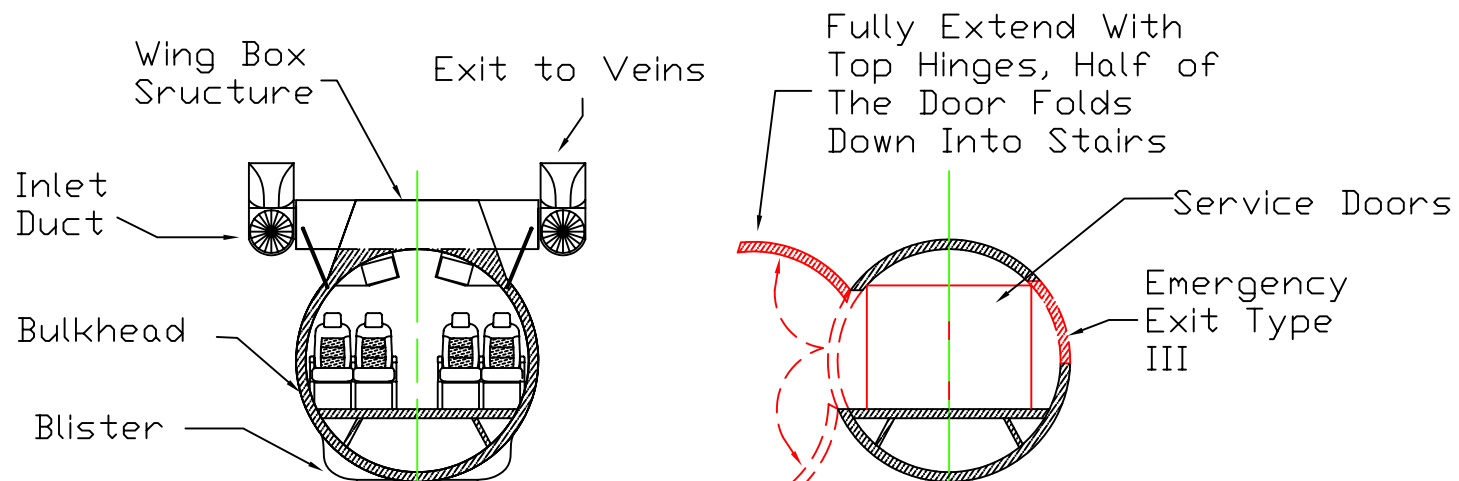
ORIGINAL SCALE 1:84

DATE: 10 APRIL 2004

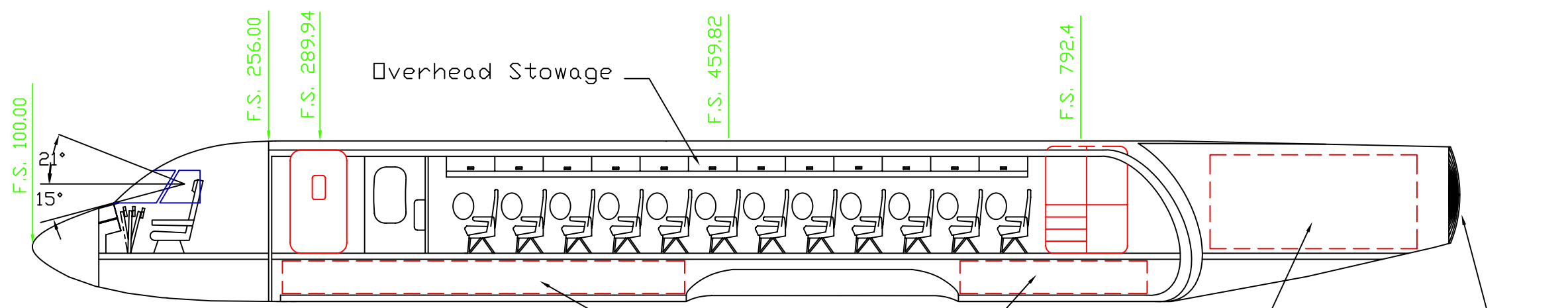
Ver.

DRAWN BY: AE and RM

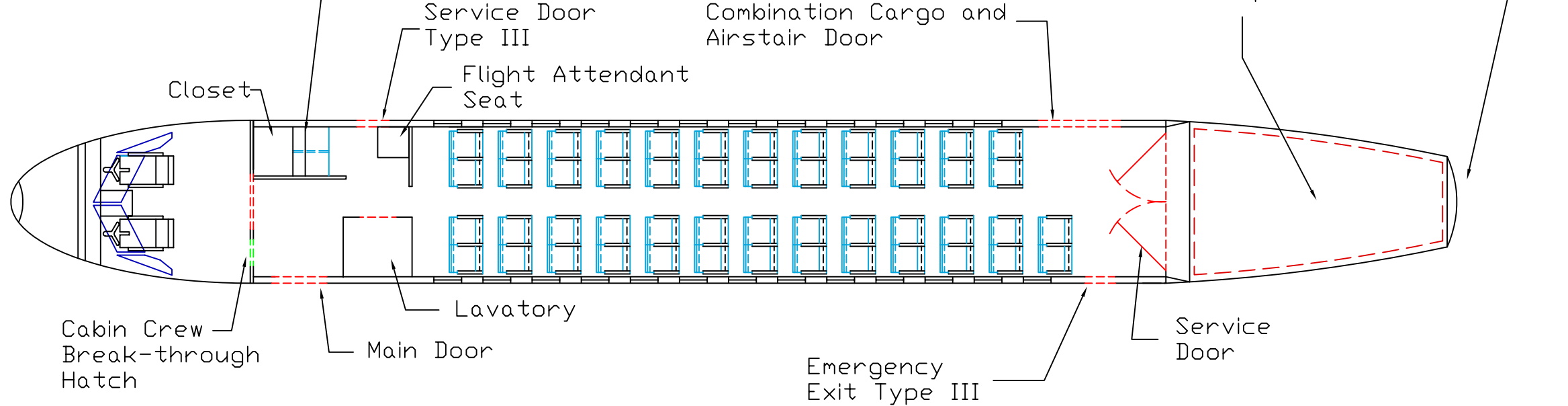
1



SIDE VIEW



TOP VIEW



PRODUCED BY AN AUTODESK EDUCATIONAL PRODUCT

PRODUCED BY AN AUTODESK EDUCATIONAL PRODUCT

THE PEREGRINE

VIRGINIA TECH AEROSPACE ENGINEERING

COMPONENT DESIGN: TEAM ASCENT

ORIGINAL SCALE 1:204

DATE: 10 APRIL 2004

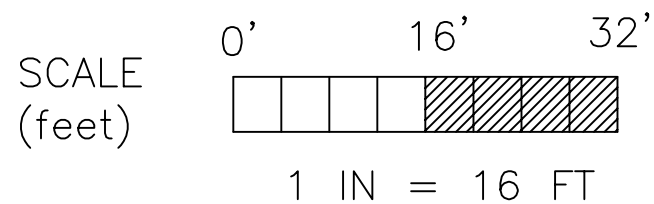
Ver.

DRAWN BY: AE and RM

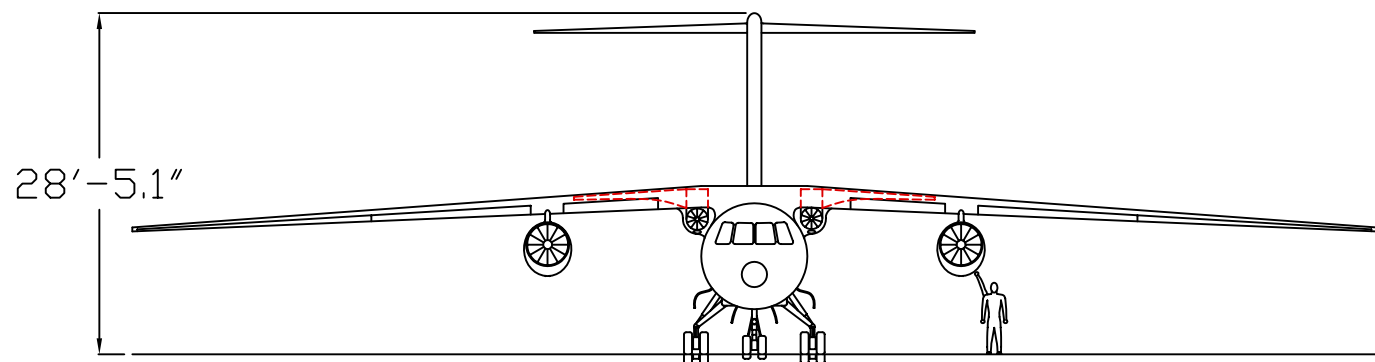
1

DATA SUMMARY

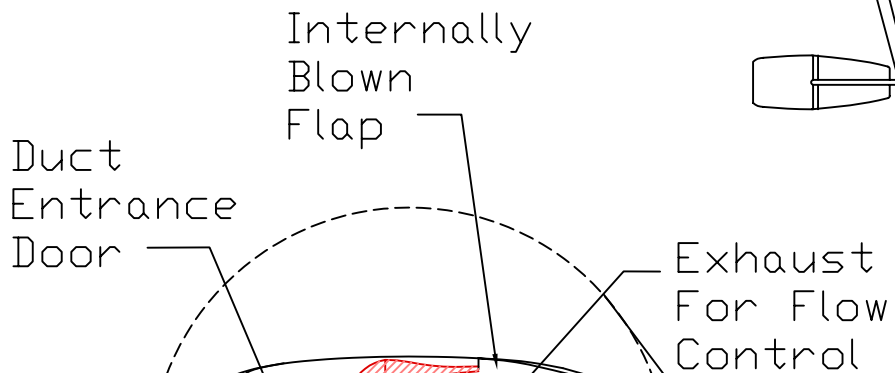
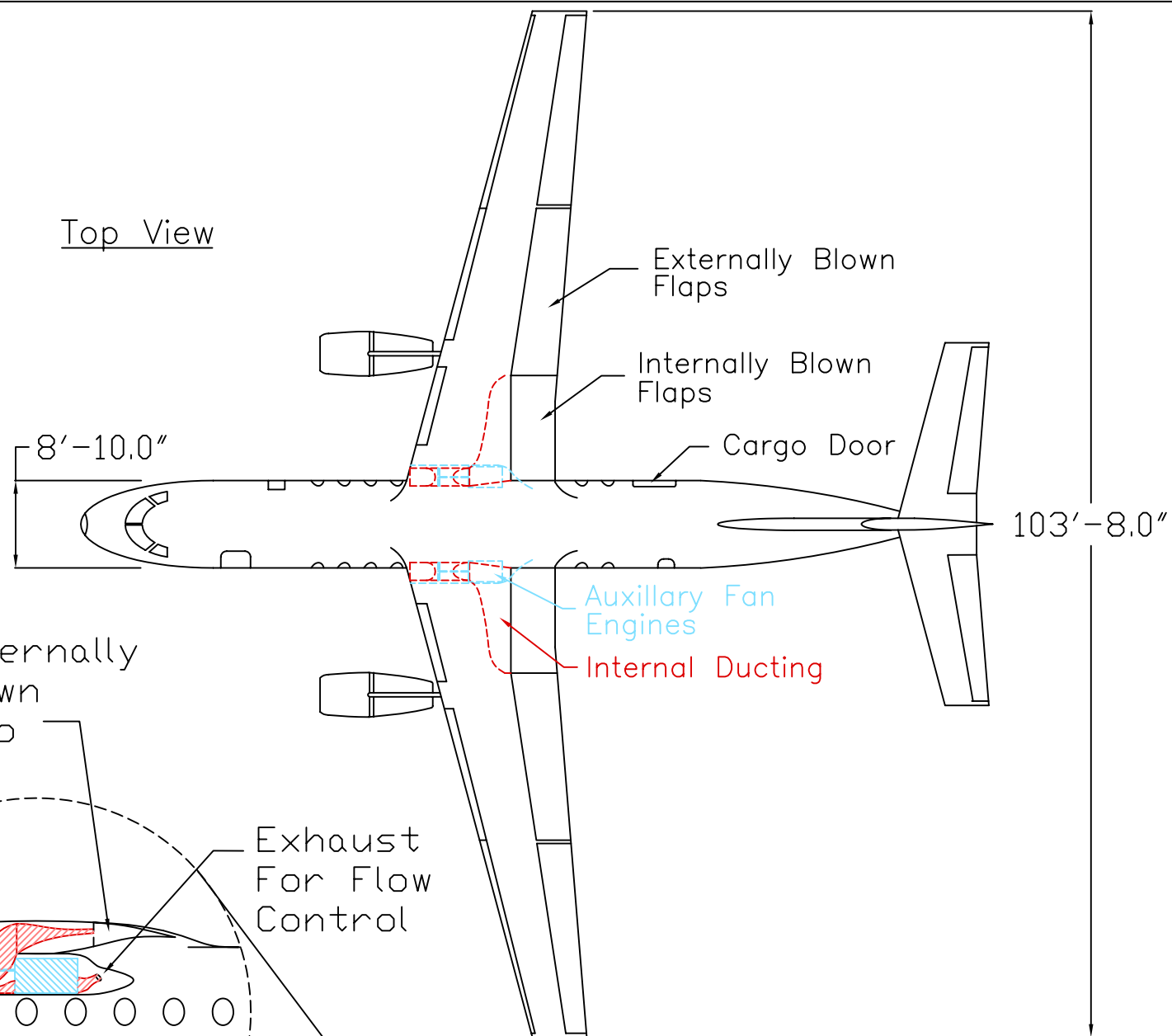
	WING	H TAIL	V TAIL
AREA (REFERENCE)	1080 FT ²	225.3 FT ²	215.5 FT ²
ASPECT RATIO	10.11	5.85	1.11
SPAN	103.7 FT	36.6 FT	16.1 FT
ROOT CHORD	15.00 FT	8.09 FT	16.16 FT
TIP CHORD	5.50 FT	4.42 FT	12.74 FT
TAPER RATIO	0.366	0.546	0.788
ANHEDRAL ANGLE	3 DEG	-	-
VOLUME COEFFICIENT	-	0.903	0.100
T/W RATIO	0.335		
TAKE OFF GROSS WEIGHT	55,000 LB (-100 SERIES)		



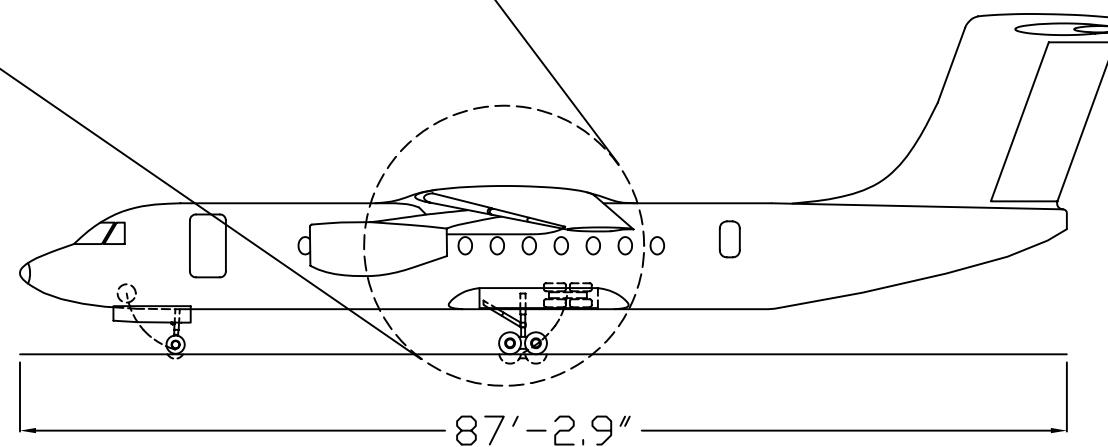
Front View



Top View



Side Elevation





During future growth, the fuselage will be extended evenly about the center of gravity with fuselage plugs to allow for 65 passengers (128 in. longer) in the -200 series and 81 passengers (256 in. longer) in the -300 series. The three different models in this series can be seen in Figure 3.5

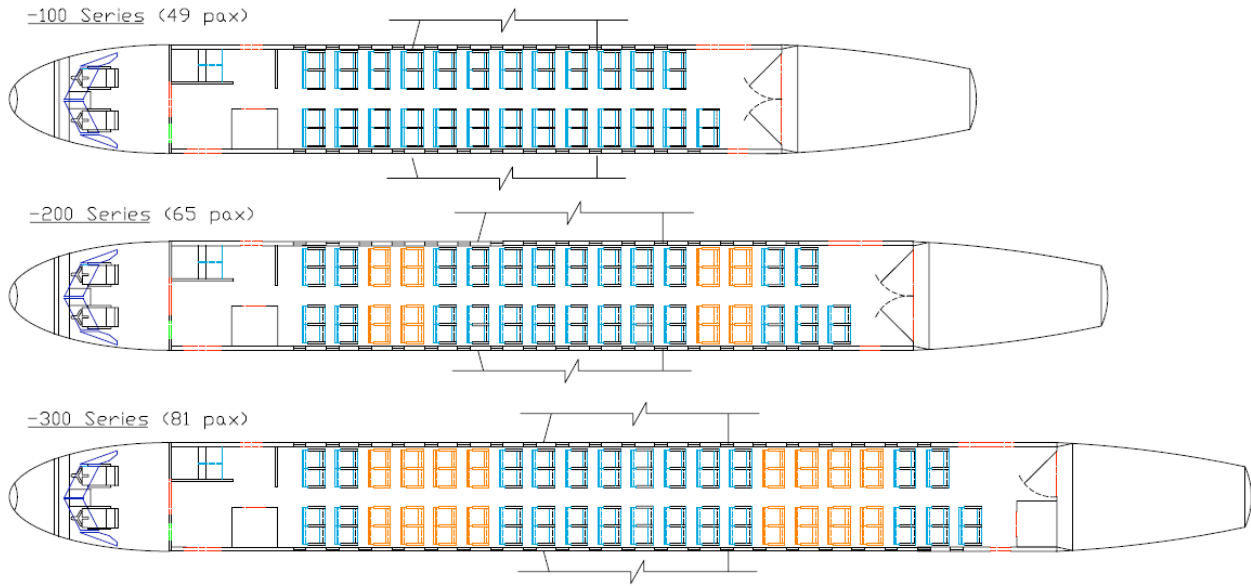


Figure 3.5 Future Growth

Baggage volume is another important aspect of regional transport jets, which needs to be evaluated here. Considering the space beneath the seats, in overhead compartments, and in the main baggage compartment under the cabin and in the tail cone, there is enough room for the required baggage. The total baggage volume is approximately 280 ft.³ After implementing a reasonable effective baggage volume of 85%, the new available volume is 238 ft.³ The average luggage weight for a mission is 2205 lbs. with a commercial luggage density of 12.5 lbs./ft.³. The average required volume is 176.4 ft.², leaving 35% more room for increased mission flexibility.



Chapter 4: Aerodynamics

The RFP presents the challenge to design a regional jet that can take-off and land within a balanced field length of 2,500ft. The landing sequence must involve a simultaneous non-interfering approach and spiral descent even with an engine out. The required maximum lift coefficient necessary to perform these maneuvers is 6.06. To achieve this lift coefficient a hybrid lifting system was implemented. Leading edge slots, trailing edge flaps and both internal and external blowing are all combined to meet and exceed the take-off and landing requirements. The main focus of the aerodynamic analysis that will be presented in the following section is; high lift devices, selection of the airfoil, C_L capabilities and drag behavior.

4.1 High-Lift Technologies

The STOL requirements laid out by the RFP necessitate innovative design. The Peregrine incorporates powered lift with a unique hybrid scheme in the form of external blowing supplied by the two main engines and internal blowing supplied by two small auxiliary engines mounted near the fuselage. Double-slotted flaps extend during take-off and landing and then are retracted when the auxiliary engines are turned off. This configuration allows for the achievement of ESTOL operations. Fig. 4.1 shows the planform area of the wing with flaps and engine location. Figures 4.2 and 4.3 depict the cross section of the externally and internally blown flaps respectively.

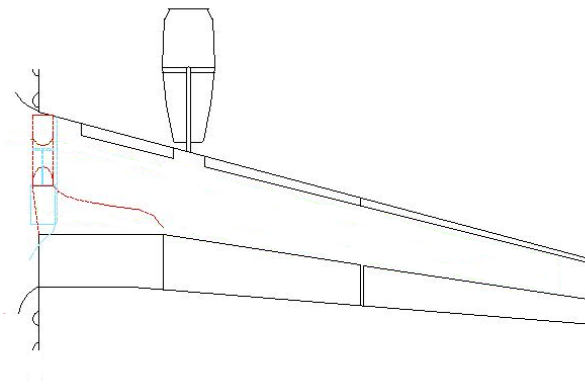


Figure 4.1 Planform Diagram of Wing

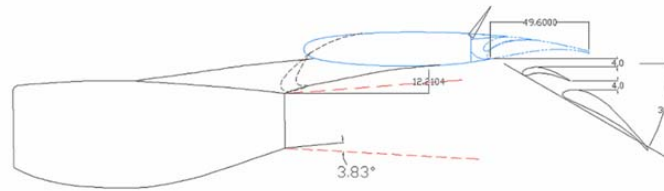


Figure 4.2 Externally Blown Double-Slotted Flap Arrangement

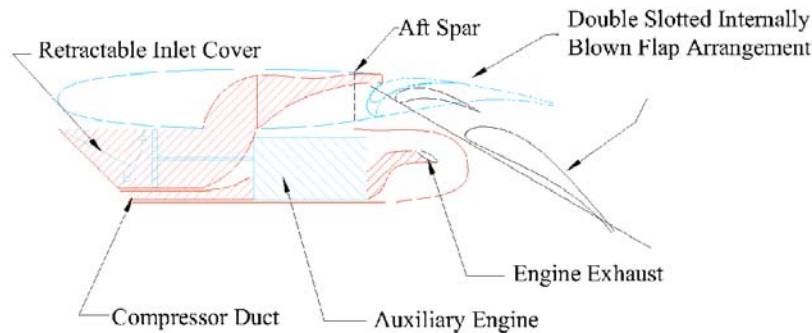


Figure 4.3 Internally Blown Double-Slotted Flap Arrangement

The flap dimensions for internal blowing are approximately 127 in. x 42 in. The flap dimensions for the externally blown configuration are 203 in. x 42 in. The flaps are double-slotted and deflected a maximum of 30° during take-off and landing.

4.2 Airfoil Selection

The first airfoil analyzed was the NACA 23012 because its two dimensional lift coefficients were among the highest of the NACA airfoils (Ref. 5). However, the Peregrine is required to fly at Mach 0.7. Accounting for the wing sweep of just 15°, the resultant Mach normal to the wing is 0.68 during cruise conditions. Because of the possibility of the flow over the wing entering the transonic region, a supercritical airfoil was analyzed. Supercritical airfoils are designed to reduce the shock strength and move the shock aft in transonic flight, thereby minimizing the region of separation. While decreasing the adverse affects in the transonic region, the supercritical airfoil maintains adequate lifting characteristics. The two airfoils were analyzed for inviscid flow using X-foil program (Ref. 6) at the cruise Reynolds number of 16×10^6 , the normal Mach of 0.68, and the cruise C_L of 0.285. The resulting pressure distributions of the NACA 23012 and the supercritical are shown in Figures 4.4 and 4.5 respectively.

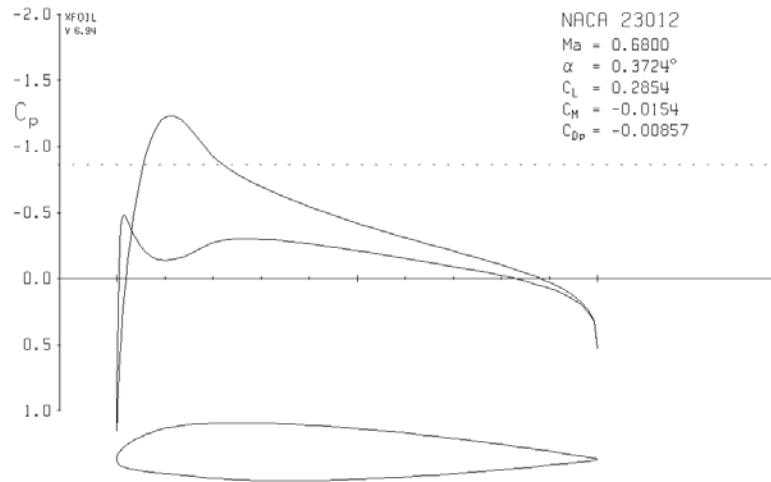


Figure 4.4 NACA 23012 at Cruise C_l

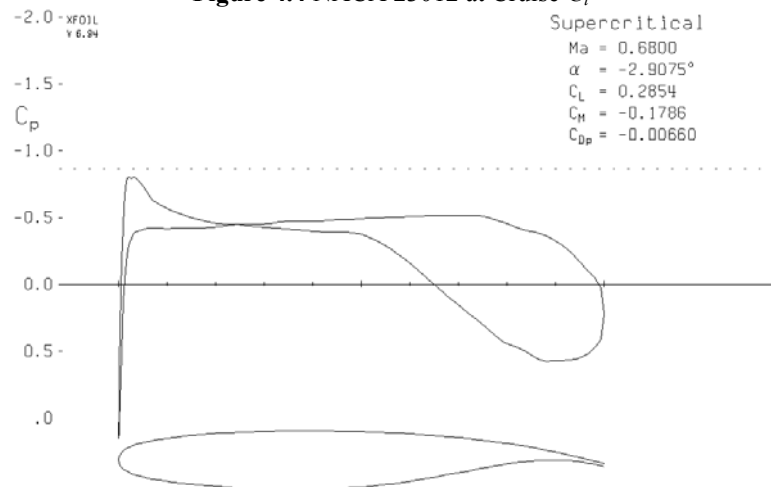


Figure 4.5 Supercritical at Cruise C_l

The supercritical airfoil has a quick recovery on the upper surface, before the point of maximum thickness, which delays separation and stall. The pressure gradient relaxes so as to delay separation. The rear camber creates additional lift that can be seen in the increased area of the rear section of the pressure distribution. The NACA 23012 has a widely distributed recovery region over a large percentage of the upper surface which thickens the boundary layer leading to early separation.

The final decision was to use the supercritical airfoil with a t/c of 0.14 occurring at 43% of the chord, a MAC of 10.608 ft and an aspect ratio of 10.1. The t/c was selected to be a bit larger than the optimum thickness ratio of 0.12 due to structural considerations in the wings.



4.3 Lifting Capabilities

In order to meet the additional missions, air ambulance to urban and rural areas, air transport to and from combat areas and emergency evacuation, it was necessary to achieve a shorter take off distance than was required for the primary mission. External blowing alone would not produce enough lift to meet these requirements, therefore, an additional source of lift was required. An internally blown flap arrangement was integrated into the Peregrine utilizing auxiliary engines and double-slotted flaps.

To determine the three-dimensional lift coefficient resulting from this configuration, a combination of methods and equations from Roskam (Ref. 5) and McCormick (Ref. 7) were used. From Roskam the two and three-dimensional lift coefficients for a clean wing were calculated, and then for flaps extended 30°. The equations for blown surfaces were used from McCormick and the C_l values were found using equations 4.2 – 4.4. These equations relied heavily on the blowing momentum coefficients of the engines, which are defined in equation 4.1.

$$C_{\mu} = \frac{\dot{m}_{jet} V_{jet}}{qS} \quad \text{Equation 4.1 (Ref. 7)}$$

$$C_l = C_{l_} + C_{l_} \quad \text{Equation 4.2 (Ref. 7)}$$

$$C_{l_} = 2\pi(1 + 0.151\sqrt{C_{\mu}} + 0.219C_{\mu}) \quad \text{Equation 4.3 (Ref. 7)}$$

$$C_{l_} = [4\pi C_{\mu} (1 + 0.151\sqrt{C_{\mu}} + 0.139C_{\mu})] - \quad \text{Equation 4.4 (Ref. 7)}$$

The contribution of each high lift device for two-dimensional lift coefficients is shown in Fig. 4.6.

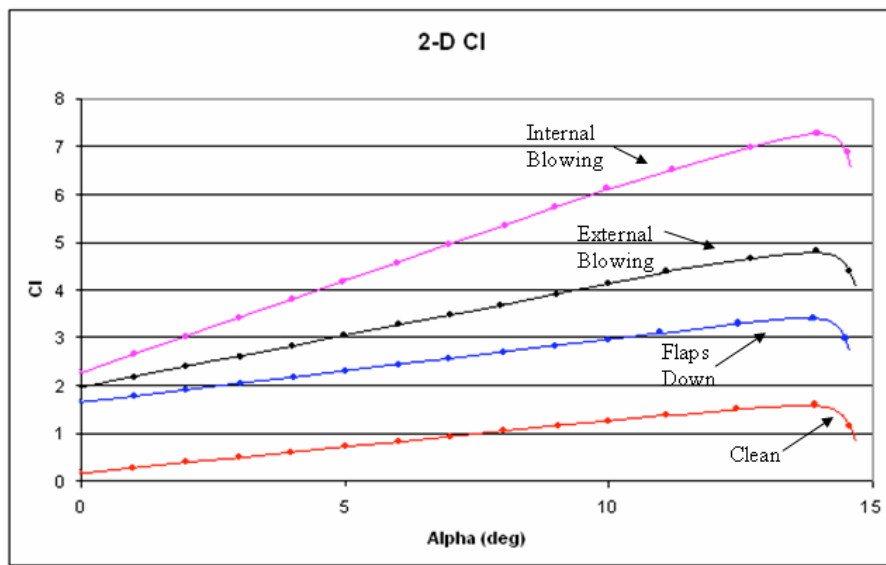


Figure 4.6 2-D Lift Coefficient



The results show the Peregrine wing divided into four 2-D sections; clean, flaps down, externally blown and internally blown. It is evident that the highest lift contribution comes from internal blowing which is explained by the high C_l achieved by the auxiliary engines. The 3-D lift coefficients were found using the calculated 2-D lift coefficients and the methods outlined in Roskam. Figure 4.7 shows the effects of flaps and blowing on the 3-D lift curve slope. Both Fig. 4.6 and 4.7 include an approximation for stall based on analysis of the wing in X-foil (Ref. 6). This is a conservative estimate because the blowing systems will delay separation during take-off and landing.

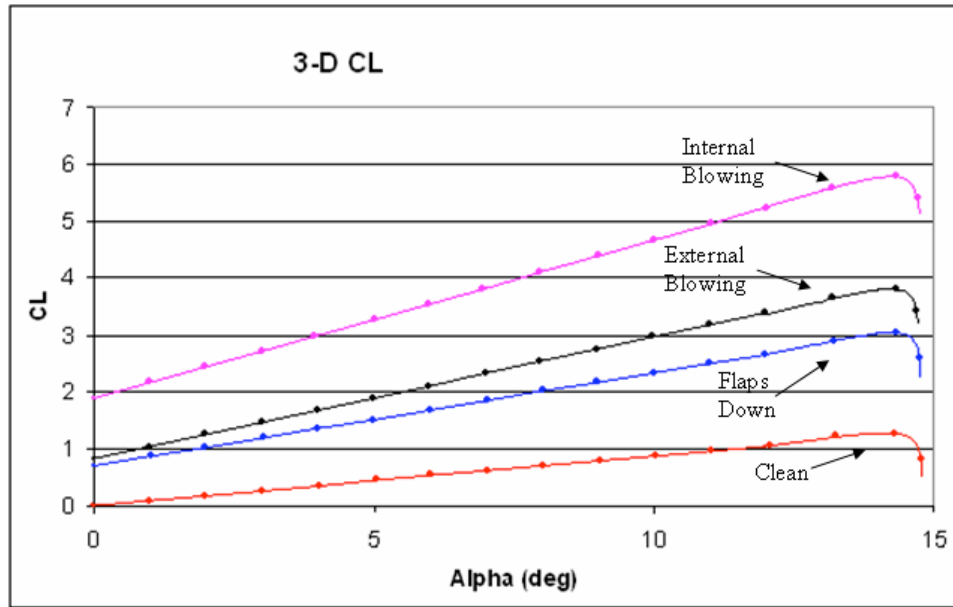


Figure 4.7 3-D Lift Coefficient

The resulting C_{Lmax} from the combination of all the high lift devices is 8.75. This lift coefficient allows for a margin of safety for engine out scenarios and provides the ESTOL capabilities necessary to complete the additional missions.

4.4 Drag Analysis

The Friction program (Ref. 8) was used to analyze the drag incurred by each of the major components of the aircraft during take-off, cruise and landing. The flow was assumed turbulent over the entire surface of the aircraft. The trim drag was determined using stability calculations and equations found in Raymer (Ref. 9). Table 4.1 shows the C_{D0} contribution of each component.



Table 4.1 Component Contribution to C_{D0}

Conditions	Takeoff	Cruise	Landing
Altitude	Sea-Level	30,000 ft.	5,000 ft
Flaps	30	0	30
Gear	Extended	Retracted	Extended
Flap Deflection	30°	0°	30°
Component C_{D0}			
Fuselage	0.00471	0.00384	0.00487
Wing	0.00822	0.00657	0.00854
Landing Gear	0.00423	0	0.00467
Landing Gear Pods	0	0.00034	0
H Tail	0.00180	0.00143	0.00188
V Tail	0.00149	0.00120	0.00155
Nacelles	0.00080	0.00064	0.00084
Pylons	0.00018	0.00014	0.00018
Auxiliary Nacelle	0.00066	0.00054	0.00070
Flaps	0.00173	0	0.00180
Total C_{D0}	0.02382	0.0147	0.02503

The drag polar was calculated using the given C_{D0} values with equations 4.5 and 4.6.

$$C_D = C_{D0} + KC_L^2 \quad \text{Equation 4.5 (Ref. 9)}$$

$$K = 1/\pi Ae \quad \text{Equation 4.6 (Ref. 9)}$$

The Oswald efficiency factor was calculated to be 0.75 for the wing and 0.87 for the horizontal tail using an equation found in Raymer (Ref. 9). Trim drag was found in a similar manner using data from the horizontal tail (Ref. 9). The drag polar for take-off, cruise and landing scenarios, which include trim drag, are shown in Figures 4.8, 4.9 and 4.10 respectively.

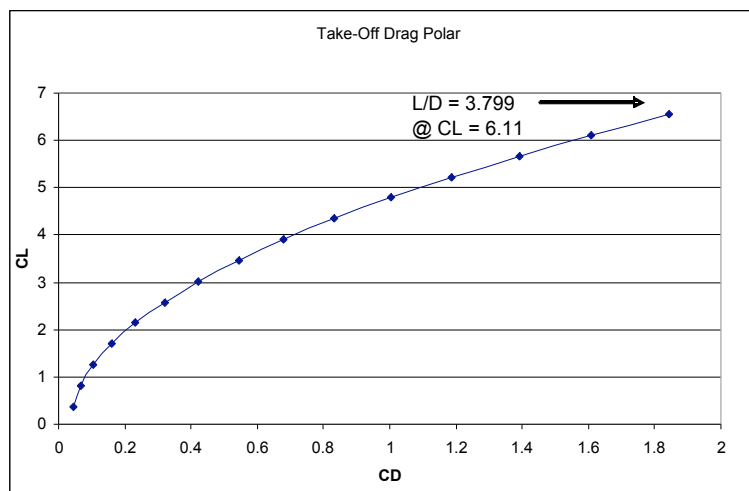


Figure 4.8 Peregrine Drag Polar for Take-Off

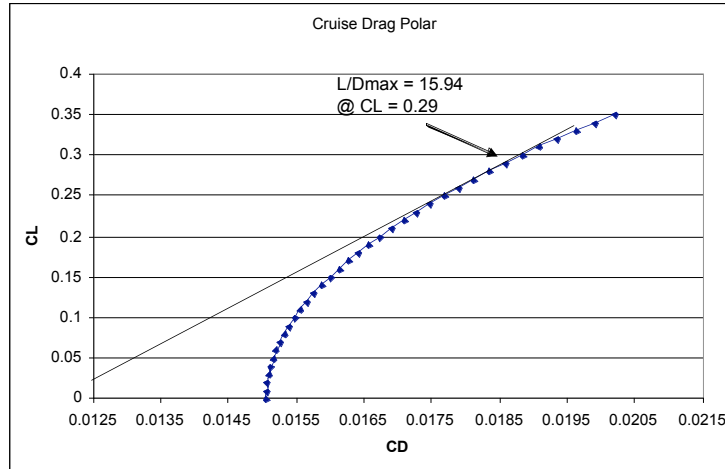


Figure 4.9 Peregrine Drag Polar for Cruise

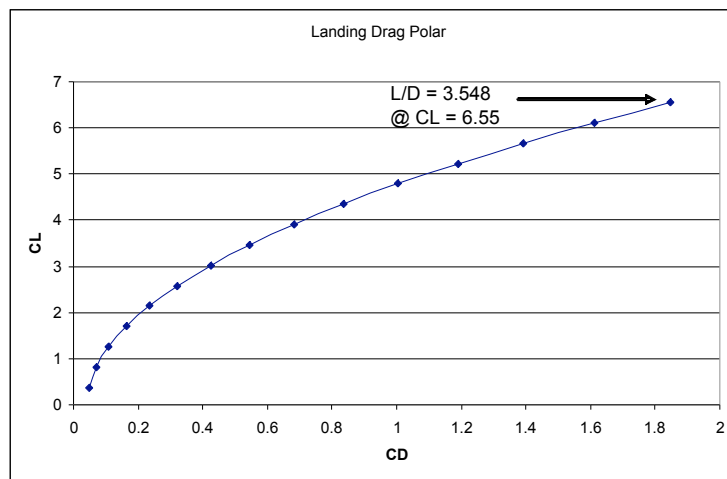


Figure 4.10 Peregrine Drag Polar for Landing

The L/D_{\max} achieved is 15.94 during cruise. The lift-to-drag ratios achieved during take-off and landing are 3.8 and 3.5 respectively. While these ratios may seem low, the extremely high lift coefficients achieved by the Peregrine explain the reason for the high induced drag. The tail's induced drag is high because of its size, which is necessary to counteract the large pitching moment produced by the Peregrine's high lift system. Although the drag is relatively high during take off and landing, it is not unreasonable because of the use of high lift systems.



Chapter 5: Propulsion and Powered Lift

5.1 Introduction

To meet the STOL requirements of the RFP, the Peregrine incorporates a hybrid, powered lift, double-slotted flap system. The two sources of powered lift include the two main thrusting engines (General Electric CF34-3), and two auxiliary, turboprop engines (Rolls Royce 250-C40B). The main engines produce lift through an externally blown flap arrangement. Internal blowing is used to produce lift from the auxiliary engines (Figure 5.1).

The most critical requirements that impacted the power plant selection and the powered lift design were:

1. For the primary mission, balanced field takeoff length must not exceed 2,500 ft. on a hot day (95°F) at sea level (FAR §25).
2. For the wildfire support mission, the aircraft must land within a balanced field length of 2,000 ft. at an altitude of 5,000 ft.
3. Cruise at best cruise altitude and $V_{tas} \geq 400$ knots.
4. When conducting the SNI Landing, the aircraft must be able to continue the SNI landing with the failure of one engine.

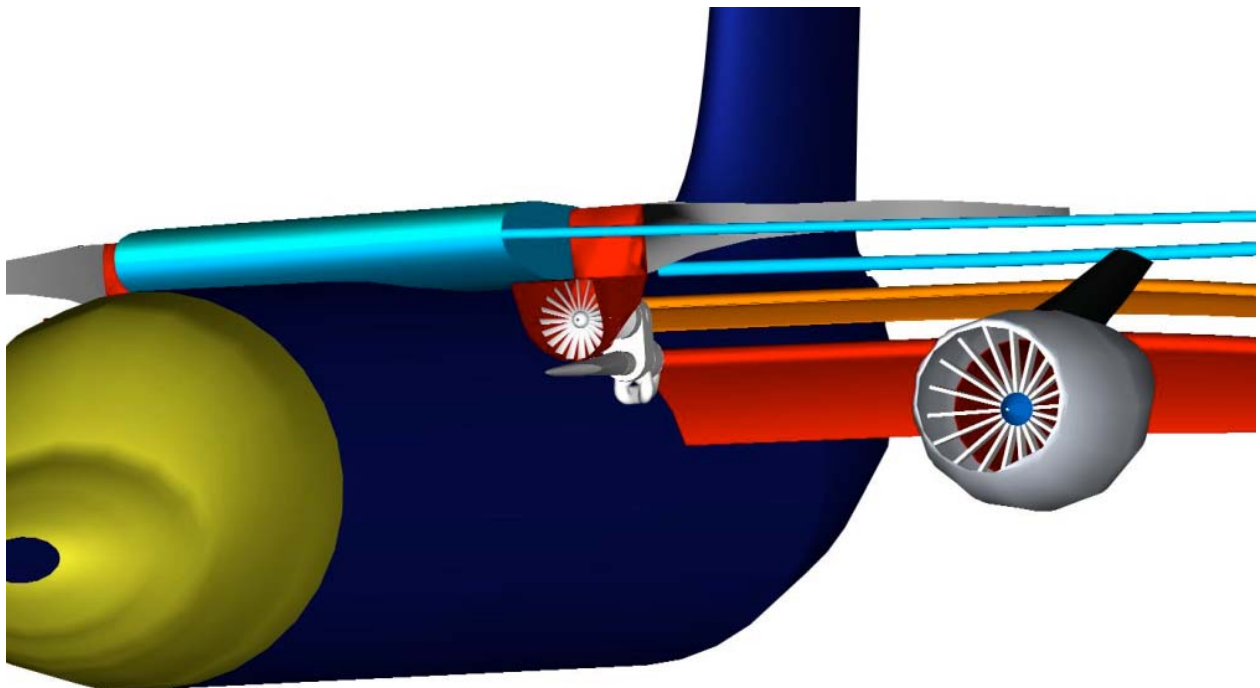


Figure 5.1 Propulsion and Hybrid Powered Lift Configuration



5.2 Main Engine Selection

The Peregrine will operate at Mach 0.7 which dictates the choice of a high bypass ratio turbofan engine. With a TOGW of 55,000 lb. and an increased thrust-to-weight ratio of 0.335 to accommodate for the additional missions, the maximum installed thrust was determined to be 18,440 lb. Because the auxiliary fans provide negligible thrust, each main engine requires 9,220 lb of thrust. The best engine to choose for this requirement is the CF34 turbofan engine, which is rated as a 9000 lb. to 14000 lb. class engine. The specific model chosen was the CF34-3, producing a maximum sea level thrust of 9,220 lb.

The engine nacelle was designed based on the dimensions of the bare engine. Figure 11 shows the nacelle schematic where the nacelle diameter is 10% greater than the bare engine, the inlet extends 60% of the nacelle diameter in front of the fan, and the inlet area is 70% of the maximum diameter of the bare engine (Ref. 10)

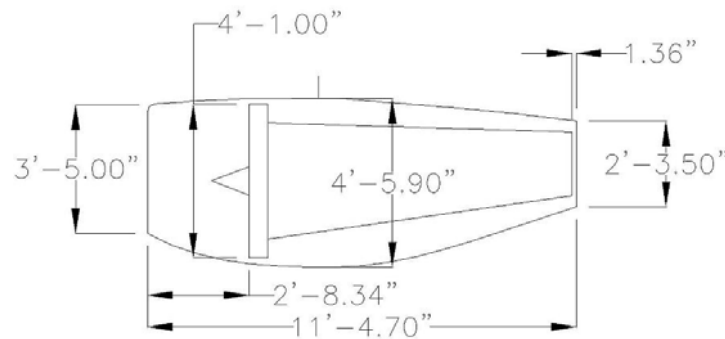


Figure 5.2 Engine Nacelle for the CF34-3 Turbofan Engine

Based on the engine data provided on the AIAA website, it was possible to determine the engine operating limits and capabilities of the CF34 turbofan engine by plotting the relations between Mach number, thrust, and thrust specific fuel consumption. It is apparent from Figures A.1 and A.2 of Appendix A, that the two CF34-3 turbofan engines will allow the Peregrine to cruise at 35,000 ft. and Mach 0.7.

In addition to the considerations mentioned above, an innovative advanced technology will be integrated into the Peregrine that will reduce the temperature of the exhaust plume that impinges on the flaps. The technology is called Active Core Exhaust (ACE) control and is currently in development for use on the C-17 (Ref. 11). By reducing the exhaust plume temperature, removal of the Core Thrust-Reverser (CTR) is permitted and the thermal loads on the trailing edge flaps are reduced. Figure 5.3 displays a fully installed ACE for a turbofan engine. In addition to the enhanced performance specifications of the aircraft, the application of this device will also reduce the



production cost and weight of the aircraft. The C-17 production cost per aircraft is reduced by \$1.2 million and the weight is decreased by 1,200 lbs.

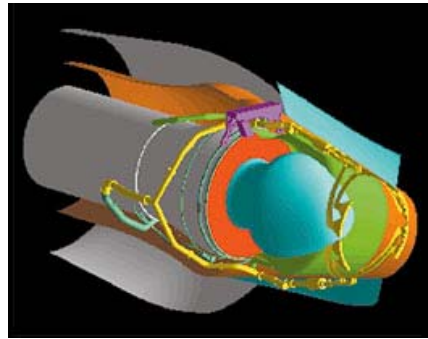


Figure 5.3 Installation of Active Core Exhaust (Ref. 11)

5.3 Powered Lift: External Blowing-Main Engines

External blowing requires proper engine placement and flap configuration (Figure 5.4). The exit plane of the engine is placed so that the exhaust plume expansion of 3.83° produces a plume diameter of 36.3 in. at the leading edge of the first deployed flap and a plume diameter of 44.7 in. at the leading edge of the second deployed flap. This engine placement combined with a conventional vertical spacing of 2.78% of the wing chord (measured behind the centerline of the engine) maximizes the additional lift generated by the blown flaps. By using a vertical spacing of 4.0 in., the exhaust plume diameters at the appropriate flap segments, and the main engines operating at maximum thrust, a C_L of 3.2 was calculated at the required stall speed of 65 kts.

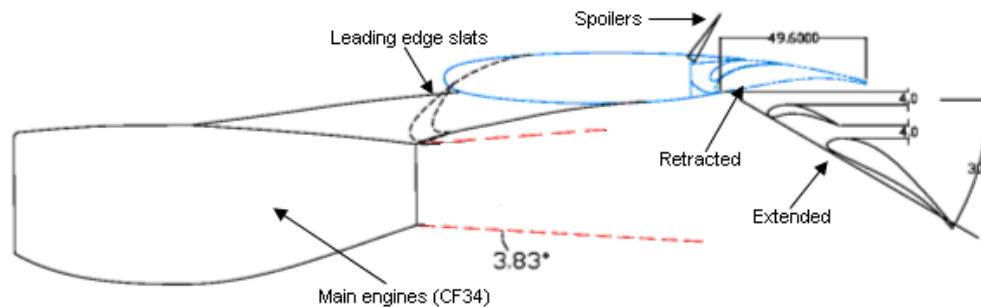


Figure 5.4 Externally Blown Flap Configuration with the CF34-3 Turbofan Engine



The C_L generated from external blowing is dependent on C_{Lc} and the effective flap length. As a result of the dissipative effects on the exhaust plume as it spreads span-wise along the flap, a conservative effective length of 80 in. was used to calculate the maximum C_L achieved. Accounting for the lift produced by the externally blown flaps and the wing, the maximum C_L achieved was 3.484. This C_L is insufficient to meet the STOL requirements of the RFP, therefore, an additional source of lift is required.

5.4 Powered Lift: Internal Blowing-Auxiliary Engines

The auxiliary fan concept is a revolutionary idea that is currently being researched by Kenneth Razak, Dean of Engineering, at Wichita State University (Ref. 12). In his research, he is incorporating an auxiliary fan device into a concept aircraft known as the “Model J”. This concept aircraft has a TOGW of 22,000 lb. and is powered by two 3,600 lb. fan jets yielding a takeoff thrust-to-weight ratio of 0.327; it should be noted that the auxiliary fan does not contribute to the thrust-to-weight ratio because its sole purpose is to provide mass flow for the powered lift system. With the combined technologies of the two fan jets and the blown flap auxiliary fan configuration, this aircraft is estimated to takeoff, over a 50 ft. obstacle in 1,600 ft. As can be seen the integration of an auxiliary fan is a very effective way to meet the STOL requirements that the Peregrine is expected to perform.

To provide enough power to execute an engine out, SNI landing at 5,000 ft. MSL, the limiting condition, the auxiliary fans of the Peregrine would require a 450 shp turboprop engine. To achieve the lift conditions for the additional ESTOL missions, more power is needed. To meet this requirement, the Peregrine will incorporate two auxiliary fans, each powered by a 715 shp, Rolls Royce Model 250-C40B turboprop engine (Figure 5.5). With the application of this engine, the Peregrine will not only meet the constraints of the additional missions but will only have a cost and weight increase (per aircraft) of 0.36% and 0.27%, respectively. Other advantages for selecting this model include its light weight (280 lb. per engine) and compact design.

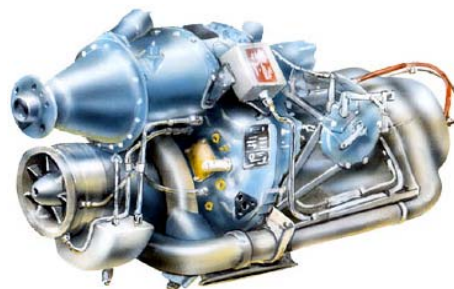


Figure 5.5 Rolls Royce Model 250-C40B Turboprop Engine (Ref. 13)



To reduce the complexity of ducting, the assembly is located next to the fuselage, under the wing root, near the primary source of application, the inboard trailing edge flaps. The main ducting will curve up into the bottom of the airfoil and fan out towards thirteen, 2 in. x 9 in. cutouts within the aft wing spar creating an exit area of 306.8 in.² (Figure 5.6). Although a smaller exit area would have increased the lift coefficient, it would have produced unreasonable noise levels by accelerating the exit flow velocity above Mach 0.8. A feature that cannot be seen in the figure but will be incorporated into the configuration will be a relatively large panel located directly under the engine that will allow easy removal and access for maintenance and repair.

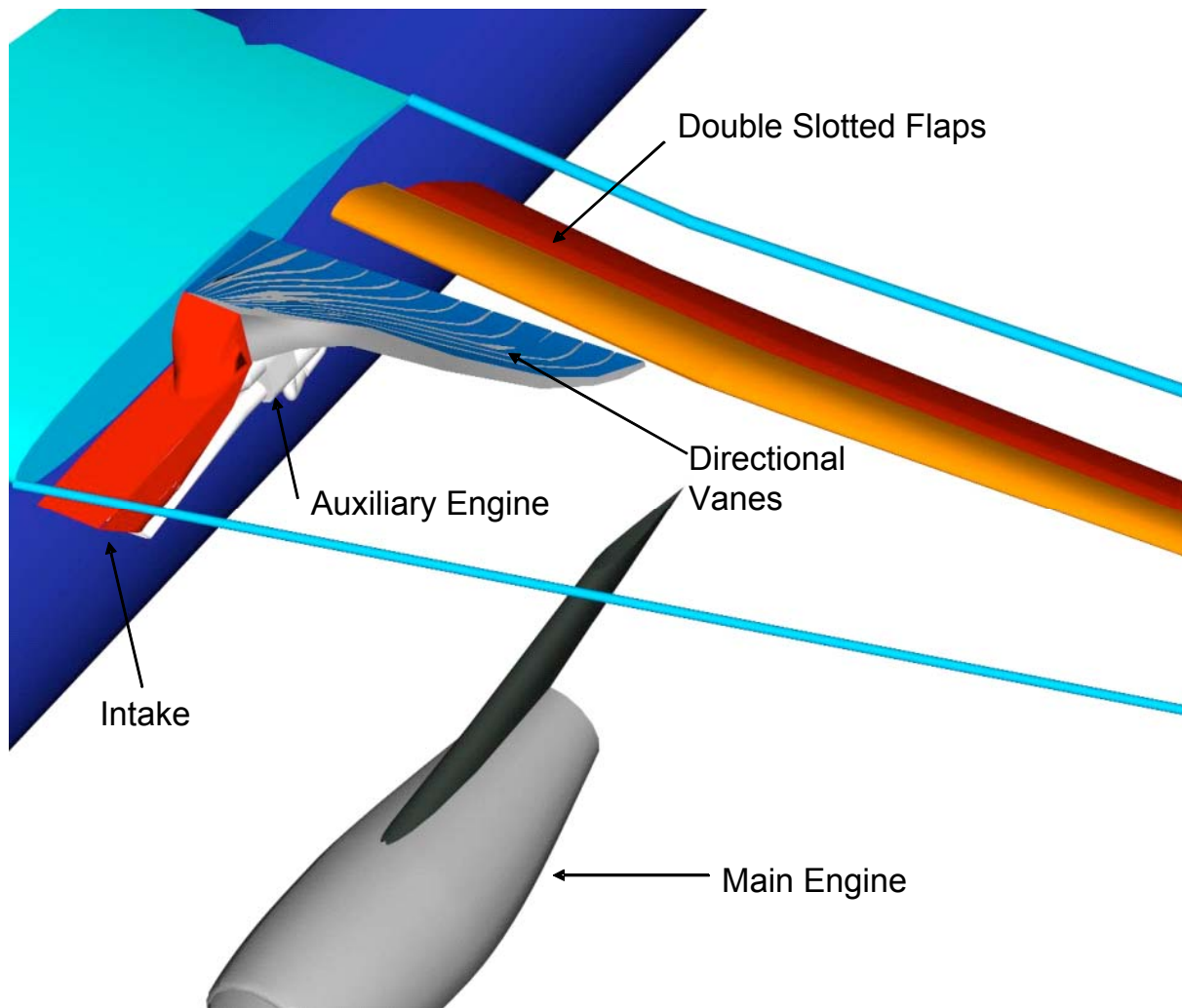


Figure 5.6: Installation of Auxiliary Fan Assembly with the Wing and Inboard Trailing Edge Flaps



Each turboprop engine is connected to a high efficiency fan ($\eta = 0.8$). A small inlet duct, which extends from the bottom rear of the nacelle, allows airflow to enter the compressor of the turboprop engine. Similarly, the engine exhaust is ducted to an exit port located on the aft portion of the nacelle (Figure 5.7). This provides flow control near the underside of the wing-fuselage intersection.

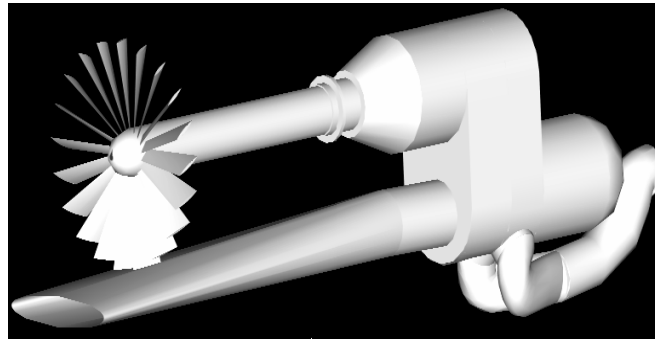


Figure 5.7 Model 250 Turboprop Shafted to the High Efficiency Fan, with Extended Compressor Inlet Duct and Exhaust Duct

The large C_L necessary to perform the STOL requirements dictates that the auxiliary fans only need to be operated during the takeoff and landing portions of flight. To reduce aerodynamic drag and alleviate the affects of inlet spillage drag within the duct after shutdown, a retractable door will extend from the roof of the intake to cover the inlet at a 45° angle (Figure 5.8).

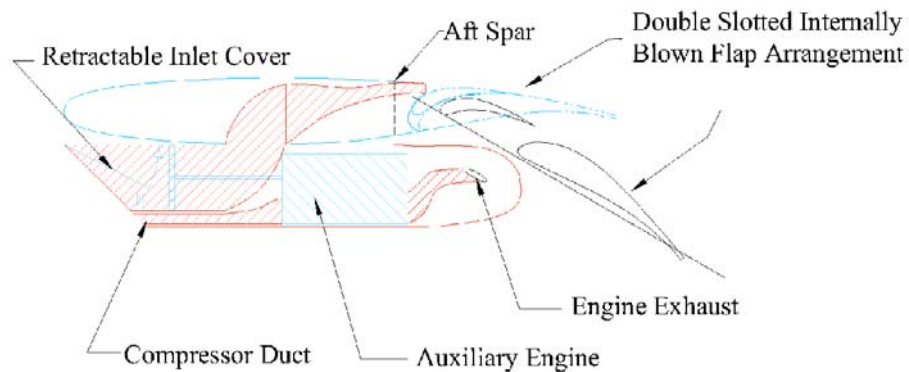


Figure 5.8 Installation of Auxiliary Fan with Ducting Highlighted

5.5 Benefits of the Auxiliary Fans

Table 5.1 clearly emphasizes the benefits for integrating the auxiliary fans to the Peregrine. For a similar aircraft to takeoff in approximately the same distance as that of the Peregrine, only utilizing two main engines in an externally blown flap configuration, would decrease the efficiency of the aircraft. The total thrust required is more than doubled which makes it necessary to use a larger engine, thereby increasing the TOGW. The greater thrust also



yields a high T/W ratio. Once airborne, the additional thrust of the larger engines will be useless because, to meet the cruise requirements, the aircraft only needs a total thrust of 18,440 lb. The most important difference to note is that to operate a two engine configuration, the cost of the propulsion devices would almost double.

Table 5.1 Benefits of the Hybrid Lift System; Auxiliary Fan Concept vs. Two Engine Configuration

	Peregrine	Equivalent (2 Engine)
STOL system	EBF & IBF	EBF
Takeoff distance (ft)	846	834
TOGW (lbs)	55,000	59,747
Total thrust (lbs)	18,440	44,000
T/W	0.335	0.736
Cost-Propulsion (USD)	2,537,000	4,279,000

5.6 Take-off Analysis

To analyze the takeoff run of the Peregrine, a program was used from the VT Aerospace Aircraft Design Software Series (Ref. 14). To ensure the validity of the program, the ATR-72 was used as a test case. After confirming the pertinent aircraft data for the ATR-72, it was found that the balanced field length output from the program was 0.8% less than the actual balanced field length. The test case confirmed the validity of the program and allowed for an accurate analysis of the Peregrine.

After calculating the lift coefficients for the takeoff conditions (sea level on a hot day, 95° F, for the primary mission and 5,000 ft. MSL for the secondary mission) it was possible to analyze the takeoff runs. At the suggested stall speed of 52 knots, the required lift coefficients for the primary and secondary missions are 5.97 and 6.48 respectively. With the auxiliary fans and the main engines operating at maximum power, the Peregrine achieves a C_{Lmax} of 8.75. The excessive lift produced allows for a takeoff distance of 846 ft. and a BFL of 1,016 ft. during primary mission operations and a takeoff distance of 1,018 ft. and a BFL of 1,244 ft. during secondary mission operations. Although the lift coefficient and the takeoff distance may seem atypical, even for STOL aircraft, it is important to take into consideration that the two 715 hp auxiliary engines are employed only to provide powered lift. The auxiliary fans generate 151.4% more lift than the externally blown flaps and the remaining wing section combined.



5.7 Landing Analysis

After calculating the lift coefficients for the landing conditions (5,000 ft. MSL at $\frac{1}{2}$ take off power) it was possible to analyze the landing performance. At the suggested stall speed of 52 kts, the required C_L is 6.48. As a result of the achieved lift coefficient of 8.75, the Peregrine is capable of landing at the stall speed of 52 kts at an angle of attack of 8.7° and a sink rate of 12.0 ft/sec.

5.8 Engine Out Landing

After calculating the lift coefficients for the main engine out landing conditions (5,000 ft. MSL) it was possible to analyze the landing performance (Table 5.2). At the required stall speed of 65 kts, the C_L is 4.15. As a result of the achieved lift coefficient of 6.91, the Peregrine is capable of landing at the stall speed of 65 knots at an angle of attack of 4.4° and a sink rate of 12.0 ft/sec.

After calculating the lift coefficients for the auxiliary engine out landing conditions (5000 ft. MSL) it was possible to analyze the landing performance (Table 5.2). At the required stall speed of 65 kts, the C_L is 4.15. As a result of the achieved lift coefficient of 6.12, the Peregrine is capable of landing at the stall speed of 65 kts at an angle of attack of 7.9° and a sink rate of 12.0 ft/sec.

Table 5.2 Engine Out Landing Analysis at 5,000 ft. Altitude

	External Out	Internal Out
Velocity (kts)	65	65
AOA (deg)	4.4	7.9
Rudder Deflection	30	0.5
Sink Rate (ft/s)	12	12
Thrust	5,650 lb	6,915 lb (75%)



Chapter 6: Structures

Team Ascent has developed an aircraft structure that uses composite materials in approximately 80% of the load bearing surfaces, structure, and miscellaneous parts. The decrease in manufacturing costs, maintenance frequency and number of parts will lead to manufacturing savings and lowered direct operating costs. The structure employed in the Peregrine enables it to be competitive with current regional jets as an adaptive airport transport (AAT) and fulfill the government's requirement for an easily convertible aircraft that can be used in a variety of Homeland Defense missions.

6.1 Loads

An aircraft experiences aerodynamic loads induced by the pilot and loads induced by atmospheric turbulence. Pilot induced load limits are quantified in a maneuvering V-n diagram. Gust loads that result from sudden wind gusts are calculated by forming a gust V-n diagram. An aircraft must be designed for both limit and ultimate loading. FAR §25.301 defines a limit load to be the maximum load an aircraft is expected to see in service. Ultimate loads are limit loads multiplied by a factor of safety. The factor of safety applied to a commercial aircraft is defined to be 1.5 by FAR §25.303. The following excerpts from FAR §25.305 explain the structural requirements for the two load categories:

§25.305 Strength and deformation.

- (a) The structure must be able to support limit loads without detrimental permanent deformation. At any load up to limit loads, the deformation may not interfere with safe operation.
- (b) The structure must be able to support ultimate loads without failure for at least 3 seconds.

By incorporating both limit and ultimate loads into the V-n diagrams the aircraft can be designed to meet the FAR standards. Figure 6.1 incorporates both maneuver and gust V-n diagrams to provide the performance envelope for the Peregrine. Calculations were made at sea level and takeoff gross weight.



of 12 fps. However, the RFP requires that the aircraft be designed to allow descents of 15 fps. This stems from the SNI landing requirement for the primary mission. In addition, the secondary mission will require a faster-than-average descent rate because of the need to land on a 2000 ft. runway with 50 ft. obstacles at each end, with a 25 knot cross wind and 5 knot tail wind. FAR §25.237 requires an aircraft to demonstrate safe landing and takeoff ability in a 90-degree cross component of wind that is at least 20 knots or 0.2 VS0 but not greater than 25 knots.

2. Longitudinal loads are caused by “spin-up”, braking, friction and bumps. Longitudinal loads occur when the wheels first contact the runway during landing. This condition is known as “spin-up”. Loads induced from braking and rolling friction also play a role as well as bumps in the runway.

3. Lateral loads occurring during cross-wind taxiing and turning (Ref. 15). Lateral loads happen when the aircraft has to “crab” on a crosswind landing. Ground turning also provides lateral loading, although not to the extent that crabbing does.

6.2 Material Selection

Approximately 80% of the Peregrine structure will be composite materials. This decision follows the trend that Boeing and Airbus are taking with their respective aircraft, the 7E7 and A380, in which composites are used for primary structural members. Advances in manufacturing are the key to decreased cost in the realm of composites. Procedures such as resin transfer moulding (RTM), resin infusion, fiber placement and laser beam curing have yielded cost savings of almost 50% for Lockheed Martin (Ref. 16). Weight savings from composites are indisputable with typical values in the 20-25% range (Ref. 17). This leads to decreased fuel burn and lowered operating costs. Composite ailerons were tested on the L-1011 and entered service in 1982 (Ref. 19). Table 6.1 illustrates the weight savings and decreased complexity associated with the composite aileron.

Table 6.1 Conventional vs. Composite Aileron on L-1011
(Courtesy of Lockheed Aeronautical Systems Co., Ref. 43)

	Aluminum	Composite
Weight (lb)	140.5	103.9
Weight saved (lb)	0	36.5 (26%)
No. of ribs	18	10
No. of parts	398	205
No. of fasteners	5253	2574

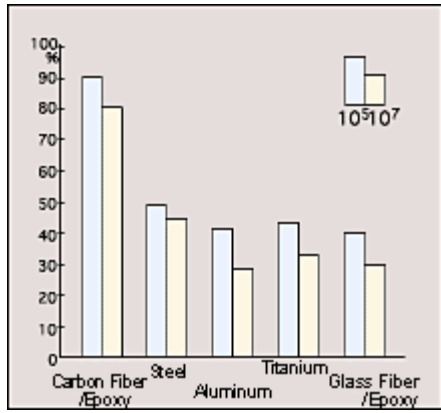


Using composites keeps the Peregrine ahead of competitors such as Embraer and Bombardier. These companies are known to be observing the development of resin infusion and GLARE (employed on the A380), viewing them as potential candidates for future aircraft (Ref. 16). The use of composites on commercial aircraft is steadily increasing. While they have long been used in numerous secondary structures, composites have seldom been employed in primary structural members. Table 6.2 illustrates the various locations of composite materials on commercial aircraft in comparison with the Peregrine.

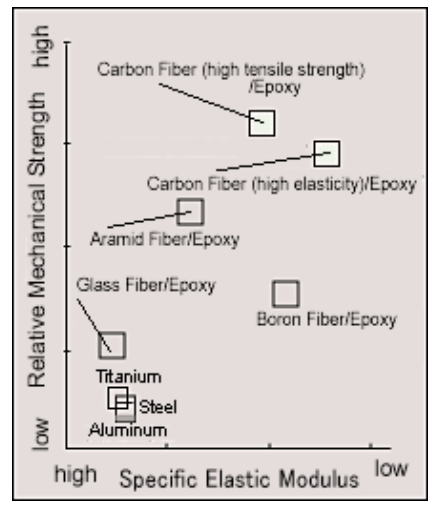
Table 6.2 Composites Used in Commercial Aircraft (Adapted from ASM International, Ref. 44)

Composite component	A340-500/600	ATR 72	B-757	B-767-400	B-777	Lear Fan	Peregrine
Doors	x	x	x	x	x	x	x
Rudder	x	x	x	x	x	x	x
Elevator	x	x	x	x	x	x	x
Vertical tail	x	x	x	x	x
Horizontal tail	x	x	x	x	x
Aileron	x	x	x	x	x	...	x
Spoiler	x	x	x	x	x	...	x
Flap	x	x	x	x	x	x	x
Wing box	...	x	x	x
Body	x	x
Fairings	x	x	x	x	x	x	x

Most structural components will be built out of Carbon Fiber Reinforced Plastic (CFRP). CFRP is 60% carbon fiber and 40% synthetic materials. Automatic production of CFRP components using new gore-folding machines, as is being done for the A380, provides increased productivity and lowered manufacturing costs (Ref. 18). Large individual sheets of carbon fiber are handled like rolls of fabric and heated together with synthetic materials and then molded to shape (Ref. 18). CFRP features extremely high strength and low weight making it ideal for structural applications. It also demonstrates superior resistance to fatigue and thus an increased lifespan. Figure 6.2 demonstrates the superiority of CFRP over other composites and metals.



(a) Fatigue Resistance



(b) Relative Mechanical Strength

Figure 6.2 Comparison of Fatigue Resistance and Mechanical Strength of CFRP with Other Structural Composites and Metals (Courtesy of The Japan Carbon Fiber Manufacturer’s Association, Ref. 22)

Almost all wing ribs and spars, the central wing box, longerons and other structural applications are built with CFRP. Glass fiber reinforced aluminum or GLARE will be used for the upper fuselage shell and all fixed leading edges. It is a laminate in which layers of glass-fiber reinforced adhesive and aluminum are alternated. GLARE is 10% less dense than aluminum yet it can support 20-25% higher loads at fatigue-critical locations (Ref. 20). It provides superior impact and fatigue resistance. GLARE is being used for the first time on the A380. Table 6.3 illustrates the materials selected for use on the Peregrine and their respective locations.

Table 6.3 Peregrine Material Locations

Material	Wing	Fuselage	Empenage	Powerplant
CFRP	wing box, spars, ribs, internally/ externally blown flaps	gear doors, center bulkheads, frames	vertical/horizontal tail box, rudder	cowling, aux. fan nacelles and ducting
Glare		upper fuselage	vertical/horizontal tail leading edges	
Toughened CFRP		floor beams		
Hybrid		wing-body fairing	leading/trailing edge panel on vertical/horizontal.	
Fiber Glass		radar nose		main engine strut cowling
Alcoa Alloys		belly skin, cockpit protective plate		
Kevlar/Epoxy		fwd.press. bulkhead	aft. press. bulkhead	
Honeycomb	ailerons	fuselage skin	vertical/ horizontal TE	



A chief concern for the externally blown flap system is the flap material itself. The active core exhaust control system (ACE) is being developed by the Air Force for use on the C-17. One of its primary purposes is to reduce the thermal loading on the trailing edge flaps used in external blowing (Ref. 11). Figure 6.3 shows that it can reduce exhaust temperatures up to 50% at five nozzle diameters behind the nozzle exit.

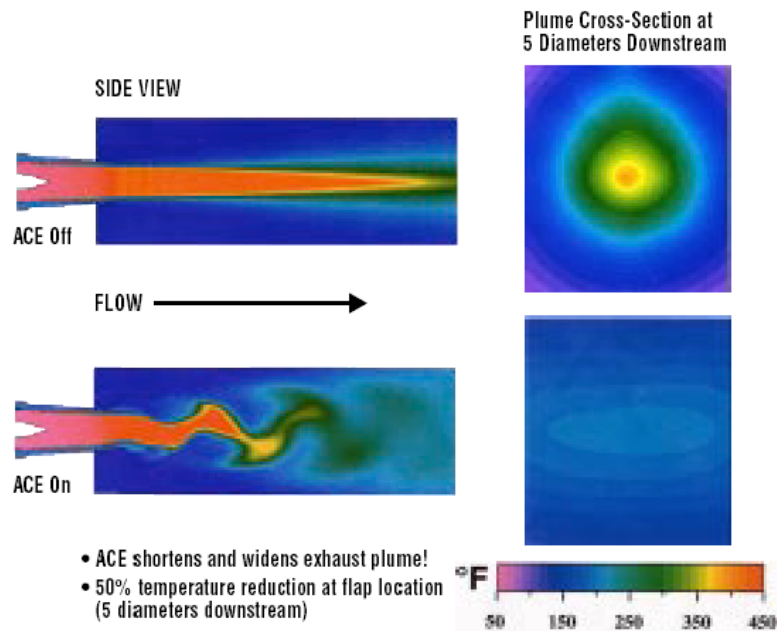


Figure 6.3 ACE Implementation Reduces Thermal Loading on Flaps
(Courtesy of Air Force Research Labs, Ref. 21)

The C-17 uses titanium plating on its externally blown flaps. With the ACE system it will be able to use high-temperature aluminum instead (Ref. 21). The Peregrine's externally blown flaps are 3.64 nozzle diameters down the flow. Thermal loading will not be lowered as much as the C-17 so Peregrine's flaps are made out of CFRP. Figure 6.4 illustrates the superior thermal properties of CFRP in comparison to aluminum alloys and other composite materials.

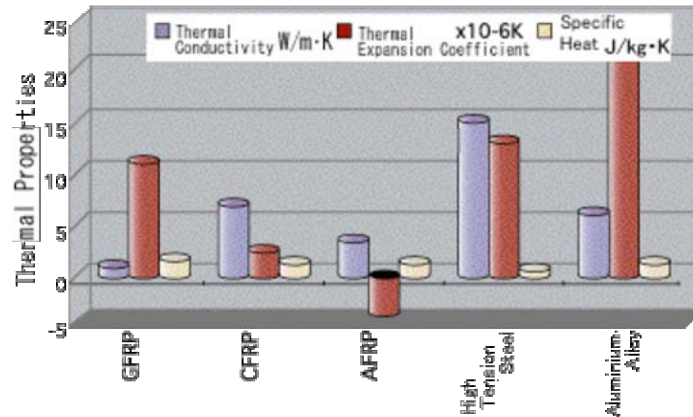


Figure 6.4 Comparison of Thermal Characteristics of CFRP and Other Materials
(Courtesy of The Japan Carbon Fiber Manufacturer’s Association, Ref. 22)

The low thermal expansion coefficient lends itself to better retention of mechanical properties under thermal loading. The use of ACE allows CFRP to be used for the externally blown flaps rather than titanium, a dramatic weight reduction.

6.3 Structural Concept

The use of composite materials leads to weight savings of approximately 20-25%. A portion of the weight savings is attributed to the large decrease in part count due to integrally formed parts and “gluing” rather than riveting and various attachment methods.

The fuselage is built out of eight bulkheads, fourteen frames and four longerons. Four longerons will run the length of the fuselage. The two lower longerons run flush with the floor beam supports. The two upper longerons run along the fuselage at the end of the passenger carry-on baggage compartments. The cockpit structure consists of the forward pressure bulkhead, two frames and bulkhead number 1. The two frames support the windshield framework and are connected to the pressure bulkhead and bulkhead 1 by longerons. Bulkhead 1 separates the cockpit from the cabin and begins the constant cross section fuselage. Four frames maintain shape and integrity between the first bulkhead and the central structure. An additional four frames are located between the central structure and bulkhead 5. After bulkhead 5 the fuselage tapers into the empennage where four more frames are located. Bulkhead 6 and the aft pressure bulkhead translate the empennage loads to the rest of the fuselage. Foldouts 3 and 4 provide a 3-view of the structure and a 3-D structural schematic, respectively.

PEREGRINE STRUCTURES

VIRGINIA TECH AEROSPACE ENGINEERING

COMPONENT DESIGN: TEAM ASCENT

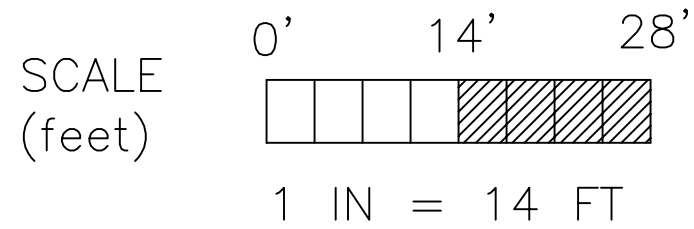
ORIGINAL SCALE 1:204

DATE: 10 APRIL 2004

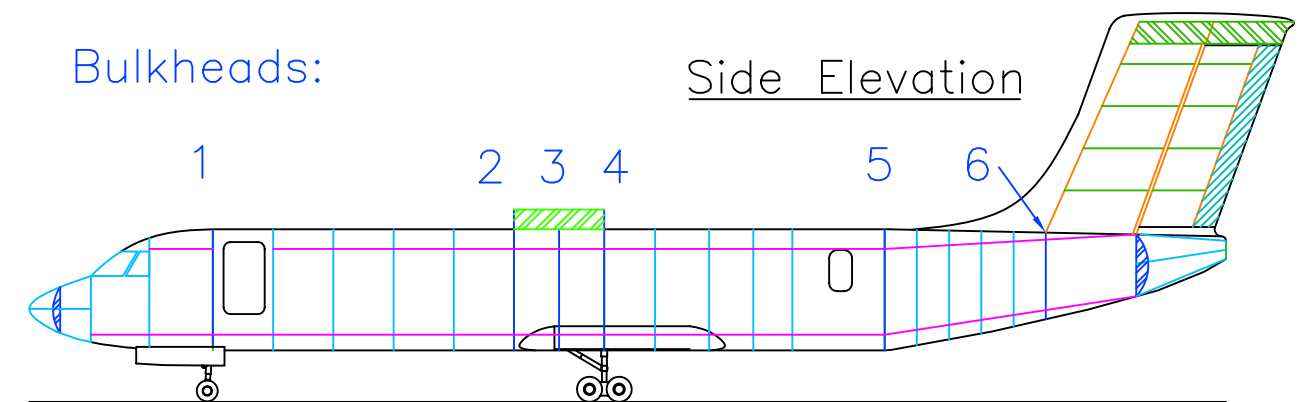
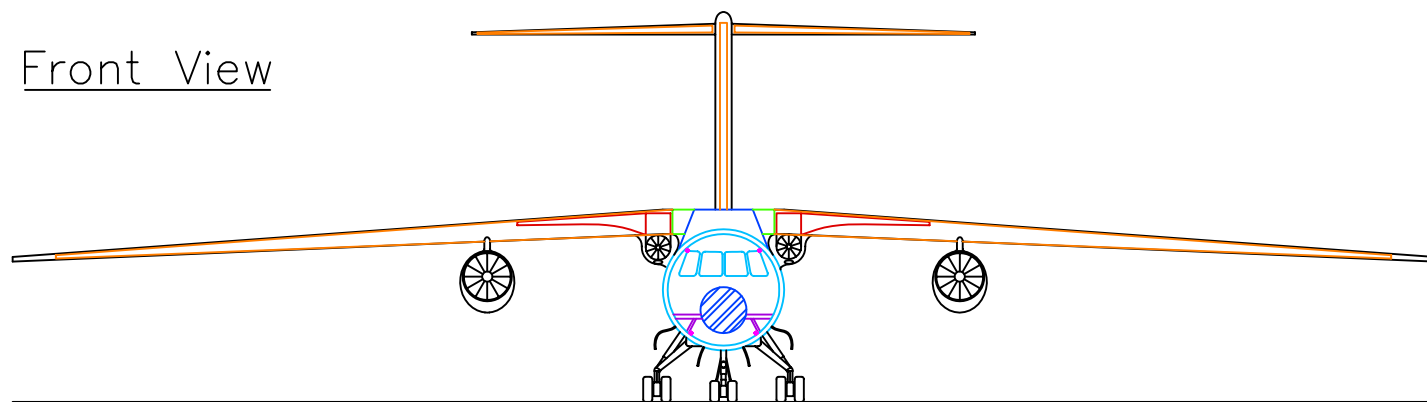
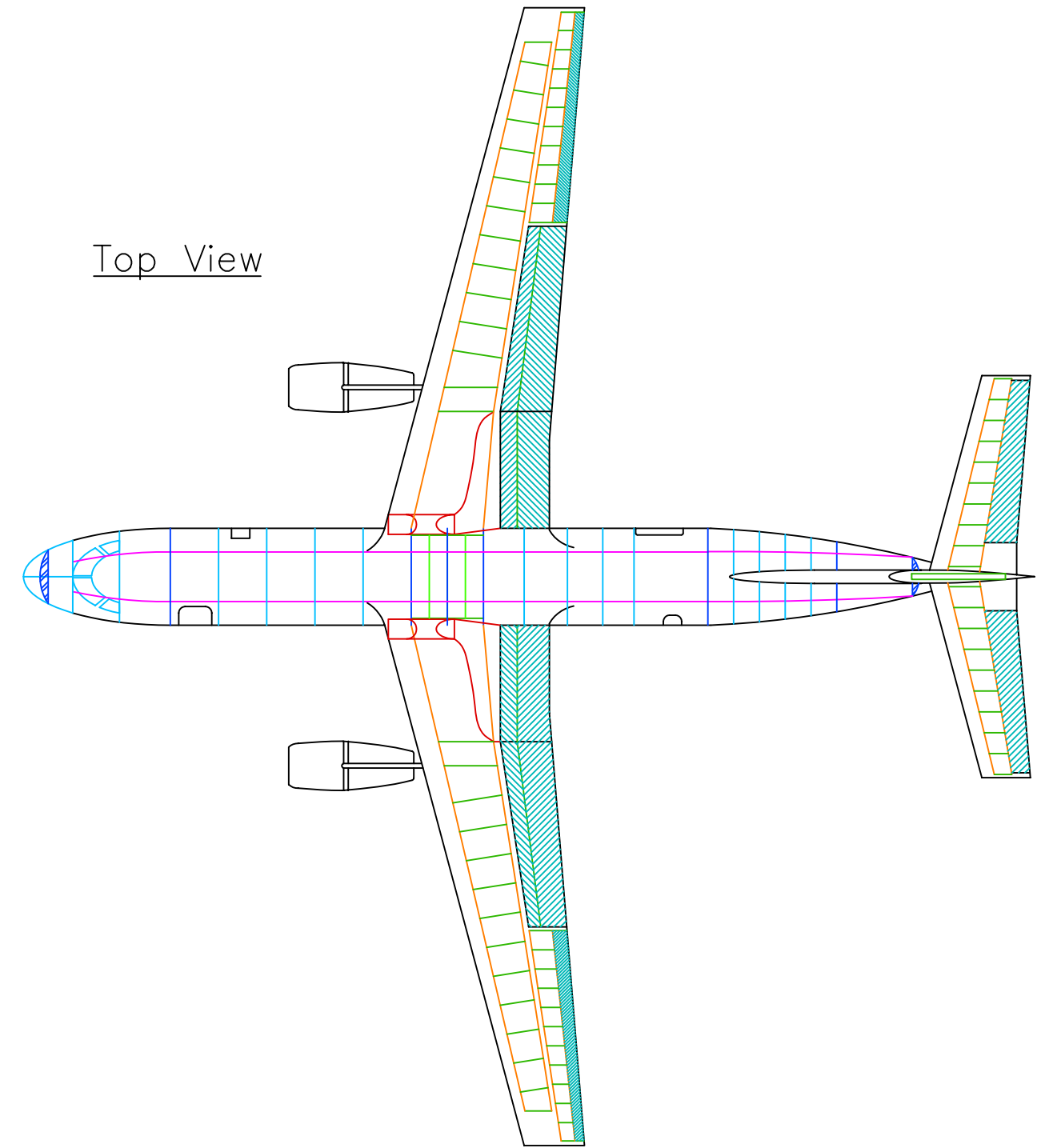
Ver.

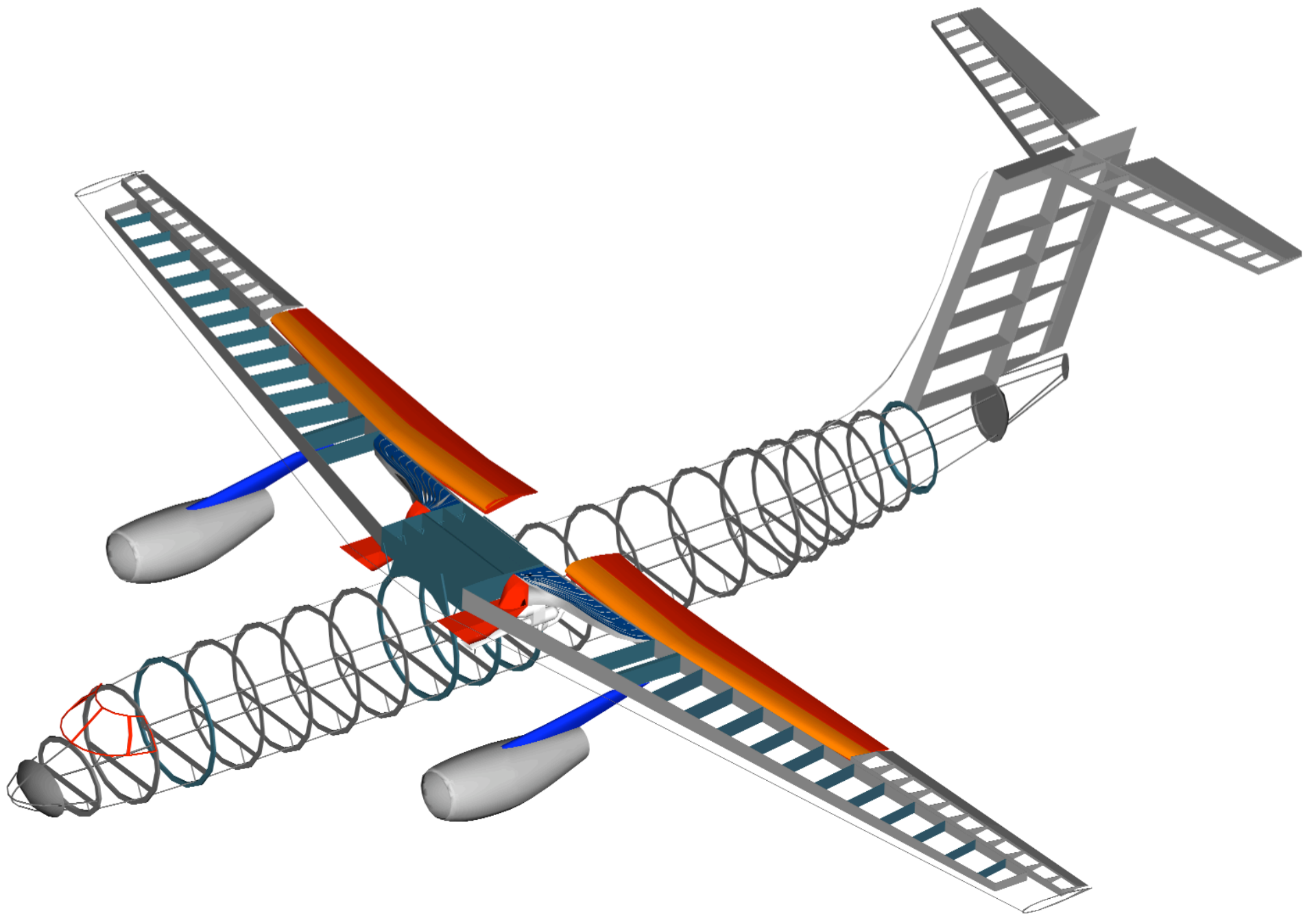
DRAWN BY: AE and RM

1



- Bulkheads
- TE Surfaces
- Floor Beams/Supports
- Frames
- Longerons
- Ribs
- Spars
- Wing Box
- Aux. Fan Ducting







The central support structure is designed to carry and share multiple loads. Heavy bulkheads numbers 2, 3, and 4 are located in the center of the fuselage. They are integrated into the central wing box to help support wing loads and also support the main landing gear loads. A framework of small beams runs between the wing box and the bulkheads to provide added support for the wing. The auxiliary fan and engine are integrated into the root of the wing. The auxiliary fan engine has two mounting locations. A reinforced rib will run directly next to the ducting system and provide a set of engine mounts directly above it. The beams built between the bulkheads and wing box will provide lateral mounts. Of crucial importance is the rear wing spar reinforcement. The internally blown flap system actually ducts the air through the aft spar at 13 locations. In between the duct locations will be reinforced vertical webbing and horizontal spar additions. The top and bottom spar caps and flanges will retain their integrity for the length of the spar so they continue to provide the best bending strength. The central structure is depicted in Figure 6.5, integrated with the rest of the aircraft.

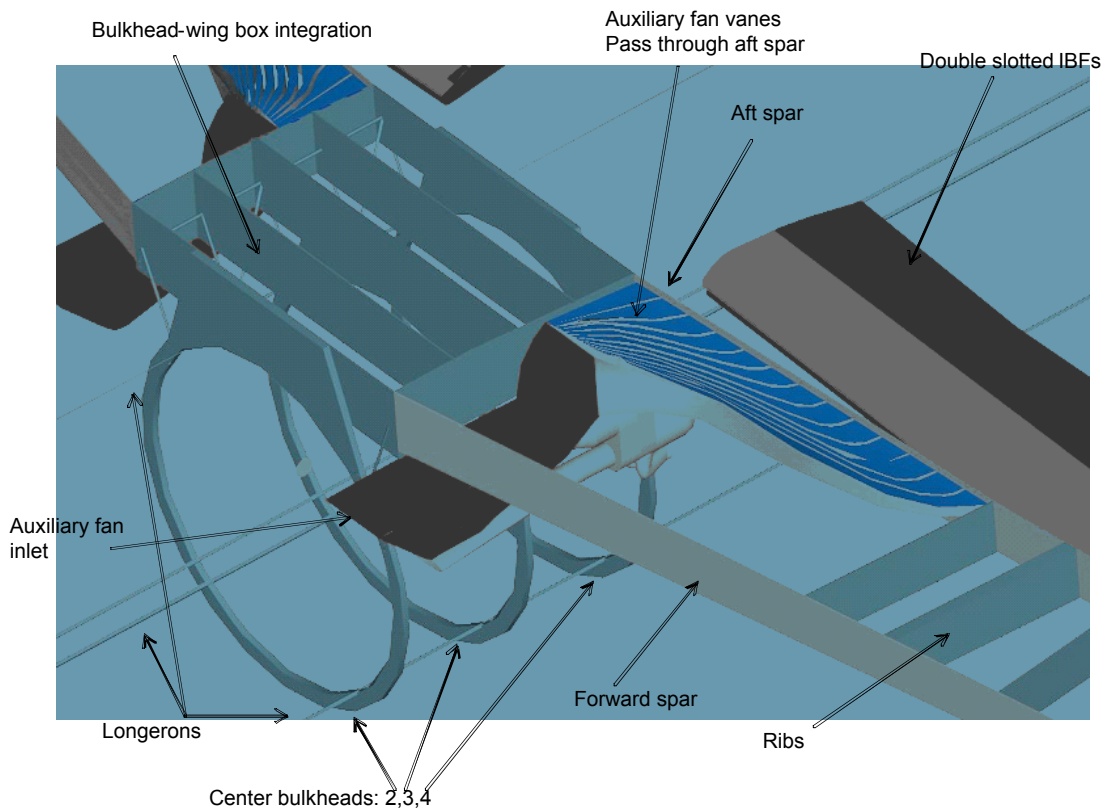


Figure 6.5 Bulkhead-Wing Box Integration



Reinforced rib and spar structure is located at each main engine station to support the engine pylon and resulting loads. All control and flap surface hinges are located where a rib meets the aft spar.

The nose gear loads are translated into bulkhead 1, which separates the cockpit from the cabin, by mounting the strut directly off of the bulkhead. Each main gear bogey is supported by a central shock strut and drag strut. Each strut is attached to one of the central fuselage bulkheads; drag struts to bulkhead 3 and shock struts to bulkhead 4. Each bulkhead is integrated into the wing box and auxiliary fan mount. Figure 6.6 clearly depicts this structural concept.

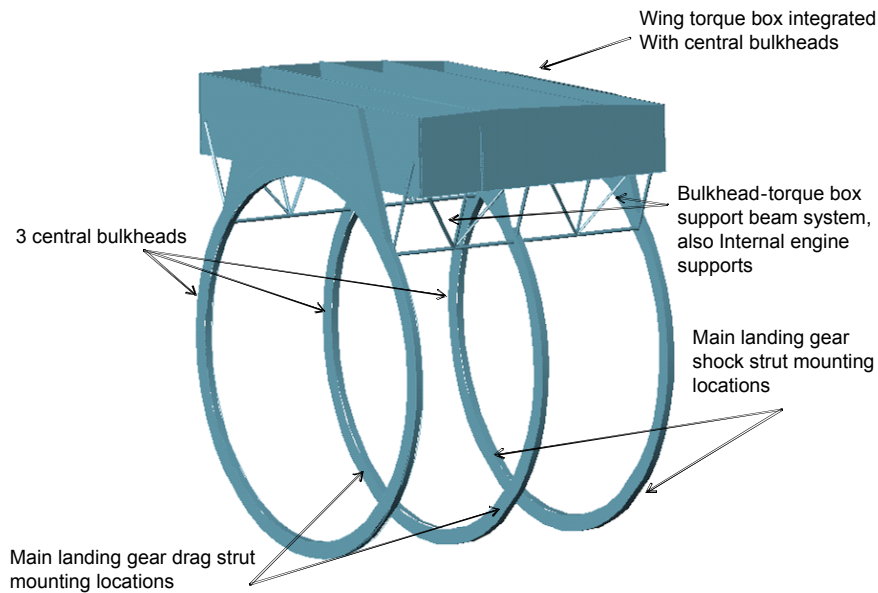


Figure 6.6 Location of Peregrine’s Main Landing Gear Mounts

Controls surfaces and wings are built with two spars each and ribs connecting them. Control surfaces are constructed with a single spar and ribs connecting the spar to the trailing edge honeycomb-core wedge. Wing skins are integrally stiffened.



Chapter 7: Systems

7.1 Electrical System

Hamilton Sundstrand will supply the electrical systems package for the Peregrine (Ref. 23). Their integrated electrical system architecture includes both primary and secondary power distribution assemblies (PDA/SPDA) and all components required for complete incorporation into the aircraft and its electrical subsystems.

Figure 7.1 shows how the integrated electrical system is placed in the aircraft.

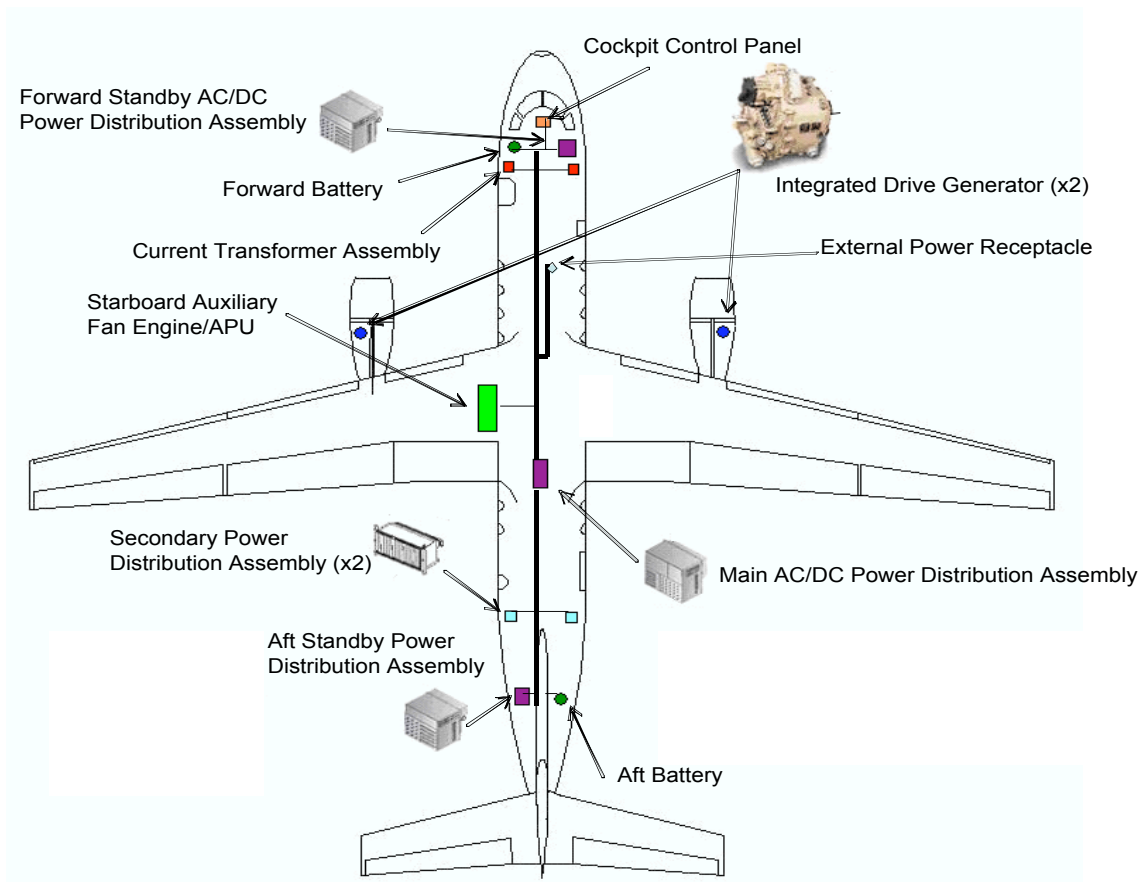


Figure 7.1 Peregrine's Integrated Electrical System (Adapted from Hamilton Sundstrand, Ref. 23)

The electrical system is built with the modular concept in mind. This significantly decreases maintenance time and complexity and increases operating efficiency. Cost is reduced by the consolidation of multiple components, leading to less



wiring, lower weight, better reliability, and reduced manufacturing hours. The Hamilton Sundstrand integrated system is an excellent choice for the Peregrine, enabling it to meet AAT requirements through cost reduction and increased operating efficiency. Typical systems that are supported by the electrical network are listed in Table 7.1.

Table 7.1 Aircraft Sub-Systems Requiring Electrical Support (Adapted from Roskam, Ref. 15)

Commercial Aircraft Electrical Sub-Systems
Exterior Lighting
Flight Compartment Lighting
Passenger Cabin Lighting
Galley
Toilets
Entertainment
Windshield Heating
Avionics
Air Conditioning
Fuel
Electro-Hydrostatic Actuation (EHA)
Flight Control
Electrical Power (converted to DC)
Cargo Handling
Miscellaneous

7.2 Auxiliary/Emergency Power

The Peregrine auxiliary fans are not only used for the internally blown flap system, they double as auxiliary power units (APUs). Most commercial aircraft have a single APU located in the empennage. An APU typically supplies power to main engines for start up so an external power source is not needed. It is also a source of in-flight emergency power, should the main systems fail. If additional hydraulic or electrical power is needed the auxiliary engine can be operated in flight. The typical power requirement for an APU is 37 kW or 50 SHP at sea level (Ref. 24). With the surplus power from the auxiliary fans there is more than enough to supply what is needed for backup power. Because the engines are located at the wing root, they are near the center of gravity and do not require a mass balance as would conventional commercial aircraft APUs. The starboard auxiliary fan engine will be wired to double as an APU. The economy of the engines is conserved by utilizing them for both high lift and auxiliary power. Easy access to the APU/Auxiliary Fan Engine will be possible through nacelles at the fuselage-wing root mount.



7.3 Air Management System

Hamilton Sundstrand will provide Peregrine’s air management system. Their systems have logged more flight hours on regional jets than any other supplier and are currently supporting greater than 50% of all the aircraft in the 30- to 70-passenger range (Ref. 23). The air management system is composed of three major systems. The pneumatic system or engine bleed air system (EBAS) utilizes ducting from the main engines to deliver compressed air to the other systems. The second system uses the bleed air to protect the airfoil, engine cowl, and windshield against ice and frost. Thermal anti-icing is accomplished by directing the bleed air along the leading edge, cowl, and windshield using a valve and tubing system. The third component is the air conditioning system (ACS) and cabin pressure control system (CPCS). These systems keep the aircraft comfortable. ACS uses the bleed air to satisfy heating, cooling, ventilation, and pressure requirements. A system of outflow valves, controller, selector panel, and redundant positive pressure relief valves makes up the CPCS. Pressure is maintained by modulating discharged airflow from the cabin using several outflow valves.

Cabin pressurization will be maintained automatically, based on a predetermined schedule that works as a function of altitude. Internal pressures will range from 5.0 psi at 10,000 ft. to 8.5 psi at a cruising altitude of 30,000 ft. (Ref. 15). Positive pressure relief valves are set for a pressure differential of 9-10 psi (Ref. 15).

7.4 Hydraulics

A new control technology developed by Messier-Bugatti called electro-hydrostatic actuation (EHA) will be installed in the Peregrine to actuate virtually all of the systems that typically rely on hydraulics. Table 7.2 lists the systems that will utilize EHA.

Table 7.2 Electro-Hydrostatic Actuation Applications

Primary Control Surfaces	Secondary Control Surfaces	Other
Ailerons	Externally blown flaps	Landing gear actuation
Elevator	Internally blown flaps	Landing gear doors
Rudder	Trim control	Auxilliary fan inlet doors
Spoilers	Leading edge slats	Landing gear brakes
		Nose wheel steering
		Thrust reversing (ACE)

Instead of the traditional centralized hydraulic pump and accumulator, EHA provides complete mini-hydraulic systems located at each control actuator through a combination of electrical and hydraulic power.



Continuous monitoring of these individual systems allows problems to be located immediately. This drastically cuts maintenance time and costs by allowing individual components to be easily located and replaced in their entirety, rather than draining the whole system. Safety and reliability are enhanced now that a system failure means only the component it controls becomes inoperative rather than the entire network. Figure 7.2 shows how EHA incorporates both electrical and hydraulic components to achieve decentralized actuation.

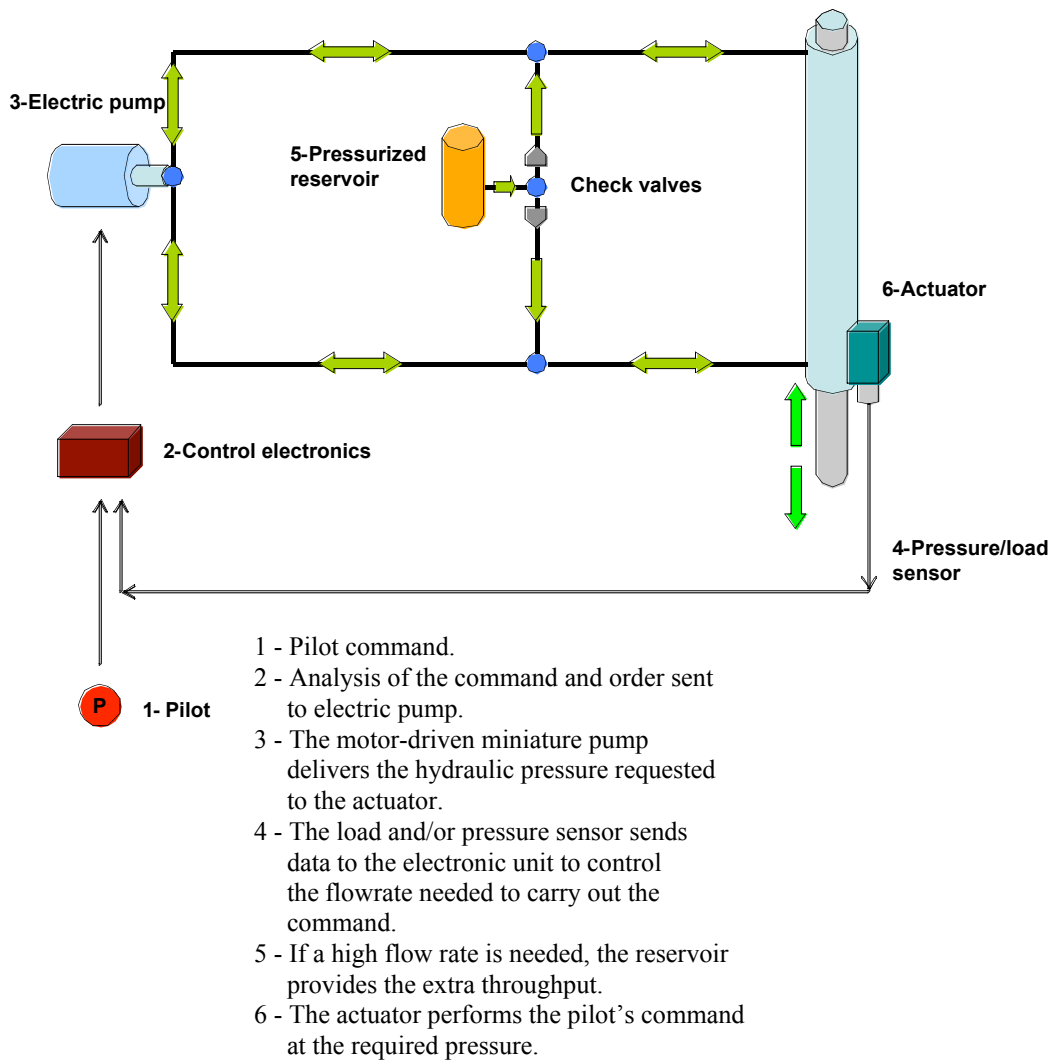


Figure 7.2 Electro-Hydrostatic Actuator (EHA) Operating Diagram (Adapted from Messier-Bugatti, Ref. 25)

The mini-pumps used on the Peregrine will operate at 5,000 psi. The combination of reduced component size, tubing, fluid required, and high operating pressure leads to generous weight savings. In addition to control



actuation, EHA systems will service high-lift devices, landing gear, brakes, doors and steering. A typical EHA pump is shown in Figure 7.3.

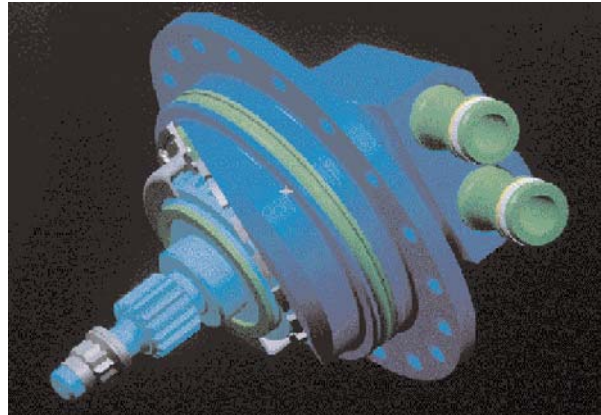


Figure 7.3 Messier-Bugatti Pump for Flight Control EHA (Courtesy of Messier-Bugatti, Ref. 25)

This cutting edge flight control actuation system will be particularly attractive to customers as it addresses problems that have plagued hydraulically operated aircraft since their inception. The decentralization of hydraulic systems provides an added degree of survivability by immediately isolating the damaged system and allowing repairs to be made that do not affect the other systems.

7.5 Avionics

Honeywell Primus, a trusted manufacturer of avionics systems for many aircraft, will be used to provide Peregrine's avionics system. The 1000 series Digital Avionics Suite, which is currently used in the Embraer ERJ-145, will be installed in the Peregrine. The 1000-series system includes all required analog displays as well as 5 large 8 in. x 7 in. digital displays. Two displays are used as flight plan maps and two are used for all primary and full rose/arc displays. There is also one display for engine and system status and for messages. In addition it has an auto-throttle and performance management system allowing for easy take-off and landing control. The avionics system also includes a heads-up display, which has been rated for use in IMC (Cat 3C) severe weather conditions. The heads-up display will also aid landing in flight conditions that will arise in the wildfire support mission where smoke, dirt and other debris may severely limit vision out of the cockpit.



7.6 Automatic Flight Control System

The Honeywell Avionics Suite has a capability to be fitted with a flight management system. A Rockwell Collins FCS-4000 series flight control system will be integrated into the system to provide temporary autonomous control of the Peregrine. It provides a 3-axis autopilot system to control the aircraft during many common maneuvers.

The system will automatically trim the aircraft during take-off and landing. It will also provide roll guidance to track a selected heading. By entering the SNI flight path into the system, it is able to provide the correct amount of roll to perform the SNI landing. The system is not completely autonomous. During engine out the pilot will have to supplement the system with additional pedal force to deflect the rudder, preventing excessive yaw.

This system greatly reduces the pilot workload during critical portions of flight, increasing safety and passenger comfort. The simplified flight paths and data control allows pilots to operate the aircraft without requiring additional training.

7.7 Fuel System

The Peregrine's total fuel capacity is 11,000 lbs. in keeping with the FAR 25 reserve requirements. Both the main and auxiliary engines operate on Jet-A. Fuel will be stored in five self-sealing bladder tanks. Two separate bladder tanks, outboard of the auxiliary fan system, will be located in each wing. The fifth bladder tank will be located in the central torque box. The combined tank volume adds to 221 ft³. The central tank has a volume of 81 ft³ and the volume for each wing tank is 35 ft³. Dry bays will be located directly above the main engines to keep the large fuel quantity away from high heat areas.

Fuel pumps will carry the fuel from the tanks to the engines. Fuel lines are able to carry 1.35 lbs/sec of Jet-A. This flow rate is 1.5 times the maximum required fuel flow for the main engines (Ref. 15). Pressure buildup within the tanks is prevented by the fuel venting system which maintains positive pressure in the tanks throughout flight. Fuel monitoring and control systems allow the crew to constantly monitor the level of fuel within each tank, control the flow rate to each engine, cross-feed between various tank and engine combinations, and shutoff flow to an engine if a fire should occur. As fuel levels change the center of gravity travel is minimal because the fuel tanks are located in the wing and torque box. The primary issue is to maintain equal balance in the wing tanks. The fuel control system will use the wing tanks to supply their respective engine. However, if a problem should occur, cross-



feeding will allow the fuel to be balanced to maintain roll stability. All fuel transfers will be accomplished by an automated system. Emergency backup will allow the crew to designate cross-feed should the automated system fail. In an emergency, fuel can be dumped through release valves in the wing.

There Peregrine has single-point refueling capability to allow easier refueling at smaller airports. Because the wings have anhedral, the refueling point is located at the top of the center fuel tank, above the fuselage.

Fire extinguishing systems will be installed for each engine. One tank of fire suppressant will be installed per wing, servicing both the main and auxiliary engine. Fire detectors and nozzles are mounted in strategic location within the engine nacelles.

Considerable survivability is designed into the fuel system. The potential dangers of operating the Peregrine in the Military Support and National Defense role merit such measures. As mentioned previously, self-sealing bladders are used for the fuel tanks. This protects against projectiles piercing the tank and causing massive leakage and explosions. In addition, ullage protection is implemented. The fuel ullage or area within the tank above the fuel will be filled with Nitrogen as the fuel level decreases. The oxygen levels in the tank will be maintained below 9% to prevent combustion in case of heated projectile penetration (Ref. 27). There are two possibilities to implement this system. Either the Nitrogen is stored in the aircraft in a small tank or it is generated from an Onboard Inert Gas Generation System (OBIGGS). OBIGGS actually removes the oxygen from engine bleed air and atmospheric air, creating Nitrogen enriched air which it sends to the fuel tank. However, the Peregrine will use a bottle to store Nitrogen rather than generating it. For the amount of fuel required, the bottle will need to weigh only 2.36 lbs with a volume of 0.1 ft³ (Ref. 26). The OBIGGS system weighs about 10 lbs, is 23 in. long and is considerably more complex than the storage bottle (Ref. 27).

Additional survivability is inherent in the system due to the high-wing configuration. The fuselage-mounted landing gear is 8 ft. 9 in. below the fuel system. This vertical separation protects the fuel from hazards such as hot tires and potential fuel-line damage during hard landings. In the event of a crash, collapsed main gear struts will be unable to cause direct damage to the fuel system. The high-wing also places the fuel system further above the ground, reducing potential foreign object damage (FOD) while operating out of austere environments. The fuel system layout and all the survivability features are noted in Figure 7.4.

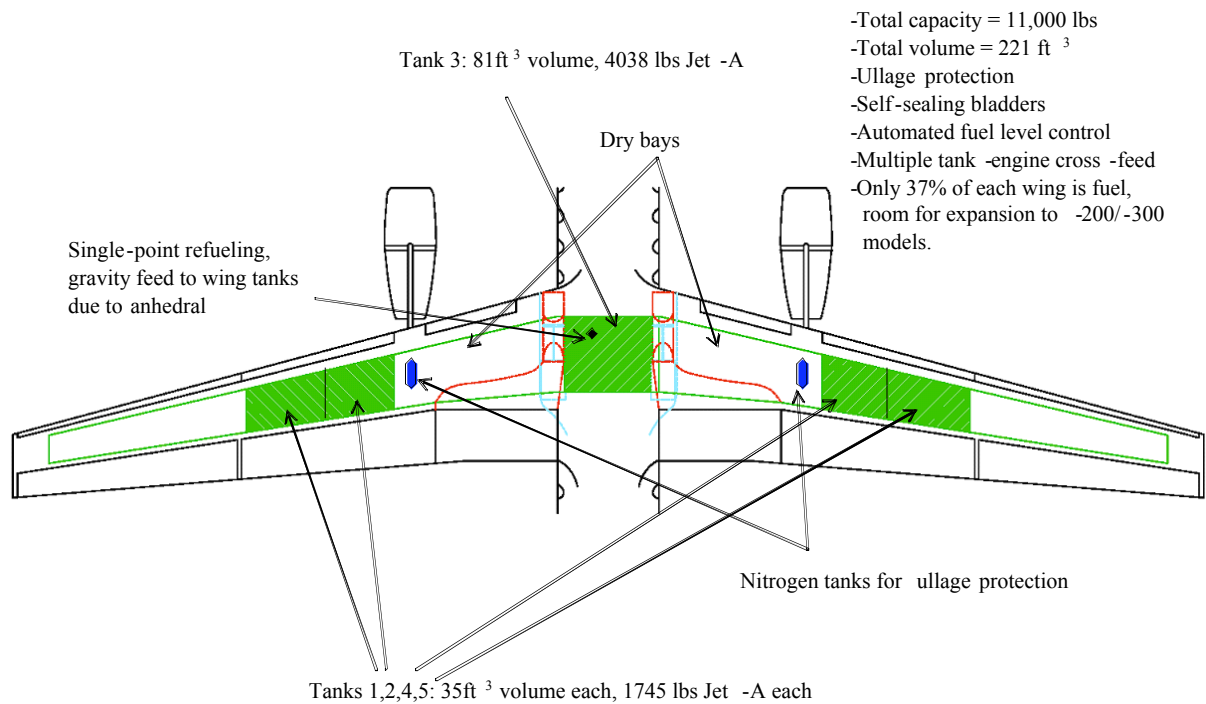
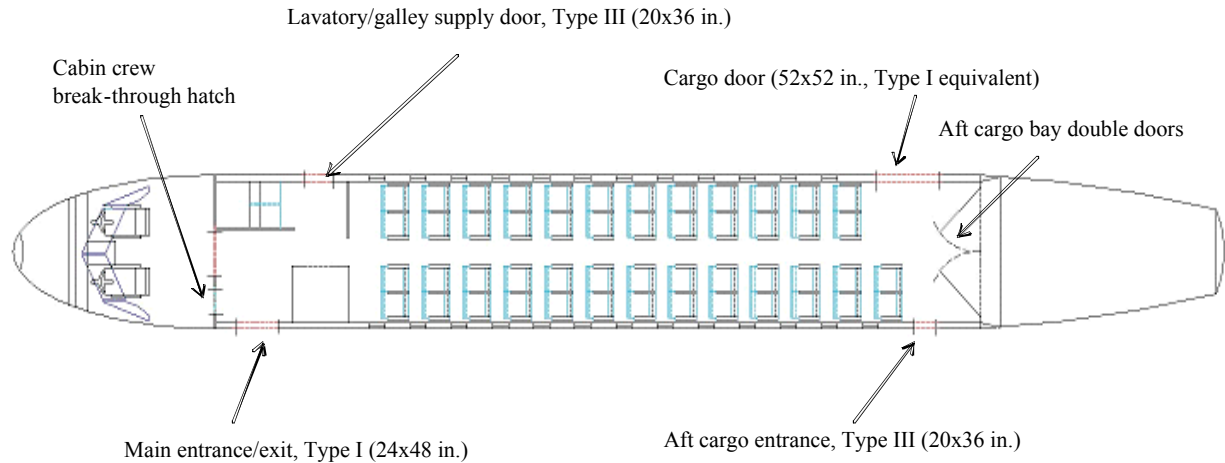


Figure 7.4 Fuel System Layout and Survivability Features

7.8 Emergency Exits and Escapes

The Peregrine is equipped with two Type I (24 in. x 48 in.) equivalent emergency exits on each side and two Type III (20 in. x 36 in.). The main door Type I dimensioned and the cargo door doubles as a Type I exit. This selection of door exits brings Peregrine into compliance with FAR § 25.807, meeting the requirements for aircraft with seating provisions from 41 to 110 seats. These provisions allow the Peregrine to be upgraded to the -200 (65 pax) and -300 (81 pax) sizes without additional emergency provisions. Internal lighting will clearly indicate the location of each exit. White lights along the floor of the aisle will guide passengers to exit locations indicated by red lights. Each exit door will be simple to operate and instructions will be clearly marked. Beneath every passenger seat will be a life vest. Because of the high-wing configuration inflatable slides are not required for the Peregrine. Each door is equipped with an automatically extendable air-stair that will enable passengers to disembark the aircraft safely. Cabin crews will exit from either of the two front passenger emergency exits. A break-through hatch in the wall separating the cockpit from the cabin will enable crew to exit the cockpit if their door is locked or jammed shut. All emergency exit provision and details are detailed in Figure 7.5.



*No changes needed for -200 (65 pax), -300 (81 pax) sizes, already meets FAR § 25.807 requirements (for 41 to 110 pax).

Figure 7.5 Emergency Exit Provisions for the Peregrine

7.9 Water and Waste System

The Peregrine's plumbing system will be able to manage 11.7 US gallons worth of water and waste. This equates to a total volume of 1.6 ft³ which is based on the value of approximately 0.3 US gallons per passenger, a standard value for transport aircraft (Ref. 15). Monogram Systems water and waste systems will be used in the Peregrine. Weight savings are achieved through trash compacting using the galley waste disposal system (GWAD). Highly efficient toilet systems that flush using minimal water lead to ultimate efficiency. Monogram's systems rely on the use of vacuums to quietly and effectively dispose of waste (Ref. 28).

7.10 Noise Reduction

The Peregrine's fuselage is specially designed to prevent discomfort for passengers due to the extreme noise of the internally blown flap system. The two problematic sources of noise are the auxiliary fans located at the wing-fuselage intersection and the resulting sound made by the ducted air as it exits the trailing edge of the wing over the flaps.

Noise requirements for all subsonic transport category large airplanes and turbojets are stated in FAR §36.201: the aircraft must have noise levels no greater than the Stage 3 limits prescribed in §C36.5(a)(3). Stage 3 noise limits applicable to the Peregrine (greater than 3 engines, 55,000 lbs takeoff gross weight) state that takeoff



noises cannot exceed 90 Effective Noise Perceived decibels (EPNdBs). Noise from the sideline must be less than 94 EPNdBs and for the approach less than 98 EPNdBs. Figure 7.6 illustrates that a typical STOL aircraft meets the FAR §36 requirements for its weight and engine classification. Peregrine is not a typical STOL aircraft, but based on the measures taken to reduce noise

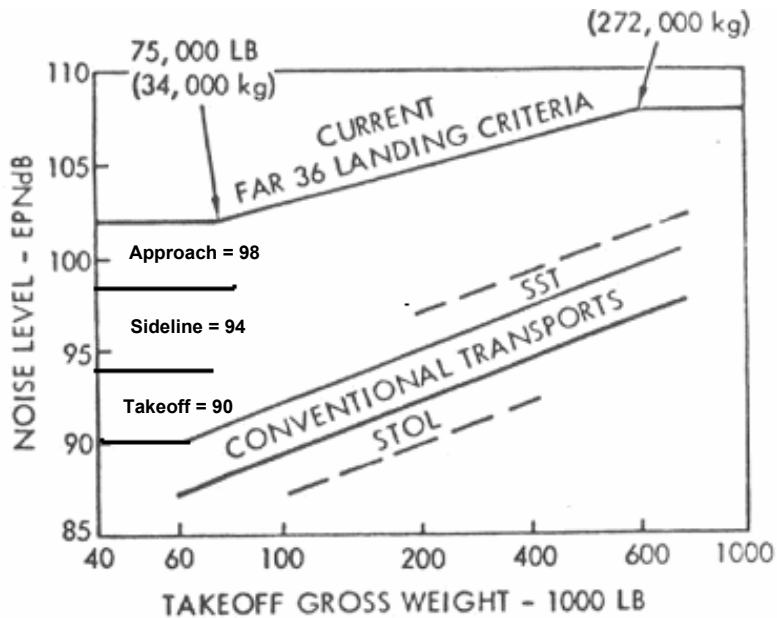


Figure 7.6 FAR §36 Noise Requirements Applicable to Peregrine (Adapted from Stanford, Ref. 7.19)

Two methods will be used to reduce cabin noise in the Peregrine: the use of a composite sound damping interior, and the application of an active noise control system. The AAR Composites, HTL® Acoustic Shell Interior will be used to decrease noise in addition to cutting weight. The interior features lightweight acoustic dampening shell panels. When the shell is attached on the interior it is mounted specifically to combat the generation of noise from the airframe through the cabin.

The use of active noise control in commercial aircraft cabins has been implemented in the large turboprops such as the King Air 350 and business jets like the Bombardier Challenger. Essentially, active noise control uses “anti-noise” or signals using frequencies that cancel out the actual noise (Ref 29). The UltraQuiet cabin, developed by Ultra Electronics, will be installed on the Peregrine. Noise throughout the cabin is detected by microphones and measured by the Controller (ANCU). The controller passes a signal to the actuators which are either loudspeakers



installed underneath the interior or Active Tuned Vibration Attenuators (ATVAs). These devices which act to cancel the noise are shown attached to an airframe in Figure 7.5.



Figure 7.7 Active Tuned Vibration Attenuator (ATVN), Decreases Airframe Vibration and Cabin Noise
(Courtesy of UltraQuiet, Ref. 29)

The ATVNs will be used on the Peregrine. In addition to canceling out noise in the cabin, it acts to dampen airframe vibration (Ref. 29). This reduces the complexity of installing loudspeakers underneath the trim and works in conjunction with the Acoustic Shell Interior, further reducing cabin noise.

Ultimately, noise will be a problem only during the takeoff and landing phases of flight. The auxiliary engines will only be operated during these times to provide the required short field performance and auxiliary power requirements. However, the extra measures taken to provide passenger comfort give the Peregrine an edge over its competitors.

External noise poses problems for flights into small regional airports where neighborhoods located near the airport do not typically deal with jet aircraft flying overhead. Noise caused by operating the auxiliary fan engines on the ground in their backup power roles will be problematic to crews loading and unloading the aircraft. External noise reduction is accomplished by manipulating the exhaust flow using noise-reduction nozzles on the main engines and a specially insulated exhaust system in the auxiliary engine nacelles. Noise reduction nozzles manipulate the exhaust so it mixes with bypass or ambient air. This lowers the exhaust gas velocity and decreases the turbulence and shear layers between the two flow fields, thus lowering noise (Ref. 7.17). A GE CF34 engine, the same type being used for Peregrine's main engines, has been tested using "chevron" shaped mixing devices. Over



2.5 EPNdBs of noise reduction have been recorded with such a nozzle without significant thrust loss at takeoff or cruise (Ref. 7.18). Figure 7.6 shows the chevron nozzle implemented on the CF34.



Figure 7.8 GE CF34 Experiences 2.5 EPNdB Noise Reduction Using “Chevron” Nozzle
(Courtesy of NASA/GE/P&W, Ref.45)

Finally, it is important to note that the noise resulting from the Internally Blown Flap system will not be substantial. The primary cause of noise is the speed of the flow exiting the slots of the wing. They were specifically designed to keep the flow subsonic, at Mach 0.8, in order to decrease the noise that is inherent with trans-sonic or supersonic flow regimes.

7.11 Landing Gear

Design of the Peregrine’s landing gear was driven by the requirement to operate out of small regional airports and then transition to unprepared runway operations with no configuration or part changes and to minimize weight in the process.

Key factors in design for unprepared runway operations were the landing gear geometry, stroke and tire types. Tip back angle, measured from the main wheel ground contact points to the aft end of the airframe was set to be 14° (Ref. 30). This sets the takeoff angle of attack to be slightly less than 14° . Of critical importance to rough field operations is the turnover angle, θ . Land based aircraft must have $\theta \leq 63^\circ$ while for “rough” surfaces $\theta \leq 50^\circ$ (Ref. 30). The Peregrine has a turnover angle of 51° . The additional weight is minimized by keeping the turnover



angle from getting smaller than it needs to be. Figure 7.7 illustrates the various landing gear geometries applied to the Peregrine; part (a) shows the tip-back angle design, part (b) shows the turnover-angle.

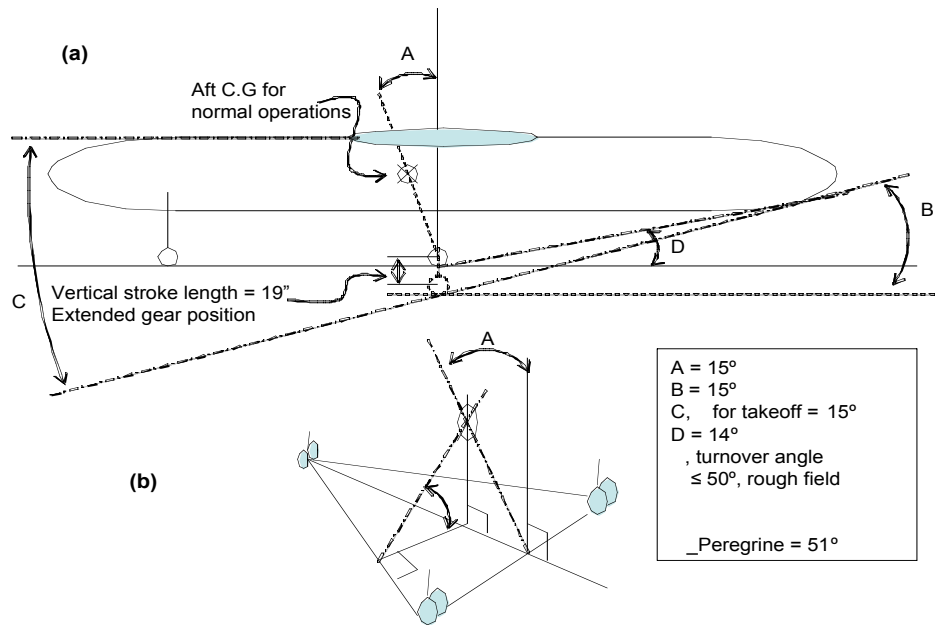


Figure 7.9 Peregrine Landing Gear Geometry

The Peregrine’s main gear stroke distance was determined to be 23 in. along the shaft translating to 19 in. vertically. Stroke distance was calculated based on a landing gear load factor of 1.75, maximum descent rate of 15 ft/sec., an oleo-pneumatic shock absorption efficiency of 0.80, and the projected landing weight (Ref. 15). An additional 20% factor of safety was added after initial calculations to produce the final stroke length of 23 in. The corresponding diameter of the shock strut is 5.28”. A long stroke allows for smoother landing despite increased descent rate. It decreases loads translated to the airframe during rough landings, lengthening airframe lifespan. The nose gear stroke is 10 in. and the shock strut diameter is 4.8”.

Tire selection for the Peregrine was driven by the requirement to land on an unprepared runway. Table 7.3 illustrates the variety of tire pressures allowed on a variety of surfaces. In order to support 55,000 lbs on an unprepared runway it is necessary to have ample load distribution.



Table 7.3 Allowable Tire Pressures for Various Surfaces (Courtesy of Roskam, Ref. 15)

Description of Surface	Maximum Allowable Tire Pressure (psi)
Soft, loose desert sand	25 – 35
Wet, boggy grass	30 – 45
Hard desert sand	40 – 60
Hard grass depending on type of subsoil	45 – 60
Small tarmac runway with good foundation	50 – 70
Large, well maintained concrete runways	120 – 200

Several measures were taken to distribute the load. Main gear bogies were set in the twin tandem configuration. Four tires per strut cuts the effective load per tire in half when compared to conventional twin tire configurations for aircraft of this size. This also reduces the weight and dimensions of the tire, allowing most of the tire to fit into the fuselage. The tire storage blister is small as a result and has minimal impact on drag. A Central Tire Inflation System (CTIS) will be installed in the aircraft. This allows the tire pressure to be changed in flight, en route to an unprepared field. Maximum takeoff and landing performance can be achieved with the pressure set to correspond to the operating surface. Peregrine’s tires and their specifications are listed in Table 7.4.

Table 7.4 Peregrine Tire Specifications

Specification	Main	Nose
Diameter (in.)	22	18.3
Width (in.)	8	7.7
Number of tires	8	2
Rated Inflation (psi)	135	90
Rated Load (lbs)	7,900	3,822
~Actual Load/tire (lbs)	6,188	2,750
Tire Weight (lbs)	27.7	15.4
Total Tire Weight (lbs)	221.6	30.8
Type	3 part name size	metric

The Peregrine’s total tire weight is 3 lbs lighter than the ATR-72 total tire weight. The ATR-72 is a versatile aircraft that has a 5,500 lb lower takeoff gross weight and the ability to operate out of short, rough fields.

Landing gear extension and retraction is integrated in the Electro-Hydrostatic Actuation system that replaces virtually all actuation actions that were previously accomplished through regular hydraulics. Landing gear doors are also operated by EHA.



The kinematics of extension and retraction were developed to be as simple as possible whilst saving space and minimizing blister size. Figure 7.8 illustrates each step in the landing gear retraction process and shows the extended gear position. For a discussion on the structural placement of the landing gear, see the Chapter 6.3.

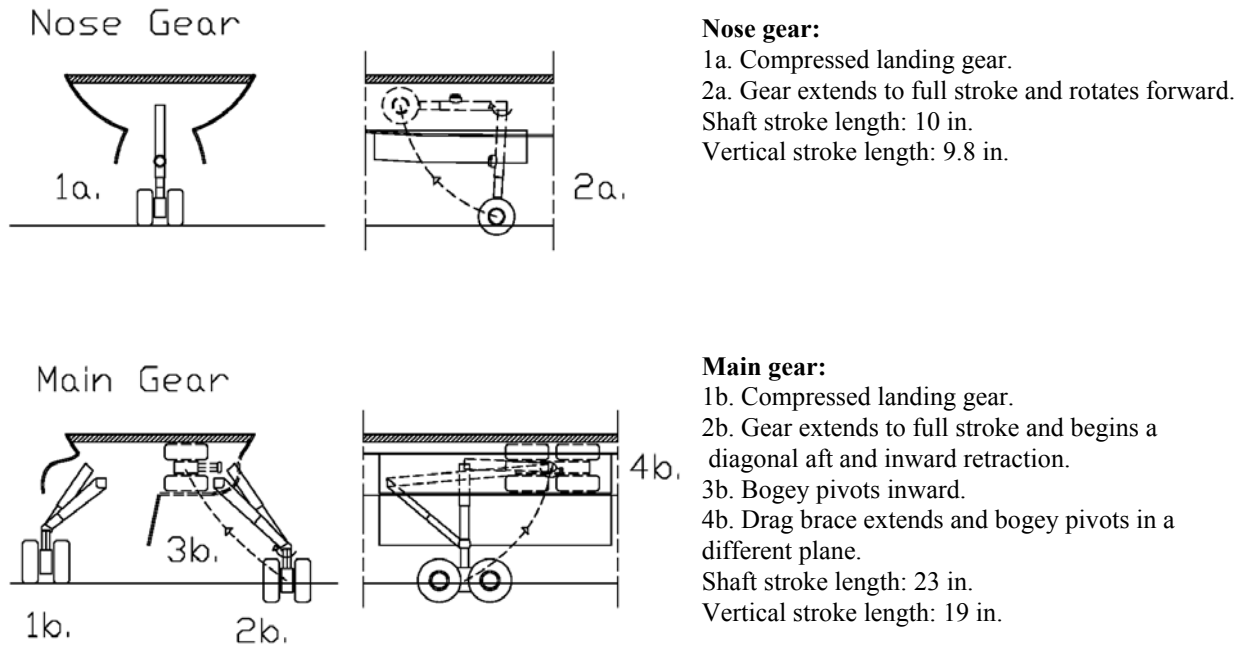


Figure 7.10 Peregrine Landing Gear Kinematics

Peregrine’s landing gear blister is small and efficient. Figure 7.9 shows that it does not extend below the lowest point of the fuselage and only extends 8.92 in. at its maximum distance from the fuselage. This decreases drag during cruise.

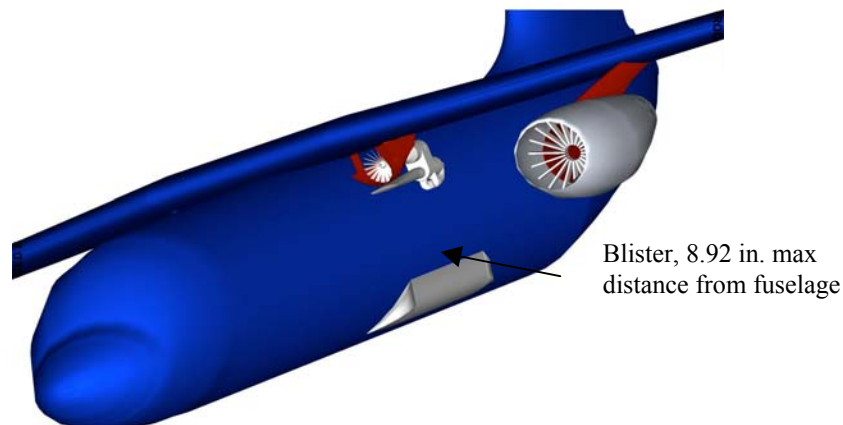


Figure 7.11 Peregrine’s Landing Gear Blister



Peregrine will utilize Messier-Bugatti's SepCarb® III Plus brakes. They feature increased 15% increased endurance over the previous generation of SepCarb brakes, bringing the lifespan to 2500 takeoff and landing cycles. Carbon brakes offer dramatic weight savings, being three times lighter than steel (Ref. 25). They perform consistently, regardless of the environment and feature unparalleled endurance. Aircraft that perform a dynamic array of missions such as the C-17 utilize SepCarb brakes (Ref. 25). Additional weight savings and increased reliability and controllability are designed into the braking system by using "brake by wire" technology. Pilot activated commands are transmitted electronically through a braking computer which passes on the actuation command to the braking EHA system (Ref. 25).



Chapter 8: Stability and Control

The Peregrine is able to perform all stability and control tasks set by the RFP and FARs. It is able to trim during take-off and landing, perform the SNI landing, even with the critical engine out, and has acceptable stability characteristics for Short-period, Phugoid, and Dutch Roll modes.

The control concept for the Peregrine is a conventional configuration: horizontal T-tail, rudder and ailerons. The T-tail configuration was chosen because the horizontal stabilizer can be extended aft of the fuselage, producing a larger moment arm, and larger control powers.

The horizontal tail, with a 37% chord elevator, provides primary pitch control as well as the primary pitch damping. The vertical tail provides the main yaw control and primary yaw damping. The ailerons, running from 75% to 90% of the wingspan, provide the primary roll control.

The simple control concept for the Peregrine was chosen for its easy analysis and maintenance. Using spoilers for roll control causes the aerodynamics to become nonlinear, making it difficult to estimate the control powers without the use of a wind tunnel model. This would make changing control configuration a complicated, timely and expensive procedure.

An important control problem to overcome is the ability to trim during the ESTOL portion of flight. The high-lift necessary to take-off and land quickly produce large nose-down pitching moments. A large horizontal tail will be needed to provide the necessary down-force to keep the nose up. However, too large a down-force on the tail may reduce the total lift necessary to take-off.

Another important aspect of the control concept is the use of different control surfaces to maintain the different attitudes of the aircraft during complex maneuvers. For example, the ailerons will be used to bank the aircraft during the turn for the SNI landing, while the rudder will be used to keep the aircraft from sideslip due to critical engine out. This prevents one control surface from being loaded to its ultimate stress while other control surfaces aren't loaded at all.

8.1 Analysis Method

Once the configuration and placement of the tail were chosen, the size had to be determined. This was done through the use of an X-plot (or Scissor-plot). The X-plot, as seen in Figure 8.1, shows the horizontal tail size required to trim at the forward most cg , and the tail size required trim at the aft most cg . Both constraints were



calculated during take-off and landing to determine the critical constraint. It was found that landing was the critical tail loading case for nose up and nose down constraints. Another nose down constraint was drawn to allow for a 10% static margin because it is important for a pilot to always be able to bring the nose of the aircraft down to avoid stall. The analysis also includes the tip-back requirement (cg in front of rear landing gear) at rest. Using the weight analysis stated in Chapter 3, the maximum cg travel was added to the plot, and placed such that it is always in the feasible region at smallest tail size.

A weight analysis was done during various loading conditions (all baggage placed in tail, then only first 3 rows filled with baggage directly beneath) to find extreme cg locations. It was determined that the forward most cg was 13.7% MAC and the aft most cg was 28% MAC during typical flight conditions.

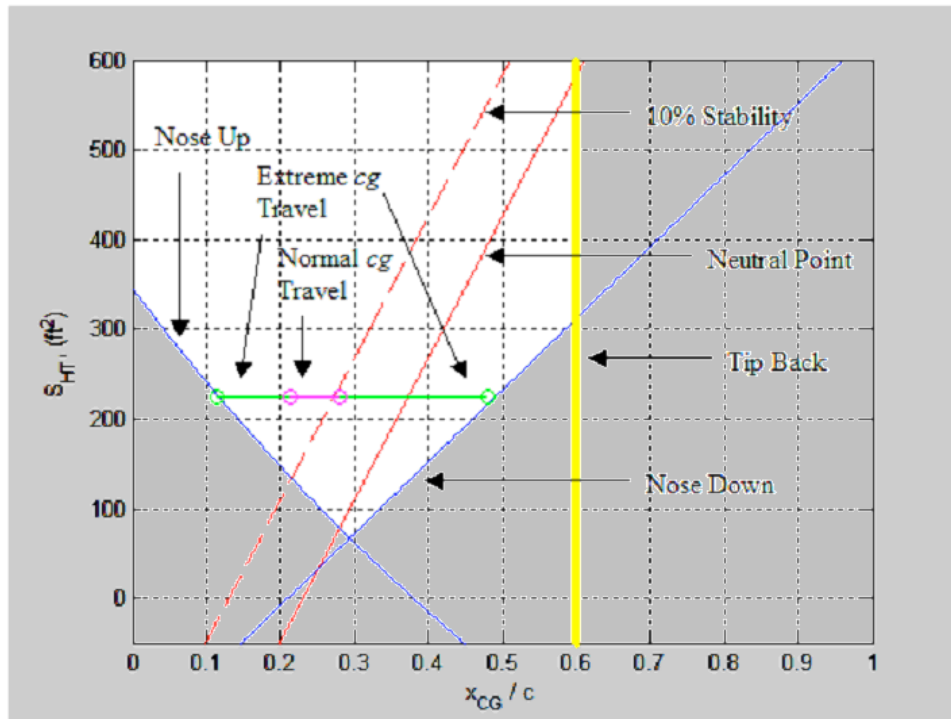


Figure 8.1 Horizontal Tail Constraint Diagram (X-plot)

With the cg travel in the X-plot, it was obvious that maintaining nose up at fore-most cg was the critical constraint, requiring a horizontal tail size of 225 ft². This gives a neutral point at 36% MAC and a static margin of 9%.



The size of the vertical tail was found using a tail volume coefficient for transport aircraft of 0.1, which is typical of STOL aircraft such as the YC-14 and YC-15 (Ref. 31). The tail volume coefficient is defined as $V_v = l S_v / b S$; using the length from *cg* to *ac* of tail, wingspan and wing size, the vertical tail size was found to be 215ft².

The control powers were found using the J-Kay Vortex Lattice program, developed by Virginia Tech faculty and students (Ref. 32). The program calculates the longitudinal and lateral-directional control powers as well as the stability derivatives for each surface using a Vortex Lattice Method. The results of the program were verified against published results for the STOL aircraft in Nelson to ensure reliability (Ref. 33). The program gave reliable results (less than 10% error) once sign corrections were made. The program results for the Peregrine are shown in Table 8.1.

Table 8.1 J-Kay VLM Program Results

Stability/Control Derivative	(rad ⁻¹)	Stability/Control Derivative	(rad ⁻¹)
$C_{m_{flap1}}$	-0.17472	C_Y	-0.64911
$C_{m_{flap2}}$	-0.77524	C_l	-0.05475
C_{l_a}	0.04378	C_n	0.14788
C_{m_a}	-0.3168	C_{Y_r}	0.50141
C_{n_a}	-0.00071	C_{n_r}	-0.17758
C_{Y_r}	-0.29992	C_{l_r}	0.04418
C_{l_r}	0.03281	C_{l_P}	-0.60333
C_{n_r}	0.11981	C_{n_P}	-0.40379

8.2 Trim

The high lift the Peregrine produces during take-off and landing creates high nose down pitching moments. Using a sum of moments about the *cg* from wing, body, tail and the horizontal stabilizer power, the horizontal stabilizer deflections necessary to trim the aircraft during take-off and landing were found. The results of the calculations show that stabilizer deflections required to trim are:

$$\text{Fore-most } cg \text{ (stabilizer)} = 16.55^\circ \text{ Aft-most } cg \text{ (stabilizer)} = -30^\circ$$

These results show that although the Peregrine produces large pitching moments, the tail is powerful enough to trim the aircraft. Also, to show that the Peregrine is able to trim during all conditions, plots of pitching moment against C_L were made for the various conditions in which the Peregrine will fly. The plots are shown in Figure 8.2 (a-d)

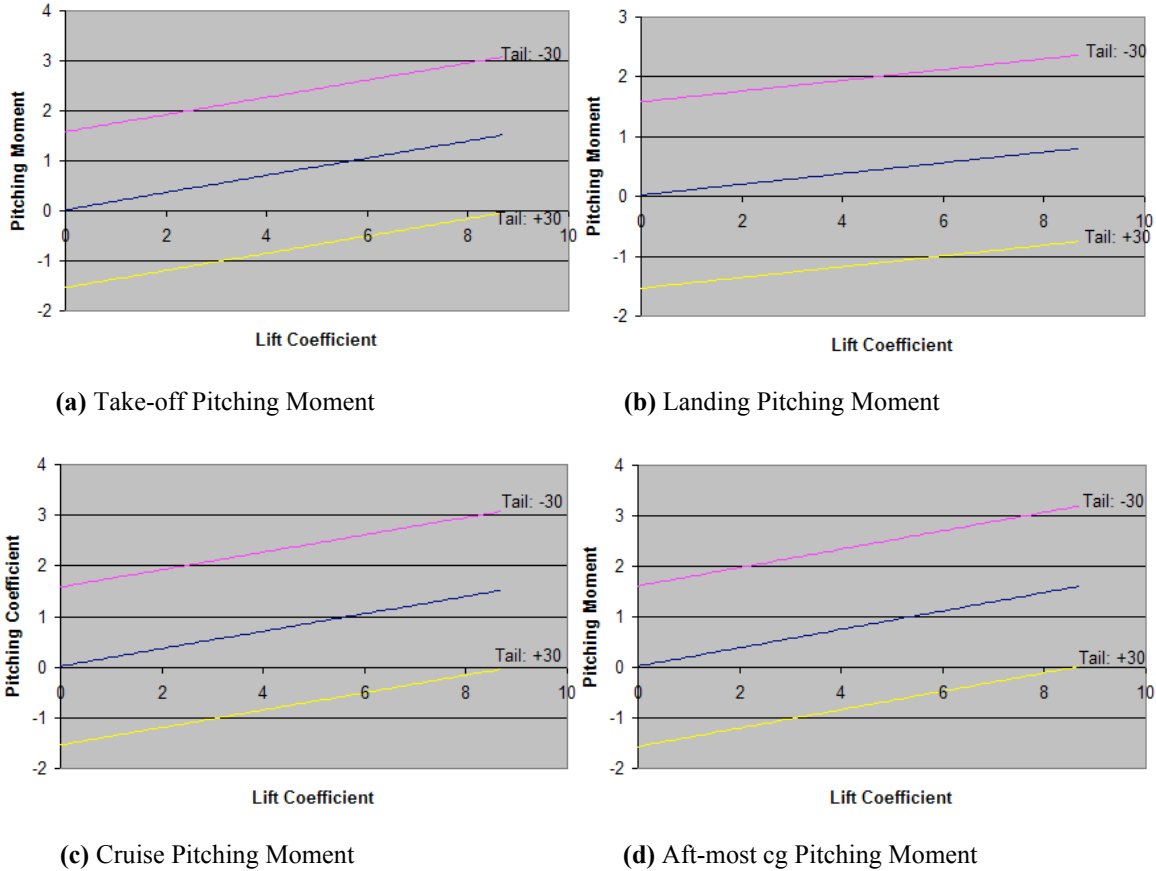


Figure 8.2 Pitching Moments for Various Flight Conditions

These plots show that the Peregrine is able to trim for every loading condition the Peregrine will experience. Although a maximum tail deflection of 30° is required during aft-most c_g location and C_{Lmax} , it is still possible, and the aircraft will not operate long during this loading condition..

8.3 Crosswind/Tailwind

The RFP contains a critical control issue; the aircraft must be able to land in a 25 kt crosswind and 5 kt tailwind (which translates to a 22° sideslip angle). Again, the STOL capability of the aircraft poses a problem, the aircraft is landing at only 65 kts minus the 5 kt tailwind, reducing the control power of the rudder to eliminate sideslip. Fortunately, the T-tail also provides a benefit; the horizontal stabilizer on the top of the tail acts as an endplate, which reduces spillover during rudder deflection, increasing its effectiveness.

The sum of side-forces, yaw-moments and roll-moments, as seen in Nelson, are solved simultaneously for rudder and aileron deflections, as well as bank angle to maintain steady-level flight (Ref. 32). The deflections for a 25 kt crosswind (65 kts & 5 kt tailwind) are:



$$\delta_{\text{(ailerons)}} = 4.7973^\circ$$

$$\delta_{\text{(rudder)}} = 23.47^\circ$$

$$\beta = 1.4456^\circ$$

These results show that the Peregrine is easily able to maintain steady level flight during the crosswind. The maximum rudder deflection is 30° , showing that the aircraft still has yaw control during the crosswind.

8.4 Engine Out

Commercial transports must be able to land with a critical engine out. This is especially important to the Peregrine, not only because of a large yaw moment created from the engines placed a considerable distance from the fuselage centerline, but also because of the large amount of powered lift each engine produces, and the slow landing speed which reduces control power.

By setting up and solving the simultaneous equations for sum of side-forces, roll-moments and yaw-moments, the rudder and aileron deflections, along with bank angle, can be found to maintain steady-level flight. One constraint is that the bank angle does not exceed 5° . Engine out control is most critical during landing due to the reduced control power from low velocity. The deflections and bank required to steady the aircraft with outboard engine failure during landing (65 knots) are:

$$\delta_{\text{(ailerons)}} = 9.24^\circ$$

$$\delta_{\text{(rudder)}} = 30.0^\circ$$

$$\beta = -2.27^\circ$$

The deflections and bank required to steady the aircraft with auxiliary fan failure during landing (65 knots) are:

$$\delta_{\text{(ailerons)}} = 5.96^\circ$$

$$\delta_{\text{(rudder)}} = 1.52^\circ$$

$$\beta = -0.11^\circ$$

Although the auxiliary fans produce more lift, they do not produce much thrust, and the moment arm is much smaller than if an outboard engine were to go out, thus making the outboard engine the critical engine for control issues. It is important to notice that rudder deflection is 30° during this engine failure, which is the maximum deflection.

8.5 SNI Landing

One more key issue from the RFP is the SNI landing; the aircraft must be able to enter a descending, decelerating spiral with a radius of 3,000 ft. at 140 kts, and come out of the spiral at 80 knots. Control power must be such that they allow for the constant turn while maintaining comfort levels for passengers and minimal load factors on the structures. The ailerons must be able to allow the aircraft to bank up to 30° , but no higher, thereby keeping the load factor below 1.15g, the maximum for allowable passenger comfort.



Because the SNI landing involves a decelerating descent, the control surfaces must vary according to the velocity. Therefore, a plot was made to show the bank angles and turn speeds for each velocity along the descent. The method for determining bank angle and turn speed from velocity are described in Roskam (Ref. 34). The conditions during the SNI landing are shown in Figure 8.3.

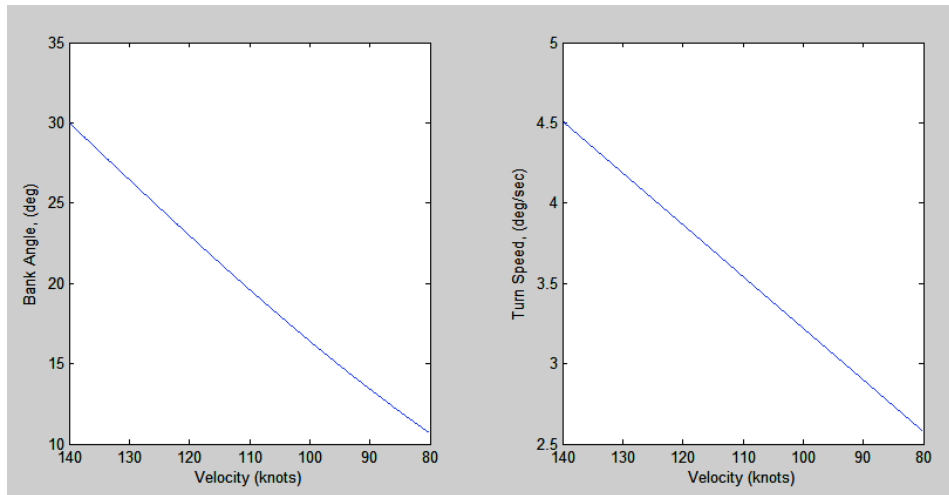


Figure 8.3 SNI Landing Conditions

Also, the aircraft must be able to continue the SNI landing with a critical engine out. However, the engine out can be used to aid the Peregrine's performance during the spiral; the roll moment produced by loss of powered lift can be used to bank the aircraft to maintain the turn. However, the rudder must still be deflected to balance the yaw moment produced by the unbalanced thrust. By combining the equations for the SNI landing with the equations for engine out, the deflections were determined to maintain the coordinated turn with the critical engine out. The resulting conditions/deflections for each velocity during the turn are shown in Figure 8.4.

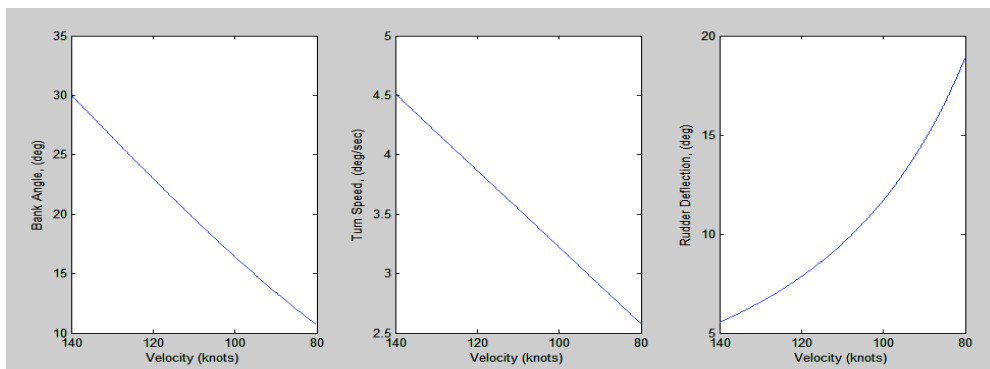


Figure 8.4 SNI Landing & Engine Out Conditions



8.6 Dynamic Response

The dynamic response of the aircraft was also analyzed using the results from the J-Kay VLM program. The analysis of the dynamic response of the aircraft was done using the methods described in Nelson and Etkin & Reid (Ref. 33 & 34). The damping ratio, ζ , and undamped natural frequency, ω_n , were used to determine the stick-fixed dynamic response of an aircraft.

The damping ratio and frequency for trim were found using the pitching moment due to angle of attack, time rate change of angle of attack, and pitching velocity. For responses to crosswind/engine out, they were found using the yaw moments due to sideslip and yaw. Finally, the dynamic motion of Dutch roll was approximated using the side-force due to sideslip and yaw, as well as the yaw moments due to sideslip and yaw. The resulting damping ratios, natural frequencies and time history of each model are shown in Table 8.3.

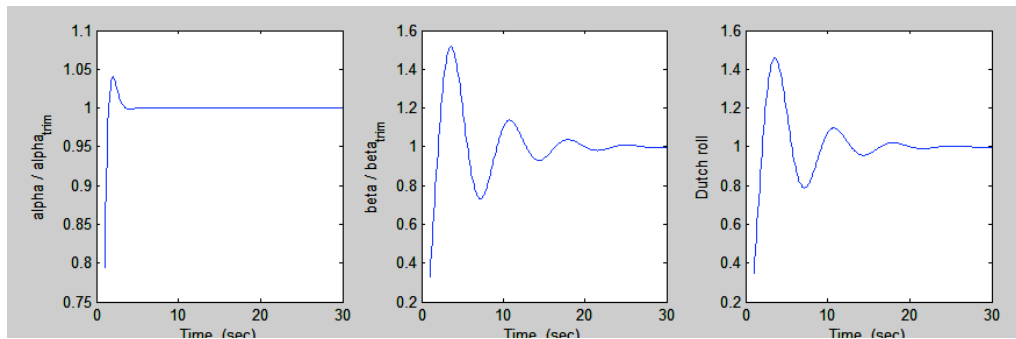


Figure 8.5 Time History of Aircraft

The frequencies and damping ratios that were calculated to determine the dynamic responses above are shown in Table 8.3 along with the FAR §25 required values.

Table 8.2 Stability Parameters

		Damping Ratio	FAR Required Damping Ratio	Frequency (rad/s)	FAR Required Frequency
Short Period	I	0.7696	0.20 – 1.30	2.6519	2.15 – 7.72
	II		0.25 – 2.00		3.10 – 12.05
Phugoid mode	I	0.7696	> 0.04	0.1572	< 0.7
	II		> 0		
Dutch Roll	I	0.2414	> 0.19	0.8983	< 1.0
	II		> 0.08		< 0.4
	III		> 0.08		< 1.0

This table shows that the Peregrine satisfies most dynamic characteristics, but not all. Specifically, the short-period mode frequency is not satisfied for class II conditions and the Dutch-roll mode frequency is also not



satisfied for class II conditions. Therefore, the Peregrine will utilize a Rockwell Collins Digital Flight Control System as discussed in Chapter 7. The FCS includes a stability augmentation system, which significantly reduces pilot workload while improving the dynamic response of the aircraft (higher damping ratios, and lower frequencies) to allow the Peregrine to meet FAR requirements for all conditions. However, all damping ratios are within required values, which can be directly attributed to the large tail and high-wing configuration.

Also calculated was the response to a 5° aileron deflection, as determined by the method in Etkin & Reid (Ref. 34). The approximate time to a steady state roll rate is 3.5 seconds. The equation for roll rate was integrated in order to solve for bank angle versus time, which was then used to determine time to bank 90°. The results for time to bank during various conditions are shown in Table 8.3.

Table 8.3 Time to Bank

Speed	Time to 90°	FAR Required
Low	2.0	1.7- 2.0
Mid	2.5	2.5 - 2.8
Max	4.0	3.4 - 3.7

This table shows that the time to bank for low and mid speeds are pushing the limits, but the maximum speed time to bank isn't exactly within the limits. For this, the flight control system will be activated to increase the aileron deflections to bank the aircraft fast enough to meet FAR values.



Chapter 9: Mission Performance

The performance of an aircraft is usually the selling point for many aircraft, next to the cost. The mission requirements reveal the critical areas of study pertaining to the aircraft with emphasis on a balanced field length of 2,500 feet. The mission performance defined in the RFP is for an aircraft capable of accomplishing multiple missions. The RFP specified required and optional missions; the primary and secondary (required), homeland security and military support (optional).

9.1 Primary Mission

The primary mission profile designated in the RFP consisted of eleven segments. The first step was a warm up and taxi at idle power for eight minutes. The aircraft must then climb to the best cruise altitude and maintain a velocity no less than 400 knots for 1,500 nm, less the distance traveled out during climb. The aircraft should be capable of conducting a Jonez Four STAR approach into Dallas Fort Worth International Airport (Ref. 35), using a simultaneous non-interfering (SNI) landing on runway 13L. Figure 9.1 illustrates the primary mission profile. Five minutes at three quarter take off power was allocated for the SNI landing if powered lift was used. The SNI approach was a two loop spiral descent from five thousand feet with a diameter of one nautical mile and a nominal sink rate of 15 fps. The RFP requires the aircraft to complete the SNI landing with one engine out. The aircraft will have a velocity of eighty knots at an altitude of fifty feet above the runway threshold when completing the approach. After landing, the aircraft will taxi in and park using idle power for ten minutes. Federal Aviation Regulations require the aircraft to have enough reserve fuel to accommodate a missed approach with a diversion of one hundred and fifty nautical miles with a forty five minute holding time at five thousand feet (Figure 9.1).

9.1.1 Take-Off Analysis

The take-off analysis conducted, estimated the ground roll including rotation, transition to climb, climb, and the balanced field length including stopping distance after decision velocity is reached (Ref. 9). The ground rolling resistance coefficient was selected to be 0.03 for dry concrete or asphalt. The height of the obstacle for clearance is 35 feet. $C_{L_{max}}$ was calculated to be 8.75, the wing areas is 1,080 ft², and the thrust provided by the two main engines is 18,440 lbs of thrust at sea level.

A take-off program was used to correlate the analysis. The program used Krenkel & Salzman's method given in their AIAA paper pertaining to takeoff analysis (Ref. 36). Modifications were made in the code to account



for rotation phase. A fourth order Runge-Kutta scheme solved the equations of motion numerically with a time step of one second. The take-off program was used on the ATR-72 for a comparison to verify the output is correct. The results of the Peregrine are given in Tables 9.1 & 9.2.

Table 9.1 Normal Take-Off

Rotation Velocity (V_r)	86.7 ft/s
Liftoff Velocity (V_{lo})	112.7 ft/s
Velocity over obs. (V_{obs})	101.2 ft/s
Rotation Distance (X_r)	394.1 ft
Liftoff Distance (X_{lo})	694.1 ft
Distance to obst. (X_{obs})	846.5 ft
Rotation Time (T_r)	8.9 s
Liftoff Time (T_{lo})	11.9 s
Time to obst. (T_{obs})	13.3 s
TOTAL TAKEOFF DIST	846.5 ft
TOTAL TAKEOFF TIME	13.3 s

Table 9.2 One Engine Inoperable

Critical Velocity (V_{crit})	76.5 ft/s
Decision Velocity (V_1)	87.7 ft/s
Velocity over obs. (V_{obs})	101.3 ft/s
Critical Distance (X_{crit})	301.4 ft
Decision Distance (X_1)	547.8 ft
Balanced Field Length (BFL)	1015.9 ft
Critical Time (T_{crit})	7.7 s
Decision Time (T_1)	10.8 s
OEI Takeoff Time (TBFL)	21.2 s

9.1.2 Landing Analysis

Landing is broken up into four segments; approach, flare, free roll, and ground roll using techniques describe in Ref. (9). The obstacle height at the beginning of the runway is 35 ft, the radius of the flare circular arc was found to be 1,809 ft, and the aircraft is assumed to free roll at touchdown speed for 3 seconds. Landing analysis is shown in Table 9.3.

Table 9.3 Landing Analysis

Segment	Velocity (knots)	Horizontal Distance (ft)
Approach	65	262.4
Flare	61.5	35.41
Free Roll	57.5	302.77
Ground Roll	57.5 – 0	251.57
TOTAL	-	852.6



Landing distance of 852 ft is achieved by the high lift coefficient produced by the powered lift scheme. The high lift coefficient provides for a decrease in stall speed, therefore landing procedures are conducted at a relatively slow velocity. Figure 9.1 illustrates the primary mission profile along with performance details pertaining to fuel, altitude, lift to drag ratio, flight time, distance traveled, and speed.

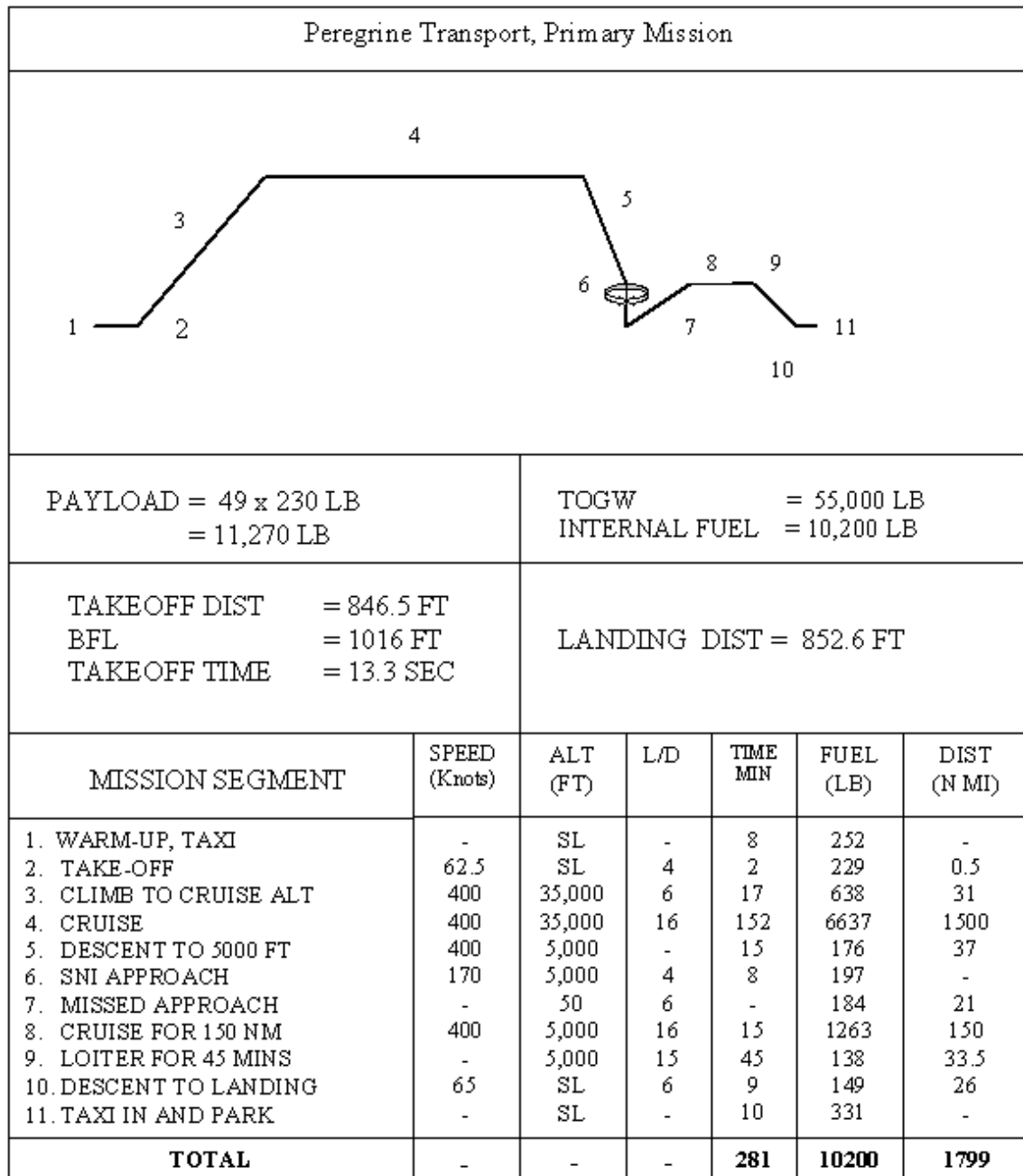


Figure 9. 1 Primary Mission



9.2 Secondary Mission

The secondary mission required in the RFP was a wildfire support mission, which included carrying twenty firefighters equipped with extra gear (144 lbs/ each baggage) and 2,000 lbs of additional fire suppressant. The first step was a warm up and taxi at idle power for 8 minutes. The balance field length must not exceed 2,000 ft at sea level on a hot day, temperature equal to 95 °F. The aircraft will climb to best altitude and cruise for 750 nm at a cruise speed no less than 400 kts then descend to 5,000 ft and land. If powered lift was used 3 minutes were allocated for landing at three-quarter takeoff power. The landing zone was blacktop with a useful area of 2,000 ft. The simultaneous non-interfering approach is not required, but the aircraft needs to be capable of landing in a 25 kt crosswind with a 5 kt tailwind component. The aircraft will then taxi in and park using idle power for 2 minutes, Figure 9.2. The passengers, baggage, and suppressant will be unloaded and the aircraft will takeoff from the same runway.

Take off analysis was conducted on the current designs to ensure fulfillment of mission requirements. The analysis was conducted the same way for the secondary mission as it was for the primary. Tables 9.4 & 9.5 show the distance and velocities achieved during takeoff. The analysis was conducted for takeoff at 5,000 ft (95°F) and on soft ground ($\mu=0.3$, Ref. 35) to mimic the conditions that would be encountered

Table 9.4 Secondary Normal Take-Off

Rotation Velocity (V_r)	89.5 ft/s
Liftoff Velocity (V_{lo})	112.7 ft/s
Velocity over obs. (V_{obs})	98.6 ft/s
Rotation Distance (X_r)	517.4 ft
Liftoff Distance (X_{lo})	820.9 ft
Distance to obst. (X_{obs})	1017.4 ft
Rotation Time (T_r)	11.5 s
Liftoff Time (T_{lo})	14.5 s
Time to obst. (T_{obs})	16.4 s
TOTAL TAKEOFF DIST (X_{to})	1017.4 ft
TOTAL TAKEOFF TIME (T_{to})	16.4 s



Table 9.5 Secondary One Engine Inoperable

Critical Velocity (V_{crit})	76.5 ft/s
Decision Velocity (V_1)	87.7 ft/s
Velocity over obs. (V_{obs})	101.3 ft/s
Critical Distance (X_{crit})	301.4 ft
Decision Distance (X_1)	547.8 ft
Balanced Field Length (BFL)	1015.9 ft
Critical Time (T_{crit})	7.7 s
Decision Time (T_1)	10.8 s
OEI Takeoff Time (TBFL)	21.2 s

9.2.1 Landing Analysis

Landing is broken up into four segments; approach, flare, free roll, and ground roll following techniques describe in reference 9. The obstacle height at the beginning of the runway is 50 ft, the radius of the flare circular arc was found to be 2,103 ft and the aircraft is assumed to free roll at touchdown speed for 3 seconds. Landing analysis is shown in Table 9.6

Table 9.6 Secondary Landing

Segment	Velocity (knots)	Horizontal Distance (ft)
Approach	65	550.6
Flare	61.5	41.17
Free Roll	57.5	302.77
Ground Roll	57.5 – 0	250.72
TOTAL	-	1145.2

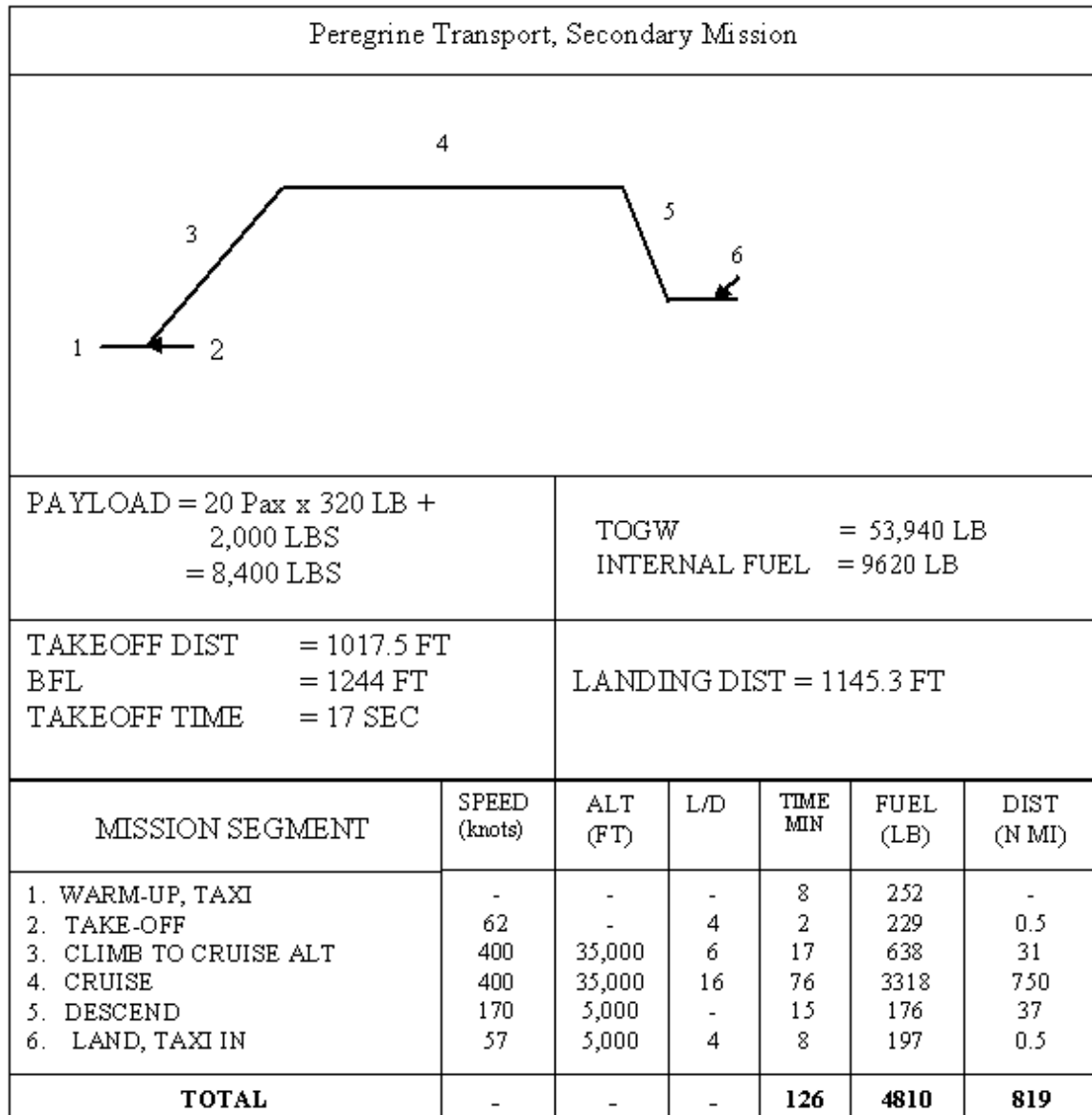


Figure 9.2 Secondary Mission

Optional missions require the aircraft to be efficiently converted from a commercial regional jet to an aircraft capable of supporting wildfire missions, homeland disaster response, military support and national defense. The survivability of the Peregrine will be enhanced for missions in combat areas to provide military support.



Chapter 10: Conversion Configuration

10.1 Baseline

The baseline aircraft is capable of completing the primary mission given in the RFP. The secondary and tertiary missions require a balanced field length of 2,000 feet with 50 ft obstacles located at each end of the runway. The Peregrine has roughly a 1,000 ft takeoff and landing capability, which is within the balanced field length required.

10.2 Additional Components

The Peregrine is capable of the short takeoff and landing requirement in the secondary and tertiary missions, but the structural integrity of the aircraft may be compromised by unprepared runways, combat areas, or large loads encountered during the missions. Landing on shorter runways with the probability of a higher descent rate will cause the loads on the landing gears and tires to increase. Therefore, the landing gear will need to be reinforced, moving the weight from 2,750 lb to 3,850 lb. The tires will need to have a higher floatation to absorb the shock and a higher stroke for more compression and a “smoother” landing. A central tire inflation system (CTIS) will be utilized to control the tire pressure in flight (Ref. 37). The CTIS will be used when taking off from regular well maintained runways and landing on softer, unprepared areas. A low tire pressure will be required for landings made on soft ground; therefore a heavier tire is required to support the loads. The number of tires will be increased from 2 to 4 per bogey to better distribute the aircraft weight on soft runways. Thus, tire weight increases from 114 lb to 320 lb. In addition to reinforcement of the landing gear, the bulkhead located at the center fuselage will need to be stronger to carry the added loads of landing in an unprepared setting.

The aircraft systems are upgraded to fulfill the survivability requirements of Military Support and National Defense missions. The vulnerability of a regional jet transport in a combat area is very high. Design features were incorporated into the Peregrine to reduce the vulnerability of the aircraft. The protection of the fuel tanks was increased with self-sealing tanks and ullage protection. The self-sealing tanks reduce the risk of a detrimental fuel leak from 0.1 to almost zero. Cost of the tanks was found from Ref. 38. Ullage protection reduces the risk of ignition of the fuel incase the tanks are penetrated by a bullet or hot projectile. Nitrogen is injected into the tank and mixes with the air between the fuel and top of the tank to reduce the level of oxygen. Cost of the ullage protection was taken from Ref. 38



Flying in combat areas, the pilot and copilot need to be protected from bullets and missiles. Therefore, aluminum plating will be placed on the floor of the cockpit to reduce the vulnerability of the crew. The aluminum plating will be 0.1575 inches thick and cover an area of 66 squared feet, the total area of the cockpit floor (Ref. 39). In addition to protective floor plates, countermeasures such as flares or chaff will need to be installed. The flares and chaff are used to deter heat seeking or radar guided missiles, respectively. The cost of the flare and chaff systems was found in Ref. 40

Another critical component are the engines. Fire extinguishers will be placed in the nacelles to reduce the risk of losing an engine due to fire. Ref. 38 provided the cost of development and installation.

Separation of redundant flight controls is also necessary to maintain control of the aircraft if a direct hit is incurred. The separation of the flight controls will be at least 0.5 meters. Therefore, a single hit should not cause rotor-burst.

The converted Peregrine aircraft must be able to land in a 25 kt crosswind with a 5 kt tailwind component with a balanced field length of 2,000 ft. Engine out was the critical constraint for control and did not effect the size of the control surfaces. Therefore the Peregrine will be able to control the landing in less than optimal orientation.

The wildfire support mission requires the aircraft to carry 20 firefighters with extra gear and 2,000 lbs of fire suppressant. The starboard seats will be taken out of the aircraft using a quick release mechanism to accommodate the firefighter's extra gear. The 12 rows of 2 seats will be removed efficiently, requiring the least amount of man hours. The quick release mechanism will be modeled after other quick release mechanisms used in conversion vans and minivans to remove the backseats in the vehicle. Hooks will be on the floors and walls located every 2 feet, and the aircraft will be equipped with 40 bungee cords (2 per firefighter) to secure the extra gear in flight. The seat removal conversion will also allow for stretchers to be carried in the aircraft, in the absence of extra equipment.

In addition to the firefighters, 2,000 lbs of fire suppressant will need to be transported. The fire suppressant will be housed in 80 pressurized canisters, each having a volume of 2.78 gallons. The canister is made from aluminum and will be in the shape of a cylinder with an internal useful volume of 0.396 ft³. The fire suppressant tanks are modeled after the AL-80C scuba diving tank (Ref. 41). The Peregrine will be able to house four rows of 20 tanks in the lower cargo compartment of the aircraft.



The additional components incorporated into the Peregrine's design will allow the aircraft to perform the secondary mission as well as tertiary missions including homeland disaster response and military support with transport to/from combat areas.

To provide enough power to execute an engine out, SNI landing at 5,000 ft. MSL, the auxiliary fans of the Peregrine would require a 450 shp turboprop engine. To achieve the lift conditions for the additional ESTOL missions, more power is needed. To meet this requirement, the Peregrine will incorporate two auxiliary fans, each powered by a 715 shp turboprop engine. With the application of this engine, the Peregrine will not only meet the constraints of the additional missions but will only have a cost and weight increase (per aircraft) of 0.36% and 0.27%, respectively.

10.3 Multiple Mission Configuration

When the government requires the use of the Peregrine it will be converted to the wildfire support mission configuration, shown below in Figure 10.1. Both sets of starboard seats and 3 rows on the port side will be removed via the rear cargo door, utilizing the quick-release seat track system. Fire suppressant canisters will be loaded in both lower cargo compartments in order to maintain proper weight and balance. Fire fighters will sit on the port side of the aircraft while their equipment will be secured on a set of hooks and bungees installed on the starboard side. Once on location, each firefighter will deploy with a fire suppressant tank and equipment to accomplish his mission.

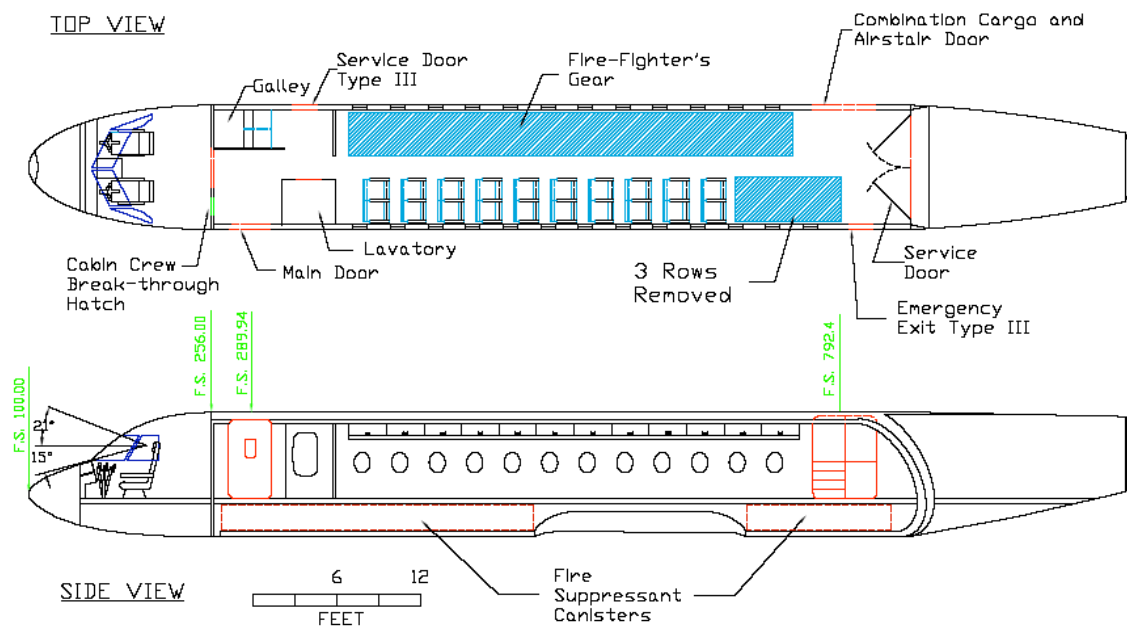


Figure 10.1 Secondary Mission Configuration



10.4 Cost Difference

The Peregrine will be able to convert to a military asset in the event of a homeland security crisis. The United States Government will subsidize the additional components on the aircraft for survivability in combat situations. Table 10.1 shows the baseline and multiple mission differences as well as the cost per aircraft and the RDT&E cost for each component.

Table 10.1 Subsidized Flyaway Cost

Category	Baseline	Multi-Mission	Difference	Cost (04'USD)	RDT&E
Landing Gear	2750 lb	3850 lb	1100 lb	\$640,000	\$994,124
Tires	114 lb	320 lb	206 lb	\$119,854	\$338,809
Bulkhead(composite)	100 lb	200 lb	100 lb	\$58,181	\$199,059
Cockpit Plates	-	66 ft ² x 0.013ft	0.86625ft ³	\$170	\$58,683
Countermeasures	-	28 lb	28 lb	\$2,229	\$78,043
Self Sealing Tank	-	1.5 kg	3.3 lb	\$1,500	\$100,000
Ullage Protection	-	1.31 kg	2.88 lb	\$2,620	\$400,000
Fire Extinguisher	-	80 kg	176 lb	\$16,000	\$100,000
Sep. Redundant controls	-	500 lb	500 lb	\$30,000	\$650,809
CTIS	-	20 lb	20 lb	\$5,400	\$60,938
Engines	450 hp	715 hp	150lb	\$200,000	\$535,562
Total			2305 lb	\$1,075,954	\$3,516,027

The United States Government will subsidize almost 900,000 dollars per aircraft and almost 3 million dollars for the RDT&E phase. The DOC incurred due to additional weight and systems for homeland security missions will also be subsidized by the United States Government. The cost of flying will be affected by the weight, reflected in the amount of fuel consumed. Maintenance cost will rise due to the amount of additional systems implemented on the aircraft. The additional structural mass and systems will increase the depreciation cost over time. Finally, the cost of financing or interest will be higher due to a more expensive DOC. Table 10.2 shows the cost breakdown. The United States Government will pay \$1.59 per nautical mile for DOC incurred due to the presence of additional equipment.

Table 10.2 Subsidized Direct Operating Cost plus Interest

DOC Category	Multi-Mission	Difference
Flying	\$0.077 / nm	\$0.08 / nm
Maintenance	\$1.05 / nm	\$1.05 / nm
Depreciation	\$0.37 / nm	\$0.37 / nm
Landing Fees	-	-
Financing	\$0.09 / nm	\$0.09 / nm
Total	-	\$1.59 / nm



Chapter 11: Cost

The Peregrine aircraft is a very affordable product considering the capabilities and technologies this vehicle offers. The United States Government will subsidize the incremental amount of flyaway cost and direct operating cost incurred on the Peregrine to perform additional homeland security missions. Typical airplane development utilizes a six step process for designing and manufacturing an aircraft family.

Six Step Process:

- 1) Planning and Design Concept
- 2) Preliminary Design and System Integration
- 3) Detail Design and Development
- 4) Manufacturing and Acquisition
- 5) Operation and Support
- 6) Disposal

The following cost analysis addresses all costs in the six step process.

11.1 Research, Development, Test & Evaluation

RDT&E account for the first three steps in the aircraft development process. There are seven factors which contribute to the cost of RDT&E: airframe engineering and design, development of support and testing, flight test airplanes, flight test operations, test and simulation facilities, RDT&E profit, and the cost to finance the phases. These factors are determined mainly from the Aeronautical Manufacturers Planning Report Weight, the cruise velocity, number of airplanes produced during the RDT&E phases, the judgment factors which account for difficulty and the effect of computer aided design. Table 11.1 and Figure 11.1 show cost breakdown.

Table 11.1 RDT&E Cost Breakdown

	Category	Cost
	Airframe Engineering & Design	\$ 130,000,000
	Development Support & Test	\$ 23,702,589
	Flight Test	\$ 326,000,000
	Flight Test Operations	\$ 3,758,497
	Financing	\$ 48,279,140
	TOTAL	\$531,740,226

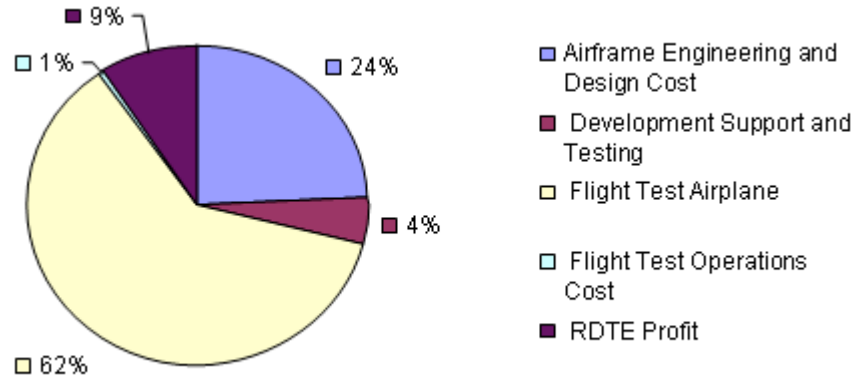


Figure 11.1 RDT&E Cost Breakdown

The airplane flight test represents the largest expenditure involved in the research, development, test, and evaluation phase of construction. The flight test performed on the aircraft involves the cost of engines and avionics, acquiring the manufacturing labor and materials, tooling costs, and the cost of quality control. The most expensive part of test flying a new aircraft is the tooling cost acquired due to manufacturing. The total amount of man hours required to produce 2 flight test planes, 2 static test planes, and 1 fatigue test plane (5 total) was estimated to be 2.4 million based on the weight of the aircraft, cruise speed, number of planes produced, and the difficulty judgment factor (Ref. 42). The tooling labor rate per hour was estimated to be \$60 an hour. Another large contribution to the test flight cost was the manufacturing labor required to produce all the materials necessary for the aircraft. The number of manufacturing man-hours required in phases 1-3 was estimated to be 2.87 million (Ref. 42). Estimated wages of \$45 an hour for manufacturing was used in the manufacturing cost calculations. The breakdown of flight test costs is given in Table 11.2 and Figure 11.2.

Table 11.2 Flight Test Cost (RDT&E)

	Category	Cost
	Engines/Avionics Acquired	\$ 7,860,000
	Manufacturing Labor	\$ 129,000,000
	Manufacturing Material	\$ 25,805,335
	Tooling Cost	\$ 146,000,000
	Quality Control Cost	\$ 16,794,192
	TOTAL	\$325,459,527

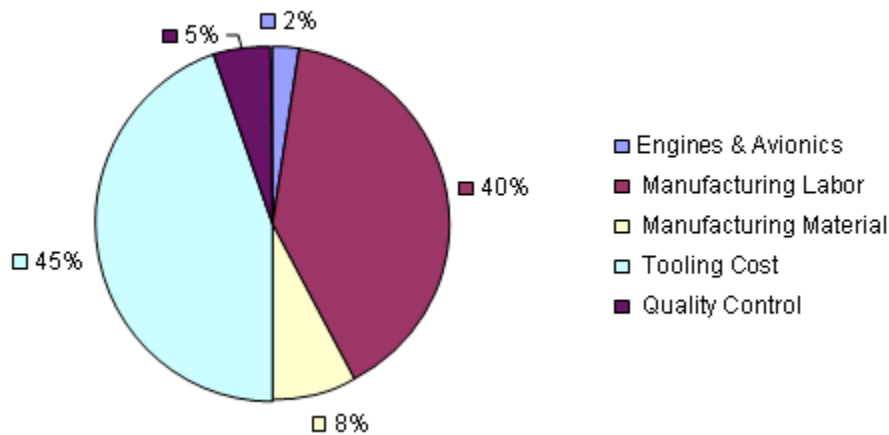


Figure 11.2 Flight Test of Aircraft Breakdown

11.2 Manufacturing

The manufacturing and acquisition of a line of airplanes is an expensive and time consuming process. The manufacturing part of the process is phase four of the cost analysis and can be broken down into four cost categories: airframe engineering and design, production cost, production flight test operations and cost of financing the manufacturing processes. The airframe engineering and design cost is incurred from sustaining engineering efforts associated with errors or changes made in the manufacturing of components or the manufacturing processes.

The production cost of manufacturing a line of airplanes includes six components: cost of engines and avionics, cost of interior, manufacturing labor costs, manufacturing material costs, tooling costs, and the cost of quality control.

The production flight test operations cost is a necessary part of the manufacturing process. Every aircraft that is manufactured must be test flown by the manufacturer before the product is delivered to the customer. For jet transports the number of flight test hours flown is generally around 10 (Ref. 42). Therefore test flights are costly because of the direct operating cost associated with flying the airplane and the overhead incurred during the production flight test.

The final cost of manufacturing is accumulated by the financing needed to get the project off the ground. Many factors come into play when determining how much money the manufacturer will need to borrow, how high of an interest rate is given, and how many calendar months it will take to pay back the money. Assuming the manufacturer will borrow money to finance the program, a reasonable interest rate is set at 6% and the money is



paid back over several years. The financing will not be more than 10% of the entire manufacturing process. Manufacturing costs for a production run of 150 aircraft is shown in Table 11.3.

Table 11.3 Manufacturing Cost Breakdown

Category	Cost
Airframe Engineering and Design	\$159.0*
Airplane Production	\$7,013.6*
Production Flight Test Operations	\$15.0*
Financing	\$431.2*
Total Cost	\$7,618.8*

*All cost are in US million dollars 2004.

11.3 Acquisition

Associated with the manufacturing cost is the cost of acquiring a line of airplanes. One airline carrier may only acquire a fraction of the airplanes built; this will affect the acquisition cost of the manufacturer.

Acquisition cost of the airplane is the manufacturing cost plus the profit made during the production. Assuming a 10% profit is made from the manufacturing, the acquisition cost is calculated as follows (Ref. 42).

Acquisition = Manufacturing Cost + Profit.

Therefore, the acquisition cost of the Peregrine is 8.4 billion dollars for year 2004.

11.4 Direct Operating Cost

The direct operating cost (DOC) of an airplane is a critical factor when a customer is interested in acquiring a large number of aircraft. The DOC must be reasonable, or the airline will not be able to make any profit. The airline must be able to sell airplane tickets at a competitive price to remain a viable company in the market.

The DOC consists of five main cost factors (Ref. 42). The DOC of flying, which includes the cost of the crew, the cost of fuel and oil, and the cost of insurance for the airframe all are essential to fly the aircraft. The DOC of maintenance required to keep the aircraft flying properly and safely as required by the FAA. The DOC of depreciation is an important element in calculating the DOC. A multi-million dollar aircraft acquires a certain amount of depreciation every time it flies. The DOC of landing fees, navigation, and registry taxes are required for the aircraft to perform legally and effectively. The Peregrine regional transport will keep all commercial operations within the United States or respective country, meaning no international flights are considered in the direct operation



cost estimation. Also included is the DOC of financing. Figure 11.3 shows the cost relation of each DOC component.

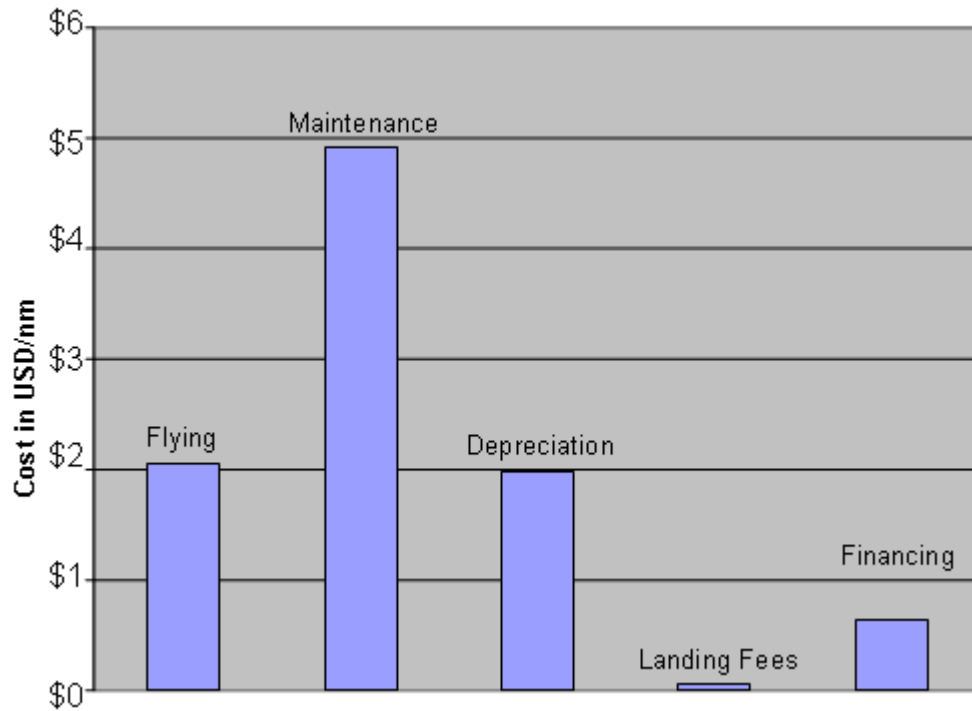


Figure 11.3 Direct Operating Cost

11.5 Disposal

The disposal cost of the aircraft is estimated to be roughly 1% of the Life Cycle Cost (LCC) of the aircraft (Ref. 42). A simple algebraic equation was used to estimate the LCC and therefore the disposal cost of the aircraft. The disposal cost of the program was estimated to be 94 million dollars.

11.6 Life Cycle Cost

The life cycle cost of an airplane production is the total cost incurred by the program for production.

$$\text{LCC} = \text{RDT\&E} + \text{Acquisition} + \text{Operating Cost} + \text{Disposal}$$

$$\text{LCC} = 531.07 + 8400 + 500 + 1$$

The Life Cycle Cost of the Peregrine is 9.4 billion US 2004 dollars



11.7 Flyaway Cost

The flyaway cost of the Peregrine depends on how many will be manufactured and where the manufacturing will take place. Production runs of 150, 500, and 1,500 aircraft have been analyzed in Figure 11.4.

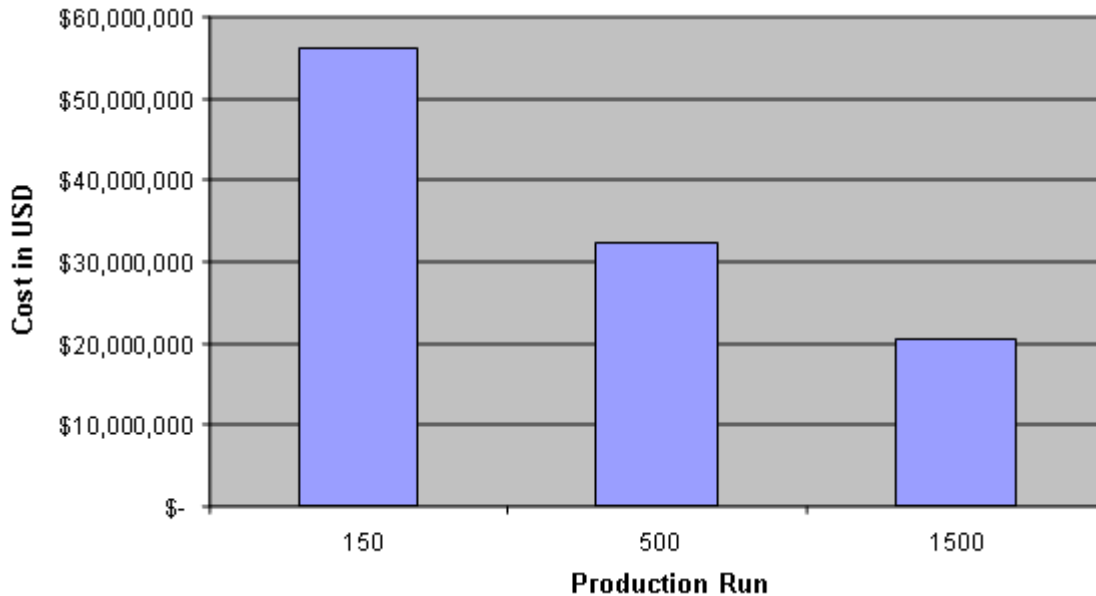


Figure 11.4 Estimated Unit Price per Plane

A production line of 1500 aircraft will create a very affordable regional jet. The cost of the aircraft goes down significantly because of the learning curve involved in production and manufacturing. Table 11.4 consists of the cost of each airplane for all three production runs plus the subsidized amount provided by the government.

Table 11.4 Total Price

Production Run	Price per Aircraft	Gov't. Subsidied	Total Price
150	\$ 56,251,879	\$ 1,075,954	\$ 55,175,925
500	\$ 32,307,324	\$ 1,075,954	\$ 31,231,370
1500	\$ 20,679,570	\$ 1,075,954	\$ 19,603,616
DOC	\$ 9.85 / nm	\$ 1.59 / nm	\$ 8.26 / nm

The cost of the Peregrine aircraft with STOL capabilities, for a production run of 1,500 aircraft, is compared with existing regional jets in Table 11.5



Table 11.5 Price Comparison

Peregrine (49 Pax-Production of 1500)	\$ 19,603,616
Embradier RJ 145 (50 Pax)	\$ 17,000,000*
Embradier RJ 170 (70 Pax)	\$ 21,000,000*
Candair RJ 900 (86 Pax)	\$ 28,500,000*

*All prices from Ref. 11.2

The price of the Peregrine is roughly 10-15% greater than current regional jets. The larger price is expected with the STOL capabilities and flexibility of the aircraft. With future growth in mind, the Peregrine becomes less expensive than current 70 to 80 passenger regional jets.



Chapter 12: Conclusion

The Peregrine provides an innovative solution to the growing problem of airport congestion as well as serving the nation through homeland security and military support. By incorporating a hybrid, powered lift, double-slotted flap system into a 49-passenger regional jet it was possible to satisfy the 2003/2004 AIAA undergraduate RFP. Team Ascent has incorporated these advanced technologies into a unique design to be a flexible, efficient and cost effective airport adaptive regional transport that will revolutionize air travel and improve national security.

The Peregrine is capable of many missions including: wildfire support, air ambulance to urban and rural areas, air transport to and from combat areas and emergency evacuation. The cost of the aircraft is split between the baseline cost of the regional jet and the additional, government-subsidized cost of converting the Peregrine to its additional mission configurations.

The Peregrine addresses the SNI approach and automated spiral by utilizing the Rockwell Collins FCS-4000 automatic flight control system. It stabilizes the spiral descent as well as aiding the pilot with pedal-force for the rudder deflections, stabilizer deflections and bank control. During engine out conditions, the high lift system allows the Peregrine to stably continue the SNI approach and achieve a stall speed as low as 65 knots with a descent rate of 12 fps.

The combination of the Peregrine's unique lifting systems allows the aircraft to achieve a BFL of 1,016 ft. during primary mission operations and a BFL of 1,244 ft. during secondary mission operations. These remarkable performance characteristics enable the Peregrine to complete multiple missions with a flexible, efficient and cost effective solution to the RFP.



Appendix A: CF34 Engine Decks

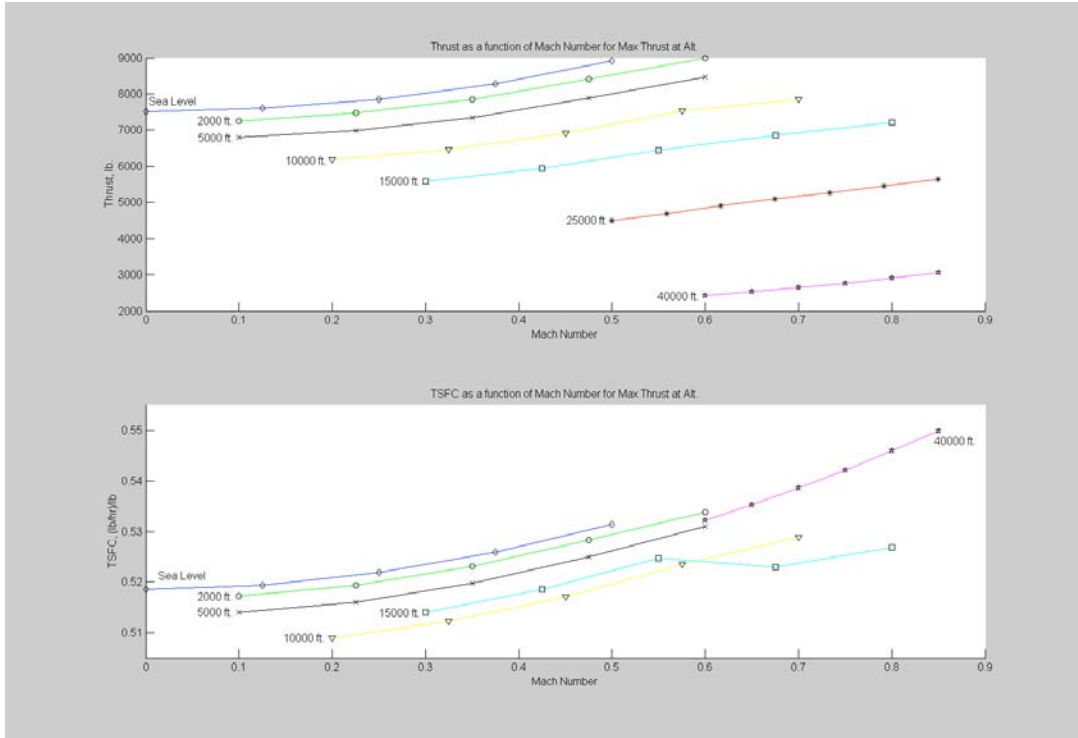


Figure A.1: CF34 Turbofan Engine Performance Charts for Maximum Thrust Setting

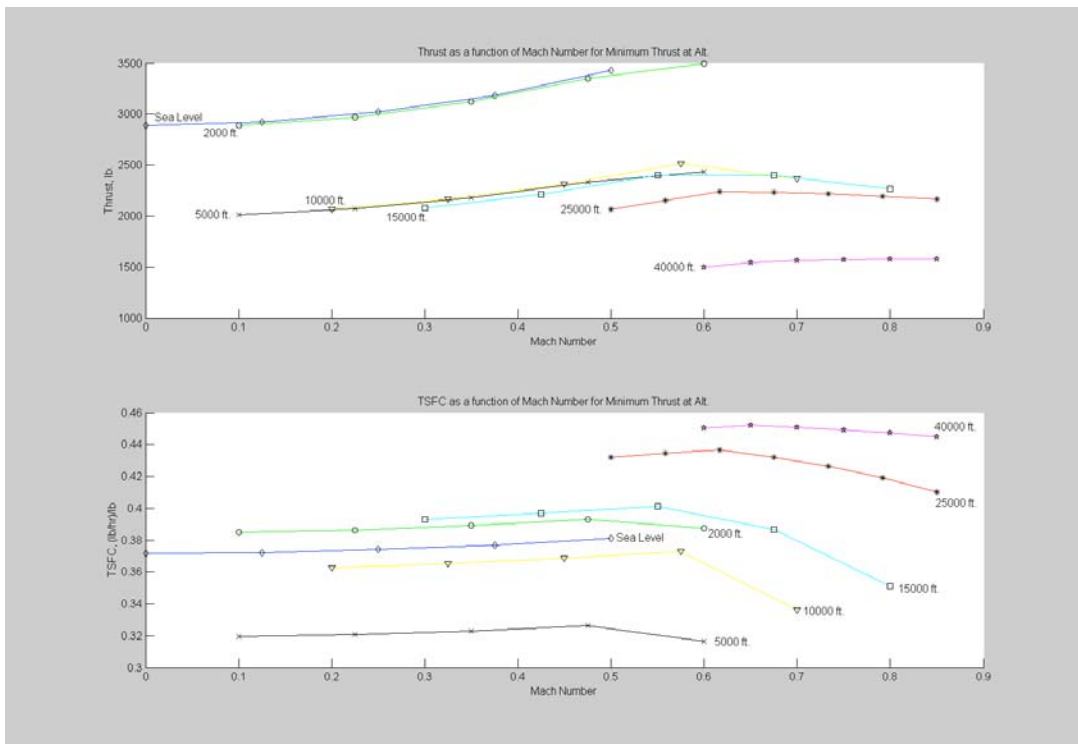


Figure A.2: CF34 Turbofan Engine Performance Charts for Minimum Thrust Setting



References

- 1 Advanced Topics in Aerodynamics, <http://aerodyn.org/HighLift/tables.html>, cited [5 May, 2004]
- 2 Roskam, J., *Airplane Design Part I: Preliminary Sizing of Airplanes*, DARcorporation, 2000.
- 3 Roskam, J., *Airplane Design Part V: Component Weight Estimation*, DARcorporation, 2000.
- 4 Roskam, J., *Airplane Design Part III: Preliminary Configuration Design and Integration of the Propulsion System*, DARcorporation, 2000.
- 5 Roskam, J., *Airplane Design Part VI*, DARcorporation, 2000.
- 6 Drela, Youngren, “XFoil”, Department of Aero & Astro, MIT, Boston, MA., Aerocraft, Inc. Dec. 2001
http://www.aoe.vt.edu/~mason/Mason_f/MRsoft.html#XFOIL
- 7 McCormick, B. W., *Aerodynamics, Aeronautics and Flight Mechanics*, 2nd Ed., John Wiley & Sons, Inc., New York, 1995
- 8 Mason, “Skin Friction and Form Drag Estimation Program”, Department of Aerospace and Ocean Engineering, Virginia Polytechnic Institute and State University, Blacksburg, VA. November 1996,
http://www.aoe.vt.edu/aoe/faculty/Mason_f/VPI-Aero_200.pdf
- 9 Raymer, D. P., *Aircraft Design: A Conceptual Approach*, AIAA Education Series, Reston, VA, 1999.
- 10 Nacelle Design and Sizing, <http://adg.stanford.edu/aa241/propulsion/nacelle/design.html>, cited [14 April, 2004]
- 11 Air Force Research Labs, www.afrlhorizons.com, cited [15 October, 2003]
- 12 Power Wing Concept, www.demand-schedule.com/specs.html, cited [22 April, 2004]
- 13 Rolls Royce, http://www.rollsroyce.com/civil_aerospace/products/regional/model250/default.jsp, cited [3 May, 2004]
- 14 The program is based on the methodology of A.R. Krenkel and A. Salzman published in the *Journal of Aircraft*
- 15 Roskam, J., *Airplane Design Part IV*, DARcorporation, 2000.
- 16 Reinforced Plastics, www.reinforcedplastics.com, cited [27 March, 2004]
- 17 Global Composites, www.globalcomposites.com, cited [28 March, 2004]
- 18 Steinke, S., and Gründer, M., “A380 Production Under Way”, www.flug-revue.rotor.com, *Flug Revue* 11/2003, pp 20.
- 19 *New Materials for Next-Generation Commercial Transports*, National Materials Advisory Board, 1996, avail: <http://books.nap.edu/books>.
- 20 The Society of British Aerospace Companies, <http://forum.sbac.co.uk/supplychain/>, cited [4 April, 2004]
- 21 Glauser, M., and Walker, S., “Active Flow Control Technology”, Air Force Research Laboratory, 1998,
www.afosr.af.mil



- 22 The Japan Carbon Fiber Manufacturers Association, www.carbonfiber.gr.jp/english/, cited [3 May, 2004]
- 23 Hamilton Sundstrand, www.hamiltonsundstrandcorp.com, cited [2 April, 2004]
- 24 Hamilton Sundstrand Power Systems, www.hs-powersystems.com, cited [2 April, 2004]
- 25 Messier-Bugatti, www.messier-bugatti.com, cited [2 April, 2004]
- 26 Ball, R. E., “How can you design your AAT to be more survivable when it is used in the ‘Military Support and National Defense’ role?”, www.aiaa.org, cited [3 April, 2004]
- 27 Air Liquide, www.airliquide.com, cited [14 April, 2004]
- 28 Monogram Systems, www.monogramsystems.com, cited [14 April, 2004]
- 29 UltraQuiet, www.ultraquiet.com, cited [14 April, 2004]
- 30 Kirschbaum, N., *Aircraft Design Handbook*, VPI Aircraft Design Series, 1994.
- 31 Mason, Durham, Lutze, Benoliel, “Control Authority Issues in Aircraft Conceptual Design”, Department of Aerospace and Ocean Engineering, Virginia Polytechnic Institute and State University, Blacksburg, VA. November 1996, http://www.aoe.vt.edu/aoe/faculty/Mason_f/VPI-Aero_200.pdf
- 32 Nelson, Robert C., *Flight Stability and Automatic Control*, McGraw Hill, Boston, MA, 1998.
- 33 Roskam, J., *Airplane Design Part VII: Determination of Stability, Control and Performance Characteristics: FAR and Military Requirements*, DARcorporation, 2000.
- 34 Etkin & Reid, *Dynamics of Flight*, John Wiley & Sons Inc. New York, 1996
- 35 AIAA, www.aiaa.org, cited [14 April, 2004]
- 36 Roskam, Jan; *Airplane Design Part VIII: Airplane Cost Estimation: Design, Development, Manufacturing and Operating*, DARcorporation, 1990
- 37 CTIS, www.xmlpitstop.com, cited [14 April, 2004]
- 38 Survivability Technical Committee, www.aiaa.org/tc/sur/index.html, cited [14 April, 2004]
- 39 Aluminum Supply, www.shapirosupply.com, cited [14 April, 2004]
- 40 Military Analysis Network, www.fas.org/man/dod-101, cited [14 April, 2004]
- 41 E-Series Steel Tanks, www.diveriteexpress.com, cited [14 April, 2004]
- 42 Aviation Today, www.aviationtoday.com/reports.htm, cited [14 April, 2004]
- 43 Niu, M. C. Y., *Airframe Structural Design*, Conmilt Press Ltd., 1988
- 44 ASM International Handbook, www.asminternational.org/hbk, cited [19 March, 2004]
- 45 Huff, D. “Technology Development for Aircraft Noise Alleviation”, NASA Research Center, 2000, www.grc.nasa.gov/WWW/AST/noise.htm